About rings and crossbands

Characterization of proteins involved in
cell division and compartmentalization in *Caulobacter crescentus*

Dissertation
zur Erlangung des Doktorgrades
der Naturwissenschaften
(Dr. rer. nat.)

dem
Fachbereich Biologie
der Philipps-Universität Marburg
vorgelegt

von

Dipl.-Nat.
Susan Schlimpert

aus Mittweida

Marburg (Lahn), Mai 2011

Vom Fachbereich Biologie der Philipps-Universität Marburg (HKZ: 1180)
als Dissertation angenommen am 05.07.2011

Erstgutachter: Jun.-Prof. Dr. Martin Thanbichler
Zweitgutachter: Prof. Dr. Lotte Søgaard-Andersen

Tag der mündlichen Prüfung: 13.07.2011

Die Untersuchungen zur vorliegenden Arbeit wurden von Oktober 2007 bis Mai 2011
am Max-Planck-Institut für terrestrische Mikrobiologie
unter der Leitung von Jun.-Prof. Dr. Martin Thanbichler durchgeführt.

Ergebnisse aus in dieser Dissertation nicht erwähnten Projekten sind in folgenden Orginalpublikationen veröffentlicht:

Möll, A., **S. Schlimpert**, et al. (2010). "DipM, a new factor required for peptidoglycan remodelling during cell division in *Caulobacter crescentus*." Mol Microbiol **77**: 90-107.

Ornston, L. N., **S. Schlimpert**, A. Buchan, and D. Parke. 2008. *Acinetobacter baylyi* genetics. In: *Acinetobacter*: Molecular Biology. U. Gerischer (ed). Norfolk, UK: Caister Academic Press. pp 141-162.

ABSTRACT

Over the past years, the dimorphic alpha-proteobacterium *Caulobacter crescentus* has emerged as an excellent model system to address various questions revolving around prokaryotic cell biology. *C. crescentus* is characterized by its asymmetric cell division, which produces two morphological distinct daughter cells. This life-style involves a high degree of intracellular organization, which is facilitated, in part, by the spatial and temporal regulation of protein localization. The localization of a protein to a distinct subcellular site is often linked to a topologically restricted function. Hence, a cytological screen was performed to identify proteins that specifically localize to midcell or the stalked pole owing to their function in cell division or stalk formation.

In most prokaryotes, cell division is accomplished by a multiprotein complex, called the divisome. The scaffold for assembling the divisome is provided by the Z-ring, which is a ring-like structure that forms during polymerization of FtsZ molecules at midcell. Coordination of Z-ring formation as well as divisome assembly and stability are crucial for successful proliferation. Several factors that stabilize the division apparatus have been characterized. However, these factors appear to be phylogenetically unrelated and to fulfill a rather species-specific function during cell division. This raises the question of what additional factors are required to ensure efficient cell division in *C. crescentus*.

Here, I report the identification of the novel cell division protein CedX (cell division protein X). CedX is a proline-rich inner membrane protein that localizes in an FtsZ- and FtsN- dependent manner to the cell division plane. Interestingly, it was found that overproduction of CedX blocks cell division and causes the formation of several non-contractile Z-rings. Functional analysis of CedX mutant derivatives demonstrated that CedX requires its membrane anchor and proline-rich region for proper localization and protein-protein interaction. In addition, coimmunoprecipation and bacterial two-hybrid analyses suggest that CedX not only interacts with FtsZ and FtsN but also with several other late cell division proteins. Colocalization experiments with fluorescently tagged derivatives of FtsZ, FtsA, FtsN and CedX further support the notion that CedX is a late recruit to the cell division apparatus. However, it remains to be elucidated under which conditions CedX becomes essential for proper cell division. Collectively, these findings suggest that CedX is an accessory divisome component that presumably supports the assembly process of late divisome components by means of its unstructured proline-rich C-terminal tail.

Apart from cell division, the formation of a prostheca, also known as stalk, is another characteristic change in cell morphology, which is a widespread phenomenon among bacteria and also an obligatory developmental checkpoint in the *C. crescentus* life cycle. In *C. crescentus*, the stalk represents a thin extension of the cell envelope that is free of DNA, ribosomes and most cytoplasmic proteins. It is segmented at irregular intervals by so-called crossbands, disk-like structures that traverse the entire width of the stalk perpendicular to the long-axis of the cell. Crossbands are generally thought to have an architectural, stabilizing function. Despite the fact that researchers have been trying to reveal the mechanisms underlying stalk formation, including the synthesis of the enigmatic crossbands, the biogenesis and function of these structures is still poorly understood.

In an attempt to identify factors involved in stalk biogenesis and morphogenesis, four novel stalk proteins, StpABCD, were identified in *C. crescentus*. Synthesis of StpABCD is initiated at the onset of stalk outgrowth. It was found that StpABCD are specifically targeted to the inner membrane and the periplasmic space of the stalk, with StpA acting as a recruitment factor for StpBCD. Additionally, coimmunoprecipitation analysis supports the idea that StpABCD interact *in vivo* to form a multiprotein complex. The four proteins colocalize in the stalk in distinct foci that display the same subcellular distribution as crossbands. Noteably, electron cryo-tomography revealed that cells deficient in StpAB consistently lack crossbands. To test for a potential role of crossbands in cellular compartmentalization, the mobility of fluorescently labeled proteins was examined in wild-type or StpAB-deficient cells using fluorescence-loss-in-photobleaching (FLIP) and pulse-labeling experiments. Interestingly, these analyses demonstrated that crossbands act as diffusion barriers for periplasmic, inner and outer membrane proteins. Based on these findings, it can be hypothesized that StpABCD constitute the crossband structures, which act as a protein diffusion barrier to compartmentalize the periplasmic space of the stalk, thereby physically separating it from the cell body. Crossband formation thus represents a novel mechanism to spatially restrict protein mobility within a cell.

ZUSAMMENFASSUNG

In den vergangenen Jahren hat sich insbesondere das Gram-negative alpha-Proteobakterium *Caulobacter crescentus* als ideales Modelsystem für die Beantwortung verschiedenster zellbiologischer Fragestellungen herausgestellt. *C. crescentus* zeichnet sich durch seine asymmetrische Zellteilung aus, welche zur Entstehung von zwei morphologisch distinkten Tochterzellen führt. Dabei durchläuft *C. crescentus* ein komplexes Entwicklungsprogramm, in dem die räumliche und zeitliche Positionierung von Proteinen und die damit verbundenen Regulationsmechanismen maßgeblich zur intrazellulären Organisation der Zelle beitragen. Zwei zentrale Aspekte im Entwicklungsprogramm von *C. crescentus* sind die Zellteilung und die Ausbildung einer Prostheka. Da die räumliche und zeitliche Positionierung eines Proteins in einer Bakterienzelle oftmals direkt mit dessen Funktion verknüpft ist, wurde gezielt nach Proteinen gesucht, die während der Zellteilung in der Zellmitte bzw. im Zuge der Stielbiogenese an den Zellpol lokalisieren.

In den meisten Prokaryoten erfolgt die Zellteilung mittels eines Multi-Proteinkomplexes, dem Divisom. Das Grundgerüst des Divisoms bildet der sogenannte Z-Ring, eine ringähnliche Struktur, die durch die Polymerisation von einzelnen FtsZ-Molekülen in der Zellmitte gebildet wird. Eine erfolgreiche Zellteilung hängt maßgeblich von der zeitlichen und räumlichen Regulation der Entstehung des Z-Rings sowie der Assemblierung und Stabilisierung des Divisoms ab. Es wurden bereits Faktoren, die zur positiven Regulation des Zellteilungsapparates beitragen wurden bereits identifiziert. Jedoch scheinen diese in den meisten Fällen eine speziesspezifische Funktion während der Zellteilung auszuführen. Es stellt sich daher die Frage, welche zusätzlichen Faktoren in *C. crescentus* für eine effiziente Zellteilung verantwortlich sind.

Im Rahmen dieser Arbeit konnte das neue Zellteilungsprotein CedX (*cell divison protein* X) identifiziert werden. CedX ist ein prolinreiches Membranprotein, welches in Abhängigkeit von FtsZ und FtsN zur Zellteilungsebene rekrutiert wird. Interessanterweise inhibierte eine Überproduktion von CedX die Zellteilung und führte gleichzeitig zur Entstehung von mehreren Z-Ringen in den Zellfilamenten. Diese Z-Ringe waren jedoch nicht mehr in der Lage, eine Zellteilung einzuleiten. Eine funktionelle Analyse von verkürzten Proteinvarianten von CedX zeigte, dass sowohl die Membranverankerung als auch die prolinreiche Region für die räumliche Lokalisation und den beobachteten Überproduktionsphänotyp von CedX eine Rolle spielen. Mittels Co-Immunpräzipitation und einer bakteriellen Zwei-Hybrid-Analyse konnte nachgewiesen werden, dass CedX nicht nur mit den essentiellen Zellteilungsproteinen FtsZ und FtsN, sondern auch mit weiteren, späten Zellteilungsproteinen interagiert. Co-Lokalisationsversuche mit fluoreszenz-markierten Derivaten von FtsZ, FtsA, FtsN und CedX bestätigten, dass CedX zu den späten Zellteilungsproteinen zählt. Bis zum jetzigen Zeitpunkt konnten jedoch keine Bedingungen ermittelt werden, unter denen CedX essentiell für die Zellteilung in *C. crescentus* wird. Zusammengefasst lässt sich feststellen, dass CedX ein akzessorisches Zellteilungsprotein ist, welches wahrscheinlich den Einbau von späteren Zellteilungskomponenten in den Zellteilungsapparat unterstützt. Dabei wird die stabilisierende Wirkung des Proteins wahrscheinlich über den unstrukturierten, prolinreichen Abschnitt im C-terminalen Bereich vermittelt.

Neben der Zellenteilung ist die Ausbildung einer Prostheka, auch Stiel genannt, eine weitere charakteristische Morphologieänderung, welche ein weitverbreitetes Phänomen unter Bakterien zu sein scheint und gleichzeitig einen obligatorischen Entwicklungsschritt im Lebenszyklus von *C. crescentus* darstellt. Der Stiel von *C. crescentus* ist eine dünne Verlängerung des Zellkörpers, welche weder DNA noch Ribosomen enthält und weitestgehend frei von zytoplasmatischen Proteinen ist. Darüber hinaus wird der Stiel in unregelmäßigen Abständen von scheibenartigen Strukturen, sogenannten Querbalken, segmentiert. Es wird vermutet, dass Crossbands eine strukturelle oder stabilisierende Funktion im Stiel übernehmen. Obwohl schon mehrere Studien zur Aufklärung der physiologischen Bedeutung des Stiels durchgeführt wurden, ist bis jetzt nur wenig über die Bildung und Funktion der Prosthecae sowie der rätselhaften Querbalken bekannt.

Auf der Suche nach Faktoren, die für die Biogenese und/oder Morphogenese des Stiels in *C. crescentus* verantwortlich sind, konnten im zweiten Teil dieser Arbeit die vier neuen Stielproteine StpABCD (*stalk proteins* ABCD) identifiziert werden. Es konnte gezeigt werden, dass die Synthese von StpABCD mit der Initiierung des Stielwachstums erfolgt. Im Zuge der Assemblierung der Querbalken im periplasmatischen Raum des Stiels übernimmt StpA eine entscheidende „Ankerfunktion" für die korrekte Lokalisierung von StpBCD. Darüber hinaus wurde mithilfe von Co-Immunpräzipitation nachgewiesen, dass StpABCD in einem Proteinkomplex vorliegen. Mittels Fluoreszenzmikroskopie konnte gezeigt werden, dass StpABCD eine charakteristische subzelluläre Position einnehmen, die mit der natürlichen Verteilung der Querbalken in den Prosthecae korreliert. Wurden in Zellen die Gene für *stpAB* deletiert, konnten keine Querbalken mehr mittels Kryo-Elektronenmikroskopie nachgewiesen werden. Um festzustellen, ob Zellen mit bzw. ohne Querbalken intrazelluläre Kompartimentierung aufweisen, wurde die Mobilität von fluoreszenzmarkierten Proteinen mithilfe von „FLIP" (*fluorescence-loss-in-photobleaching*) und „*pulse-labeling*" (zeitlich versetzte Produktion von fluoreszenzmarktierten Proteinen) Experimenten getestet. Diese Versuche verdeutlichten, dass Crossbands in der Tat für die Kompartimentierung von inneren und äußeren Membranproteinen sowie periplasmatischen Proteinen verantwortlich sind. Aus diesen Ergebnissen lässt sich daher schließen, dass StpABCD für die Synthese der Querbalken im Stiel von *C. crescentus* verantwortlich sind. Diese Strukturen wirken dabei als Diffusionsbarrieren, welche den periplasmatischen Raum zwischen Stiel und Zellkörper separieren. Die Bildung von Querbalken stellt daher einen neuen Mechanismus zur räumlichen Begrenzung der Mobilität von Proteinen in einer Bakterienzelle dar.

CONTENT

1 INTRODUCTION

In recent years it has become evident that, despite their small size, bacteria are not simple amorphous entities filled with proteins and DNA. Instead, the interior of a bacterial cell is highly organized. Like their eukaryotic counterparts, bacterial cells possess cytoskeletal elements, they dynamically move proteins and DNA to specific subcellular sites and use elaborate signaling cascades to coordinate inter- or intracellular events. These findings have not only changed the perception of bacteria in general but also led to new research questions, concerning the molecular mechanisms that regulate the progression through the cell cycle, cellular differentiation, chromosome segregation or cell division. Over the past decade, the dimorphic bacterium *Caulobacter crescentus* has emerged as a leading model organism to study the spatial and temporal organization of a bacterial cell.

1.1 *Caulobacter crescentus* – A model organism to study cellular differentiation and cell division

C. crescentus is a widespread Gram-negative alpha-proteobacterium. Although it is best known for thriving in oligotrophic aquatic environments [118], *C. crescentus* cells can also be isolated from polluted sites such as gold mines [71], contaminated water or sediments [93, 108], or from nutrient-rich sewage water [92]. The laboratory strain of choice is *C. crescentus* CB15N (NA1000), to which I will refer henceforth to as *C. crescentus*. *C. crescentus* is characterized by its unique developmental program during which two morphological and physiological distinct cell types arise: a motile "swarmer cell" and a sessile "stalked cell" (Fig. 1). Unlike many prokaryotes, *C. crescentus* duplicates its single chromosome only once per cell cycle. Hence, according to the replication state of the DNA in eukaryotes, the phases of the C. *crescentus* life cycle can be temporally distinguished into a pre-synthesis gap (G1), a DNA synthesis phase (S) and a post-synthesis/division phase (G2/M).

The life cycle of *C. crescentus* starts with a swarmer cell, which carries a single polar flagellum and several type IV pili at one cell pole (G1 phase). In order to become replication-competent, the swarmer cell needs to morph into a stalked cell. This morphological transition requires shedding of the flagellum and retraction of the pili followed by the establishment of an adhesive stalk at the same pole. Upon reprogramming into a stalked cell, DNA replication is initiated (S phase). As the cell grows, segregates its DNA and starts to constrict, a new flagellum is assembled at the pole opposite the stalk (G2 phase). The developmental program culminates in the asymmetric separation of the two siblings into a new swarmer cell and a stalked cell. The latter can immediately enter the next round of cell division, whereas the swarmer cell is temporally arrested in a "predevelopmental" state [27].

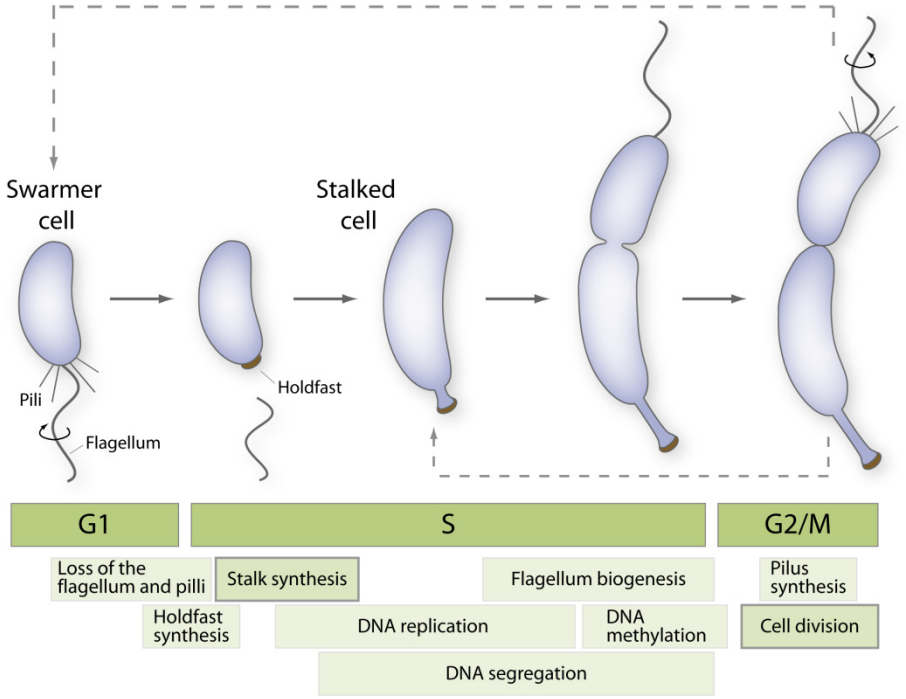

Fig. 1. Life cycle of *C. crescentus*. The motile swarmer cell posses a single flagellum and several pili (G1). During the obligatory swarmer-to-stalked-cell transition, the flagellum and pili are replaced by an adhesive holdfast and the stalk. During the S phase, DNA is replicated, methylated and segregated. At the end of the S phase, a new flagellum is assembled at the pole opposite the stalk. Asymmetric cell division at the end of G2/M produces two physiological different cell types, a swarmer cell that is unable to initiate DNA replication and cell division until it has differentiated, and a replication-competent stalked cell, which can immediately enter the next round of reproduction. The timing of various cell cycle and morphogenesis events are indicated below the cell cycle schematic. Modified from [154].

Conveniently, both daughter cell populations can be easily separated by density gradient centrifugation. Isolated swarmer cells can then be monitored as they progress synchronously through the developmental cycle, a property that greatly facilitates the study of cell cycle-dependent processes. Moreover, the genome of *C. crescentus* if fully annotated [94, 106] and a comprehensive set of plasmids for the inducible production of fluorescent protein fusions provides a suitable molecular toolbox to investigate the underlying molecular mechanisms of asymmetric cell division and cell differentiation [156].

Progression through the developmental program of *C. crescentus* is tightly regulated in time and space by an intricate network of regulatory pathways and protein-protein interactions. On the regulatory level it was found that the cell cycle-dependent transcription of at least 200 genes is governed by a cyclic cascade involving the four master regulators CtrA, GcrA, DnaA, and CcrM [86]. Together, they drive the synthesis of the flagellum, initiate stalk outgrowth, coordinate chromosome replication and segregation, ensure DNA methylation and regulate cell division. This study focuses on two spatial and temporal landmarks in the developmental program: cell division and stalk formation.

1.2 About rings - Cell division in *C. crescentus* and other bacteria

Despite the microbial diversity in nature, many bacteria, euryarchaeota, chloroplasts, and some protist mitochondria share a central player when it comes to the faithful division of the mother cell into two daughter cells (also known as cytokinesis). The by far most conserved cell division protein is the prokaryotic tubulin homolog FtsZ [88].

The wide-spread occurrence of FtsZ-dependent cytokinesis across the major branches of the phylogenetic tree has without doubt made FtsZ the key cell division protein. However, there are bacteria and archaea that have evolved different mechanisms to successfully proliferate. The exact mechanisms by which these organisms divide are in general poorly understood [3, 11].

1.2.1 The bacterial cell division machinery

In the presence of GTP, FtsZ polymerizes into a contractile ring-like structure (Z-ring) at the inner face of the cytoplasmic membrane [13, 103, 109-110]. Although the name "Z-ring" implies a closed rigid structure, high-resolution imaging has shown that the Z-ring is assembled by a loose bundle of FtsZ protofilaments that randomly overlap [46, 48]. Moreover, the Z-ring is a highly dynamic structure whose subunits turnover rapidly [46]. Nevertheless, the Z-ring serves as a scaffold for the assembly of at least two dozen proteins that are involved in different aspects of cell division [34]. Together, they act the so-called division machinery or divisome [3, 51]. Recent work on the dynamics and temporal hierarchy of divisome formation in *E. coli*, *B. subtilis* and *C. crescentus* has revealed that the divisome is assembled through the sequential association of several preformed subcomplexes [2, 49, 99-100]. The function of many divisome components is still not fully understood and most of the knowledge has been gained from studies perfomed in *E. coli* or, to some extent, in *B. subtilis*. In general, there are three major stages in the development of the cell division machinery: assembly of the Z-ring, maturation of the divisome and cell constriction.

Assembly of the Z-ring is initiated with the arrival and polymerization of FtsZ at the future cell division site (Fig. 2). Among the first cell division proteins that arrive with or shortly after FtsZ at midcell are ZipA and the actin-homologue FtsA, which tether the Z-ring to the membrane [29, 61]. Interestingly, *C. crescentus* lacks a ZipA homologue, and unlike reported for *E. coli* [2] or *B. subtilis* [49], FtsA arrives with a significant delay at the cell division plane [100], indicating that other cell division proteins may be in charge with the initial stabilization of the Z-ring. Several recent studies have identified a number of cell division proteins that directly interact with FtsZ protofilaments to induce higher-ordered structures thereby positively regulating early Z-ring assembly. To this set of proteins belong ZapA [58], ZapC [40, 62], FzlA [54] and SepF [59, 145], which have been shown to promote polymerization and/or bundling of FtsZ protofilaments *in vitro*. Additional Z-ring stimulating effects have been described for ZapB [42], which interacts via ZapA with the Z-ring, and FzlC [54], an FtsZ-binding protein of unknown function. Deletion of any of these early cell division proteins often causes only a modest phenotype, and with the exception of ZapA, they are less conserved across different bacteria species. In gram-positive bacteria, aberrant Z-ring formation is inhibited by the interaction of FtsZ with EzrA. Although EzrA is generally considered to be a negative regulator of Z-ring formation, there is experimental evidence that EzrA has multiple functions during cell division [3, 153].

The initial establishment of the Z-ring is followed by a maturation phase during which mainly essential membrane proteins are recruited to the divisome (Fig. 2). Among these so-called late cell division proteins are the ABC transporter-like complex FtsEX [6, 142], the widely distributed but

poorly characterized FtsQLB complex [23, 56], and FtsK/SpoIIIE [89, 166, 178], a multifunctional protein involved in cell division and chromosome partitioning. During divisome maturation, the peptidoglycan synthesis machinery is redirected to the midcell region. The switch from longitudinal to midcell and septal peptidoglycan synthesis is FtsZ-dependent [1, 35] and requires the recruitment of the peptidoglycan synthase FtsI (PBP3)/PBP 2B [26, 32, 116], the flippase FtsW [19, 97], and the murein-binding proteins FtsN [4, 100] and DipM [53, 99, 115]. Very late in the divisome assembly process of *C. crescentus*, the cell polarity factor TipN arrives at the division site to mark the incipient pole for future flagella biosynthesis [69, 83].

Cytokinesis culminates in cell constriction and fission of the three cell envelope layers. Inner membrane invagination is driven by the dynamics of the Z-ring [46, 110]. However, the mechanism by which the Z-ring is dismantled as it constricts is not known [3]. The coordinated inward growth of the peptidoglycan layer and the outer membrane requires the localization of additional factors (Fig. 2). Septal peptidoglycan remodeling and splitting is facilitated by peptidoglycan synthases, such as FtsI and other penicillin binding proteins (PBPs) or hydrolases, such as AmiC [12, 26, 36, 116]. Recent studies in *E. coli* have demonstrated that the "lethal" activity of peptidoglycan synthesis and hydrolysis underlies an elaborate molecular mechanism that specifically activates PBPs [112, 159] or amidases [160]. Finally, in gram-negative bacteria, outer membrane invagination is controlled by the trans-envelope TolQ/A/R-Pal complex [50, 180] and, in *C. crescentus*, DipM [53, 99, 115], a periplasmic protein that has been proposed to stimulate both peptidoglycan reconstruction and outer membrane constriction.

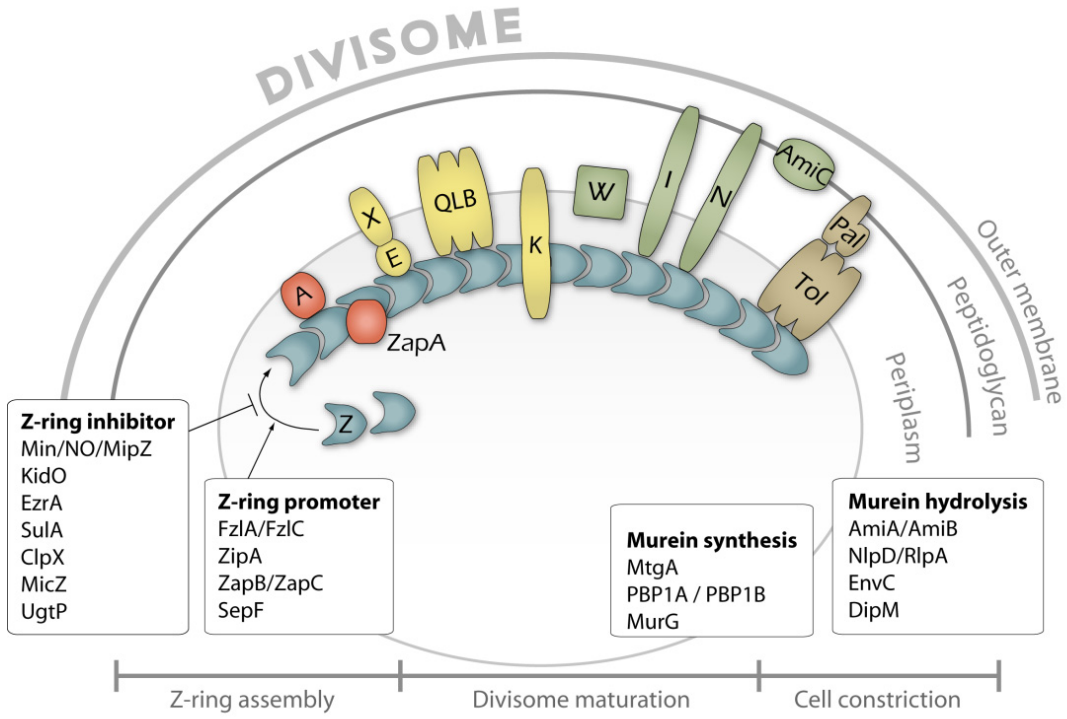

Fig. 2. The divisome. Schematic representation of the three stages of divisome assembly in *C. crescentus*, *E. coli* and *B. subtilis*. Note that schematic does not reflect order of recruitment to the Z-ring. Individual proteins were grouped according to their generally predicted function. Only functionally widespread cell division proteins are depicted. Fts protein names have been abbreviated (e.g. Z = FtsZ, A=FtsA, etc). Blue, FtsZ; red, FtsZ-stabilizing proteins; yellow, proteins involved in divisome stabilization or DNA segregation, green, proteins required for septal peptidoglycan remodeling; brown, outer membrane constriction. For clarity, additional cell division proteins are listed in a box. For further information see also [34]. For explanation of Z-ring inhibiting/promoting proteins see below (NO, nuccleoid occlusion).

1.2.2 Regulation of Z-ring assembly

The correct placement of the future division site and the timing of the physical separation of the two daughter cells need to be coordinated with a number of physiological events in the cell, such as cell growth, cell differentiation, and DNA replication and segregation. Hence, Z-ring assembly, and in particular FtsZ dynamics, must be regulated in time and space.

Spatial regulation of Z-ring assembly is achieved by three known FtsZ-inhibitory mechanisms: the Min system and nucleoid occlusion (*E. coli* and *B. subtilis*) and the MipZ system (*C. crescentus*) [155]. These molecular mechanisms prevent Z-ring formation at the cell poles or over the chromosome and establish the future division site by restricting FtsZ-polymerization to the midcell region.

Cell-cycle responsive regulation leads to a delay in Z-ring assembly in response to growth rate (UgtP), UV-induced DNA damage (SulA), or as a result of sporulation initiation (MciZ) [3]. SulA [102] and MciZ [64] target free FtsZ monomers, thereby disturbing rapid exchange of FtsZ subunits in the Z-ring and promoting Z-ring disassembly; whereas UgtP destabilizes lateral interactions between FtsZ protofilaments [171].

The largest group of Z-ring regulators comprises a number of accessory proteins that act during normal Z-ring assembly and polymerization, including the early, Z-ring promoting, cell division proteins ZapA/B/C, FzlA/C, SepF as well as the negative Z-ring regulators EzrA, KidO (unknown function) and ClpX (active against FtsZ polymers) [3, 40, 54, 62, 123]. None of these proteins is individually required for cell division and the presence of many of them are restricted to distinct bacterial phyla. Nevertheless, their function contributes to the formation of a functional cell division machinery and efficient cell division.

1.3 About crossbands - Stalk formation in *C. crescentus*

Caulobacter owes its name ("caulo" means stalk in Latin) to a polar structure – the stalk [21]. Stalks, also known as prosthecae, are produced by a number of bacteria besides *C. crescentus*, including *Asticcacaulis* spp. and *Hyphomonas neptunium*. As with bacterial cell morphologies, stalk structures come in various shapes (Fig. 3). The possible function(s) of such an appendage and the current knowledge about its synthesis in *C. crescentus* will be discussed in the following sections.

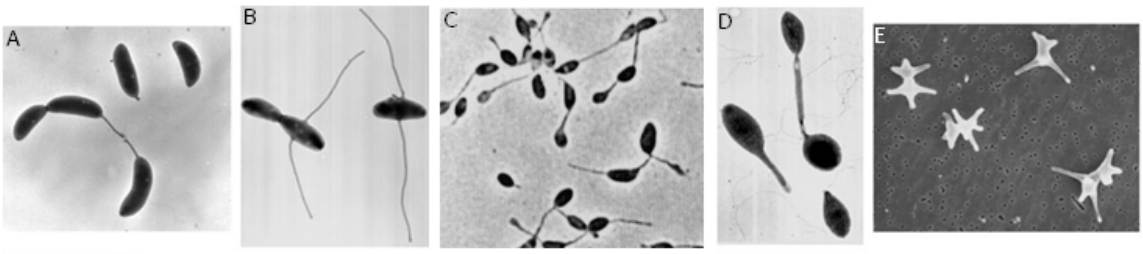

Fig. 3. Stalked alpha-proteobacteria. A. *Caulobacter crescentus*, B. *Asticcacaulis biprosthecum*, C. *Rhodomicrobium vannielii, D. Hyphomonas neptunium, E. Ancalomicrobium adetum* [41, 161].

1.3.1 *C. crescentus* stalk – structure and biosynthesis

The *C. crescentus* stalk represents a thin extension of the cell envelope of approximately 100 nm in diameter (Fig. 4). Analysis of the stalk fine structure and proteome revealed that stalks are devoid of DNA, ribosomes and most cytoplasmic proteins but are similar in their protein profile to the outer membrane [72, 117, 163]. The tip of the stalk is equipped with an adhesive organelle (holdfast), which is needed for permanent attachment of cells to biotic and abiotic surfaces [27]. The stalk is segmented at irregular intervals by so-called crossbands [117], disk-like structures that traverse the entire width of the stalk perpendicular to the long-axis of the cell. It has been suggested that crossbands require FtsZ for their formation, consist mainly of peptidoglycan, and might or might not contain a central pore [38, 74, 139, 141]. The temporal appearance of crossbands at the end of each division cycle has led to the hypothesis that the number of crossbands could be an indicator of stalk or even cell age [120, 152]. Crossbands have been observed in a variety of prosthecate species and were proposed to have an architectural, stabilizing function [74, 120, 139]. The mechanism of biosynthesis and the physiological significance of crossbands, however, remain to be elucidated.

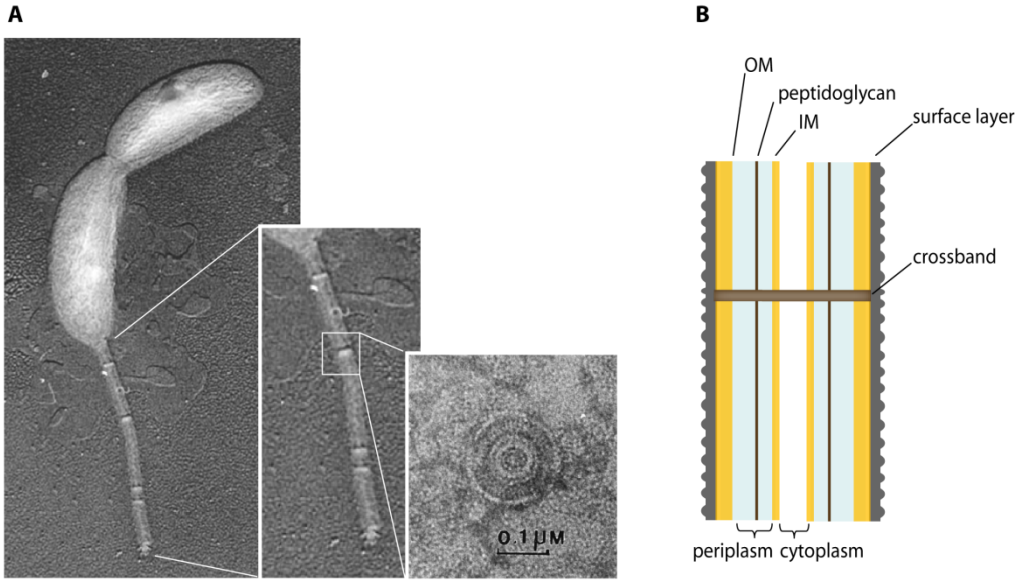

Fig. 4. Structure of the *C. crescentus* stalk. A. Electron micrograph of a predivisional cell. The magnified areas show a stalk with crossbands and a topview of a representative isolated crossband, respectively [120]. B. Schematic sideview of a stalk depicting the individual layers of the stalk envelope and the envisioned position of a crossband. Note that dimensions are not to scale.

The regulation of stalk formation has turned out to be a tough nut to crack. There are at least two pathways known to regulate stalk biogenesis. It has been reported more than 40 years ago that *C. crescentus* cells elongate their stalks in response to low extracellular phosphate concentrations [140]. The regulatory response to phosphate starvation involves the induction of the phosphate (Pho) regulon with *cis*-regulatory sequences, so-called *pho* boxes, which overlap with the promoter region of the downstream genes (Fig. 5A). It is known from studies in *E. coli* that during phosphate starvation the sensor kinase PhoR undergoes autophosphorylation and then passes on the phosphoryl group to the response regulator PhoB thereby increasing its affinity for the *pho* boxes. Phosphorylated PhoB activates the transcription of genes in the Pho regulon, including the high-affinity phosphate transport system *pstSCAB*. This phosphate transport system is composed of four proteins, a periplasmic phosphate binding protein PstS, two inner membrane channel proteins PstA

and PstC, and a cytoplasmic traffic ATPase PstB (see below) [55]. In the presence of excess phosphate, PstSCAB and PhoU repress the autophosphorylation of PhoR and activation of the Pho regulon, respectively. It has been hypothesized that PhoB~P controls the transcription of a gene(s) whose expression leads to an increase in stalk length. In fact, *phoB* mutants have short stalks, while mutations in the *pst* genes constitutively activate the Pho regulon resulting in longer stalks [55]. Yet, neither of these mutations produces stalkless cells.

In addition to phosphate starvation, stalk biogenesis occurs as part of the developmental program (Fig. 5B). Cell cycle-dependent stalk formation requires the alternative sigma factor RpoN (σ^{54}) and the response regulator TacA, the synthesis of which is controlled by CtrA, a cell cycle master regulator in *C. crescentus*. In collaboration, RpoN and activated TacA regulate the transcription of genes involved in stalk biogenesis. TacA activation is facilitated by a phosphorelay in which the hybrid histidine kinase ShkA (stalk histidine kinase A) first undergoes autophosphorylation and then transfers the phosphoryl group to the phosphotransferase ShpA, which in turn phosphorylates TacA [14]. So far, only two downstream targets of TacA have been identified - the regulator of stalk length StaR [14] and the stalked pole muramidase homolog SpmX [124]. Deletion of StaR results in short stalks, whereas overproduction of StaR leads to an increase in stalk length. SpmX is required for the localized activation of DivJ at the stalked pole, thereby ensuring proper regulation of fundamental cell cycle events [146]. Despite the identification of molecular cues that are involved in stalk biogenesis, mutants with lesions in *spmX*, *tacA*, *sta*R or genes of the phosphorelay system still synthesize a stalk in low-phosphate medium.

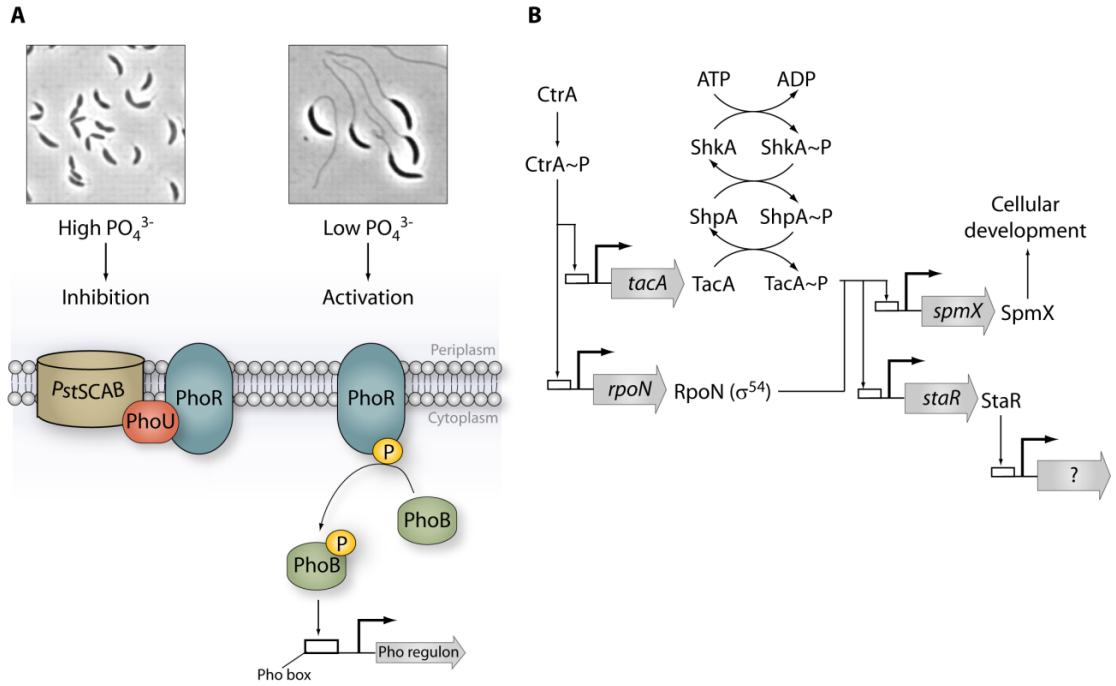

Fig. 5. Regulation of stalk biogenesis. A. Stalk biogenesis in response to phosphate starvation. In the presence of excess phosphate, *C. crescentus* cells have short stalks (phase contrast image) and autophosphorylation of PhoR and expression of the Pho regulon is repressed by the Pst complex and PhoU. Phosphate depletion (cells have long stalks) releases PhoR from the Pst complex. PhoR autophosphorylates, transfers the phosphoryl group to PhoB, which in turn binds to the Pho box sequences of promoters and activates transcription of its downstream target genes, such as *pstSCAB*. B. Cell cycle-dependent regulation of stalk biogenesis. Phosphorylated CtrA activates transcription of *rpoN* (σ^{54}) and *tacA*. TacA is activated by a phosphorelay composed of ShkA and ShpA. σ^{54} and phosphorylated TacA initiate synthesis of StaR and SpmX. SpmX is involved in cell cycle-dependent developmental events, whereas the target(s) of StaR are not known. Modified from [14, 55] and [J. Kühn, unpublished]. Phase contrast images taken from [55] (see text for details).

Synthesis of the stalk is a special type of cell elongation that occurs at the junction between the stalk and the cell body. To present, it is not known how the cell body is transformed into a tubular extension with the dimensions of the stalk. It has been shown, however, that the insertion of new stalk material depends on the cell shape-determining proteins MreB and RodA and the peptidoglycan synthase PBP2. Depletion of MreB or RodA or inhibition of PBP2 affects not only morphology of the cell body but also causes stalk deformation and prevents stalk formation, respectively [144, 162]. Recently, another peptidoglycan synthase, PbpC, and the stalk-specific protein StpX were found to support stalk elongation by a yet unknown mechanism [68, 81]. In addition, Ryan et al. recently reported that a defect in the assembly of outer membrane β-barrel proteins seems also to affect a factor required for stalk synthesis [132].

1.3.2 What are stalks good for?

The synthesis of a cell appendage such as the stalk is just another remarkable example of bacterial morphogenesis and poses the question what selective advantage is provided by having a stalk. Depending on the function of the stalk, prosthecate species can be classified into budding bacteria that use their stalk as a reproductive structure such as *H. neptunium* or *R. vannielii*, and non-budding bacteria, like *C. crescentus* or *A. biprosthecum* [138]. Interestingly, crossbands have so far only been observed in non-budding stalked bacteria. In *C. crescentus*, the synthesis of the stalk marks a switch from a motile to a sessile life style. However, production of a stalk is not required for surface attachment, as holdfast secretion is initiated before stalk outgrowth begins. Vice versa, stalk formation is independent of surface adhesion [16]. Once a *C. crescentus* cell has permanently attached to a surface, it continuously extends its stalk. The ability to elongate the stalk could be of particular advantage when the cell needs to rise above an existing biofilm into a less competitive environment. In addition, elevation of the cell body could aid in the dispersal of newborn swarmer cells, which would be released away from a colonized surface [161, 181]. The most common hypothesis favors the idea that the stalk is an organelle streamlined for nutrient uptake.

This nutrient uptake hypothesis is based on several experimental findings. First, stalk elongation appears to be significantly stimulated under phosphate-limiting growth conditions [55, 137, 140]. A similar effect was observed for other prosthecate bacteria, including *Asticcacaulis*, *Hyphomicrobium* and *Rhodomicrobium* [175, 181].

Second, the proteome of purified stalks seems to be enriched in proteins involved in nutrient binding and uptake but lacks inner membrane proteins for active translocation of nutrients into the cytoplasm [72, 163]. For instance, the abundance of TonB-dependent receptors was found to be high in stalks but the inner membrane proteins additionally required to drive the import, TonB, ExbD and ExbB, could not be detected by mass spectrometry. In addition, the periplasmic phosphate binding protein PstS was shown to be present in the stalk whereas PstA, a protein required for high-affinity transport of phosphate into the cytoplasm, was missing in whole lysates of purified stalks. Moreover, Wagner and co-workers showed that fluorescently tagged ExbB and PstA localize in the cell body but not in the stalk [55, 163].

Finally, analytical modeling suggested a biophysical advantage provided by long stalks in diffusion-limited, oligotrophic environments [163]. In other words, long and thin structures, such as the stalk, are a favorable shape for maximizing the contact with the environment to enhance nutrient uptake and, at the same time, minimizing the cost of increasing both surface area and volume. Based on the theoretical and experimental results, Wagner and co-worker proposed a "periplasmic diffusion model" for phosphate uptake via the PstSCAB proteins by the stalk (Fig. 6). In cells, nutrient

molecules can either diffuse through a pore into the periplasmic space or are taken up by a nutrient receptor in the outer membrane. Periplasmic phosphate is then captured by a specific nutrient-binding protein (PstS). This phosphate-PstS complex diffuses from the stalk periplasm to the cell body periplasm, where it is then transported across the inner membrane by PstCAB. The authors also considered an alternative "stalk core diffusion model", which describes the direct transport of nutrients from the stalk outer membrane into the stalk cytoplasm by an ABC transporter, followed by the diffusion of the nutrient molecules into the cell body cytoplasm. However, most of the experimental evidence supports the periplasmic diffusion model, which is after all just a model and may only provide a glimpse at the physiological relevance of stalks.

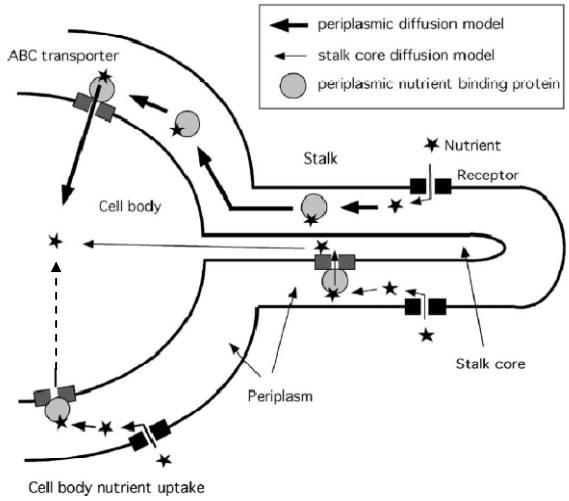

Fig. 6. Models for nutrient uptake by the stalk and the cell body. The model in the top part of the diagram (thick arrows) illustrates the periplasmic diffusion model. Nutrients (asterisk) are taken up into the stalk periplasm and bound by a nutrient binding protein. The nutrient-protein complex diffuses then from the stalk periplasm to the cell body periplasm where nutrients can be actively taken up into the cell body cytoplasm by an ABC transporter. The model in the bottom part of the diagram (thin arrows) shows the stalk-core diffusion model. Nutrients are taken up into the stalk core followed by their diffusion into the cell body cytoplasm. Nutrient uptake by the cell body is illustrated on the bottom left (dashed arrow). Diagram taken from [163].

While studying the *C. crescentus* stalk, Wagner et al. and others noticed that the stalk is compartmentalized from the cell body with respect to the protein content [72, 117, 163]. This finding was recently supported by the identification of the bitopic membrane protein StpX (stalk specific protein X), which was found to be specifically targeted to the stalk to fulfill a yet unknown function. Interestingly, not only subcellular localization of StpX was regulated but also protein mobility within the stalk [68].

1.3.3 Spatial regulation of protein mobility

Several ways of how protein compartmentalization between the stalk and the cell body could be achieved have already postulated [68, 163]. First, an unidentified physical barrier at the junction between the stalk and the cell body could prevent cytoplasmic and inner membrane proteins from diffusing freely into the stalk. So far there is no concrete evidence for the presence of a membrane or protein complex at the stalk base that could account for the observed protein compartmentalization between the stalk and the cell body. It has been suggested, however, that

crossbands or some kind of peptidoglycan structure at the stalk-cell body junction may function as diffusion barriers [74].

Second, proteins may be first localized to the nascent stalk pole by a molecular or topological cue, e.g. membrane curvature or protein-protein interaction, and then inserted into the growing stalk. Several proteins are known to localize to the stalk pole in *C. crescentus*, e.g. certain cell cycle regulators or bactofilins [81, 154], but none of these proteins is inserted into the stalk. Thus, it has been suggested that an active sorting mechanism may provide access for selected proteins into the existing stalk. Such a mechanism was recently suggested for the localization of the stalk protein StpX [68]. Yet, it remains to be clarified whether there is indeed a stalk-specific subset of proteins.

Third, proteins may be positioned in the stalk by the so-called "diffusion-and-capture" mechanism [158] meaning that proteins might diffuse into the stalk compartment where they are subsequently immobilized due to an interaction with a specific localization factor or a protein complex. Vice versa, mobility of most proteins might be simply confined to the cell body due to similar reasons. In fact, "diffusion-and-capture" appears be a widespread mechanism for both transient and persistent protein localization. For example, the positioning of the histidine kinase PleC to the cell pole in *C. crescentus*, the localization of cell division proteins to the divisome at midcell or the localization of SpoIVFB to the septal membrane during sporulation in *B. subtilis*, evidence a common principle for the subcellular localization of proteins in bacteria [130, 154].

Other ways to achieve protein compartmentalization have been developed by bacteria that produce protein-bounded or lipid-bounded organelles, such as lipid bodies, polyhydroxybutyrate granules, carboxysomes, gas vacuoles, magnetosomes of magnetotactic bacteria, photosynthetic membranes or internal membrane structures as found in *Planctomycetes* [104]. According to Murat et al. [104], the stalk structure itself does not classify as an prokaryotic organelle because it is basically an extension of the cell body, composed of the standard cell envelope, periplasm and cytoplasm.

1.4 Scope

Recent advances in fluorescent labeling methods and microscopic techniques have provided the molecular tools and the technical equipment to study the spatial and temporal regulation of protein localization and function in various biological contexts. This work aimed at the identification and characterization of proteins involved in two fundamental developmental events in the life cycle of *C. crescentus*: cell division and stalk formation.

Assembly and maturation of the bacterial cell division apparatus relies on the accurate timing and spatial organization of its components. The key component in these biological processes is FtsZ, which orchestrates the localization of an extensive set of cell division proteins. According to the different stages of cell division, complex protein-protein interactions need to be established, stabilized or destabilized. During these processes, FtsZ is the main target of regulatory proteins that in concert determine the dynamics of cell division. Although *C. crescentus*, *E. coli* and *B. subtilis* share a set of essential core cell division proteins, many of the accessory FtsZ modulators are narrowly distributed, suggesting that the repertoire of these regulatory proteins has been tailored to the specific physiological needs of the bacterial cell [129]. Given the unique developmental program of *C. crescentus*, the question arises what additional factors contribute to the structural or functional fine-tuning of Z-ring formation and cell division in the life cycle of this dimorphic alpha-proteobacterium.

Apart from cell division, stalk formation is another characteristic event in the life cycle of *C. crescentus*. Although different environmental and molecular cues that trigger stalk growth have been identified, the knowledge about the exact mechanism that control stalk biogenesis and morphogenesis, including the synthesis and function of crossbands, is still surprisingly limited. Moreover, an intriguing finding that continues to confound researchers is that the protein repertoire of the stalk is significantly reduced compared to the cell body [72, 163]. Recent work by Hughes et al. [68] about the stalked-confined localization dynamics of StpX has added another piece of information to the "stalk puzzle". Together, these findings suggest that the stalk is compartmentalized from the cell body. Yet, it is unclear whether a physical barrier or a stalk-specific protein targeting mechanism might explain the differences in protein content. It is therefore of great interest to study the molecular and structural mechanism underlying stalk biogenesis, morphogenesis and function.

2 RESULTS

2.1 CedX – a novel cell division protein of unknown function

In the first part of this chapter, I will describe the identification and characterization of the novel cell division protein CedX in *C. crescentus*. CedX is an inner membrane protein that localizes in an FtsZ- and FtsN- dependent manner to the cell division plane, where it interacts with FtsZ and other cell division proteins. Although I will provide several lines of evidence that CedX is a component of the *C. crescentus* divisome, the function of this protein remains unknown to date.

2.1.1 Identification and localization of CedX

In *C. crescentus*, precise localization of proteins is often linked to a specific function, which in turn is tightly regulated in time and space during the cell cycle. For instance, proteins involved in cytokinesis frequently display a characteristic midcell localization in predivisonal cells. The bacterial cell division apparatus is a multiprotein complex that, among other prerequisites, requires protein-protein interaction for divisome assembly and maturation. Such protein-protein interactions can be promoted by proline-rich proteins. Due to the unstructured nature of proline-rich regions [127], proteins of this class could function as a linker to mediate interactions of different cell division proteins during divisome assembly.

In an attempt to identify new factors involved in cell division, we examined the subcellular localization of proline-rich proteins. This localization screen turned our attention to the open reading frame *CCNA_02091* [94], which encodes a thus far uncharacterized hypothetical protein with a length of 309 amino acids and a predicted mass of 34 kDa. However, immunoblot analysis with a CCNA_02091-specific antibody demonstrated that apparent mass of the protein is about 43 kDa. Bioinformatic analyses indicate that CCNA_02091 contains a N-terminal transmembrane domain followed by a short α-helix and a proline-rich cytoplasmic tail. BLAST searches revealed that CCNA_02091 is only conserved in a few stalked alpha-proteobacteria. In addition, the genomic context of *CCNA_02091* does not provide conclusive information about a possible function. Based on the findings described in this study, CCNA_02091 was named CedX (cell division protein X).

To validate results obtained from the localization screen, I performed time-course microscopy (Fig. 7A) with synchronized *C. crescentus* cells, in which wild-type *cedX* was replaced by a *cedX-venus* gene fusion. In swarmer cells, CedX-Venus was localized as a distinct polar focus. During the swarmer-to-stalked-cell transition, the CedX-Venus signal became diffuse and disappeared from the cell pole. After 90 min, CedX-Venus started to accumulate at midcell forming a bright focus, suggesting a role of CedX in cell division.

In about 10 % of the cells, both polar and midcell localization was observed, reflecting the ongoing relocalization of the fusion protein. After completion of cell division, CedX-Venus was located at the new pole of the progeny cells, which was confirmed by time-lapse microscopy (data not shown).

The localization pattern observed for CedX-Venus raised the question whether polar CedX was actively degraded and newly synthesized at midcell. Therefore, CedX abundance *s* was determined over the cell cycle in synchronized wild-type *C. crescentu* (Fig. 7B). Immunoblot analysis of cells withdrawn throughout the time-course experiment demonstrated that CedX production was constitutive. Thus, the switch from polar to midcell localization is achieved by dynamic relocalization of existing CedX molecules.

According to bioinformatic data, CedX is predicted to be an inner membrane protein. To verify membrane localization of CedX, I performed protein fractionation experiments and found that CedX was exclusively detected in the membrane fraction of *C. crescentus* wild-type cells (Fig. 7C).

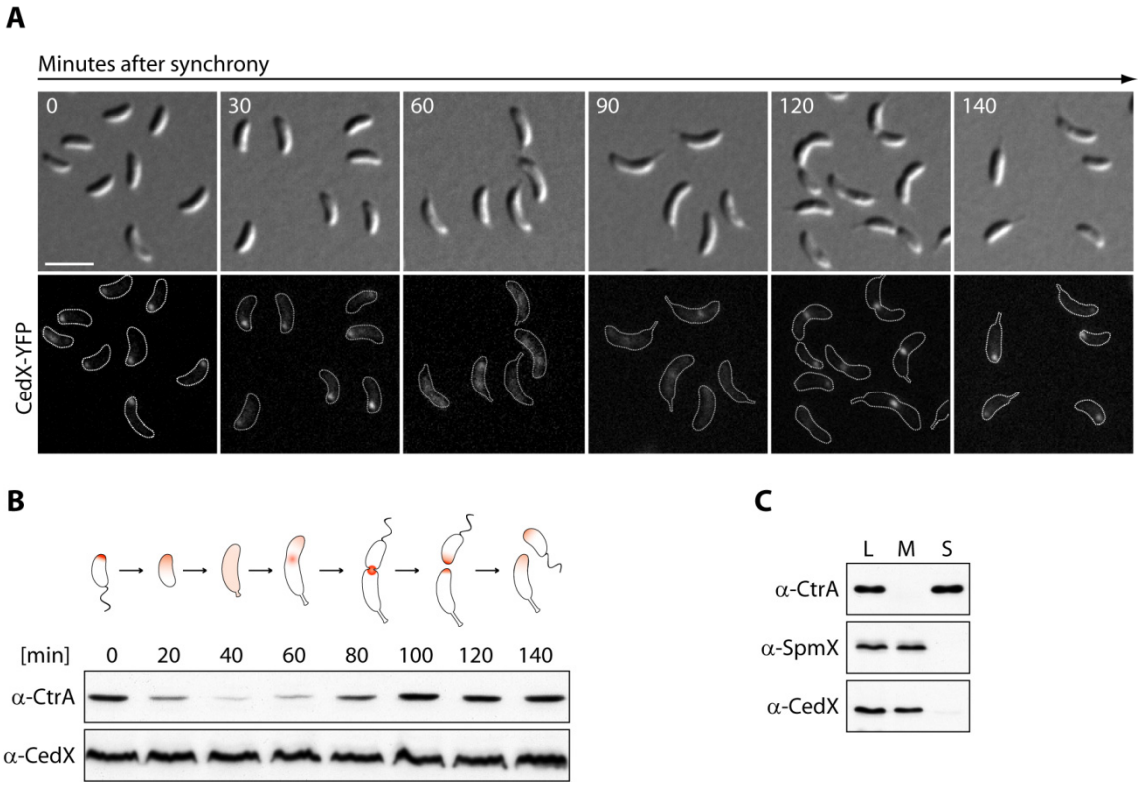

Fig. 7: Localization and abundance of CedX. (A) Cell cycle-dependent localization of CedX in synchronous *C. crescentus* cells. Swarmer cells of strain SS8 (*cedX::cedX-venus*) were grown in M2G and imaged as they progressed through the cell-cylce by DIC and fluorescence microscopy (bar: 3 µm). (B) Cell cycle-dependent abundance of CedX. Swarmer cells of wild-type *C. crescentus* (CB15N) were grown in M2G for one cell cycle. At the indicated timepoints, samples were taken from the culture and analyzed by immunoblotting using anti-CedX and anti-CtrA antiserum. The schematic illustrates the localization of CedX over the course of a *C. crescentus* cell cycle. (C) Subcellular localization of CedX. Whole cell lysate (L) of wild-type *C. crescentus* was fractionated by ultracentrifugation into membrane (M) and soluble (S) proteins followed by immunoblot analysis with anti-CedX antiserum. To control fractionation efficiency, samples of each fraction were probed for the soluble response-regulator CtrA [122] and the integral membrane protein SpmX [124].

2.1.2 CedX cellular level is critical for cell division

To investigate the function of CedX in cell division, an in-frame deletion in *CCNA_02091* was generated in *C. crescentus* wild-type cells by double homologous recombination. Mutant strains that lacked a functional copy of *cedX* did not show any phenotypic defects compared to wild-type *C. crescentus* (Fig. 8A). Although different growth conditions, such as elevated temperature, minimal medium, two-fold concentrated complex medium, or UV-stress were tested, no effect on growth rate or viability was observed in CedX-deficient cells (data not shown), indiciating that CedX is not essential under the tested conditions or fulfills a redundant function.

To rule out a role of CedX in the biogenesis of polar organelles, pili synthesis and motility were assessed in a Δ*cedX* background. First, pili synthesis was tested by incubating MT246 (Δ*cedX*) with the pili-specific *C. crescentus* phage ΦCbK [147]. Bacteriophage ΦCbK binds to polar pili in swarmer cells and causes cell lysis upon pili retraction during the swarmer-to-stalked-cell transition. Like wild-type *C. crescentus*, CedX-deficient cells were sensitive to ΦCbK infection, confirming the presence of pili (Fig. 8B). By contrast, cells that carried a deletion in the major pilin subunit gene *pilA* [147] were resistant to ΦCbK infection. Next, motility assays [148] and flagella staining [83] were performed to examine correct positioning and functionality of the flagellum (Fig. 8B). Unlike *C. crescentus* cells lacking the histidine kinase PleC, which is involved in the regulation of polar morphogenesis [167], cells that were devoid of CedX were still able to synthesize functional flagella. Moreover, polar flagella synthesis was not disturbed in these mutants.

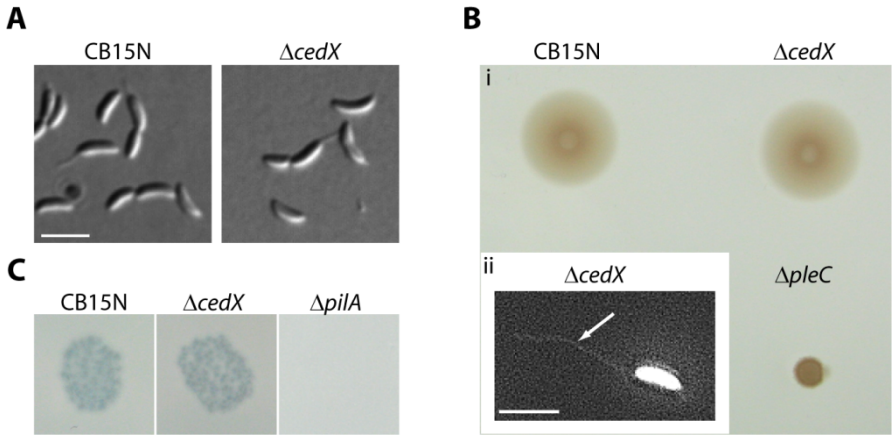

Fig. 8. Phenotypic analysis of CedX. (A) DIC images of wild-type (CB15N) and CedX-deficient (MT246) cells. (B) i, Motility assay. Exponentially-growing cells of CB15N (wild-type), MT246 (Δ*cedX*) and UJ506 (Δ*pleC*, negative control [5]) were spotted onto PYE solid media (0.3 % agar) and incubated for two days at 28 °C. ii, Flagellar staining of CedX-defiecent cells (MT246). Cells were fixed with 2.5 % paraformaldehyde, then incubated with 1.5 µg/ml DAPI to stain the flagella and imaged by fluorescence microscopy. Arrow denotes the correctly placed flagellum. (C) Test for pili biogenesis. Late exponential phase cells of wild-type *C. crescentus*, MT246 (Δ*cedX*) and LS3118 (Δ*pilA*) [147] were diluted 1:10 in soft-agar and poured onto a plain PYE agar plate. After polymerization of the soft-agar, 10 µl of ΦCbK lysate was spotted onto the plate and incubated at 28 °C for 24 h.

Previous studies in *C. crescentus, B. subtilis* and *E. coli* had shown that a stoichiometric imbalance of divisome components can disturb cell division [53, 60-61, 99-100, 102, 133, 170, 179]. Since CedX was hypothesized to be involved in cell division, I examined the effect of increased cellular CedX levels. Interestingly, overproduction of CedX from a self-replicating plasmid led to the formation of elongated cells (Fig. 9A). The observed phenotype developed rapidly in response to CedX

overproduction and was probably caused by a block in cell division. Moreover, constitutive CedX synthesis led to impaired growth due to filamentation and cell lysis (Fig. 9B).

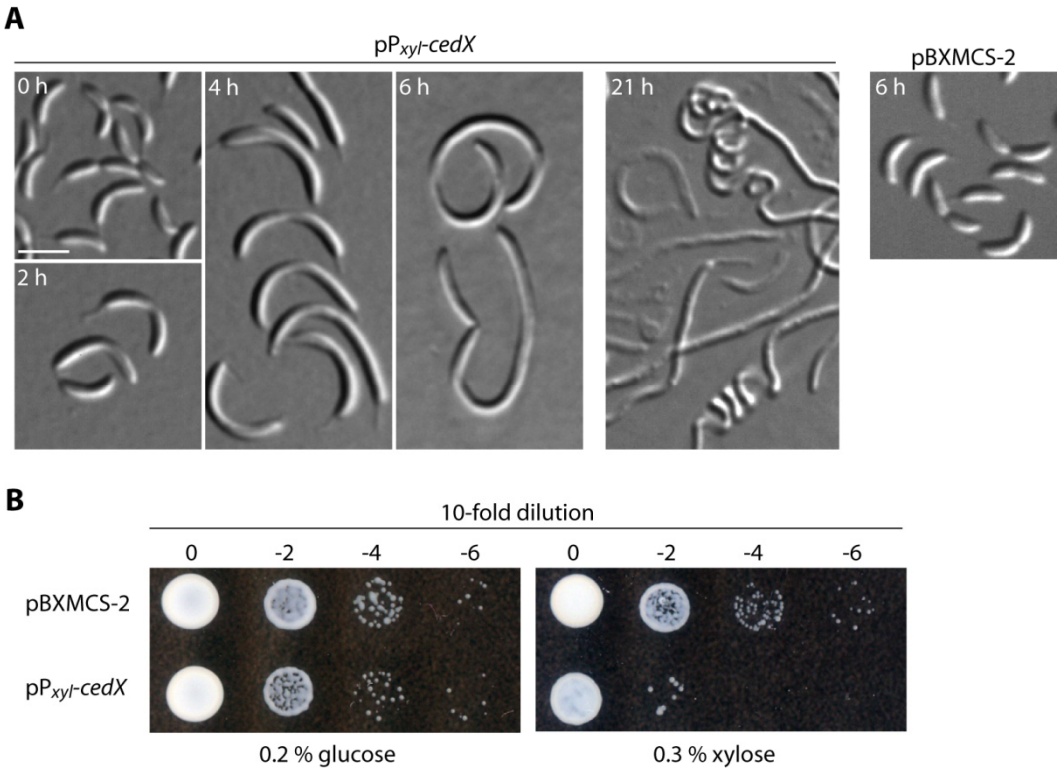

Fig. 9. Effect of CedX overproduction. (A) Filamentous growth and cell lysis induced by CedX overproduction. Cells of wild-type *C. crescentus* carrying the overproduction plasmid pMT780 (pP$_{xyl}$-*cedX,* SS2) or the empty plasmid pBXMCS-2 (SS6), respectively, were grown in PYE. CedX synthesis was induced with 0.3 % xylose. At the indicated timepoints, cells were withdrawn and imaged by DIC microscopy (bar: 3 µm). (B) Effect of CedX overproduction on cell viability. Serial dilutions of wild-type *C. crescentus* carrying the empty plasmid pBXMCS-2 (SS6) or the CedX overproduction plasmid pMT780 (pP$_{xyl}$-*cedX,* SS2) were spotted on PYE agar and incubated for two days. CedX overproduction was repressed by the addition of 0.2 % glucose and induced in the presence of 0.3 % xylose.

To further investigate the effect of increased abundance of CedX on cell division, a xylose-inducible fluorescent fusion to *cedX* was expressed from a replicating plasmid in wild-type *C. crescentus*. Surprisingly, CedX-CFP localized into several ring-like structures along the filaments after 5 h of induction. These structures resembled FtsZ rings, which prompted me to visualize FtsZ in the presence of excess CedX-CFP (Fig. 10A). Fluorescence microscopy of cells that overproduced CedX-CFP and synthesized a vanillate-inducible FtsZ-mCherry fusion clearly showed colocalization of CedX and FtsZ into multiple ring-like structures at irregular intervals along the filament. To determine whether divisome assembly was disturbed in general, I also localized FtsN in the CedX overproduction background (Fig. 10B). FtsN is the last essential cell division protein known to arrive at the division plane and it is required for the recruitment of additional factors involved in membrane invagination and peptidoglycan remodeling [30, 100]. In the presence of excess CedX, FtsN was found to localize in a similar pattern as FtsZ, forming multiple rings within the filaments that colocalized with CedX-Venus foci. To exclude that constitutive overproduction of a membrane protein is detrimental to the cell per se, I also performed overproduction experiments with truncated CedX mutant proteins. These CedX mutant derivatives did not cause the observed cell division phenotype (see below, Fig. 12B).

Taken together, the observed phenotype may be caused either by direct or indirect interference of CedX with the cell division apparatus. Filaments caused by CedX overproduction showed only rarely membrane constrictions at the site of FtsZ or FtsN localization, suggesting that Z-rings are stabilized and/or divisome disassembly and completion of cytokinesis was blocked.

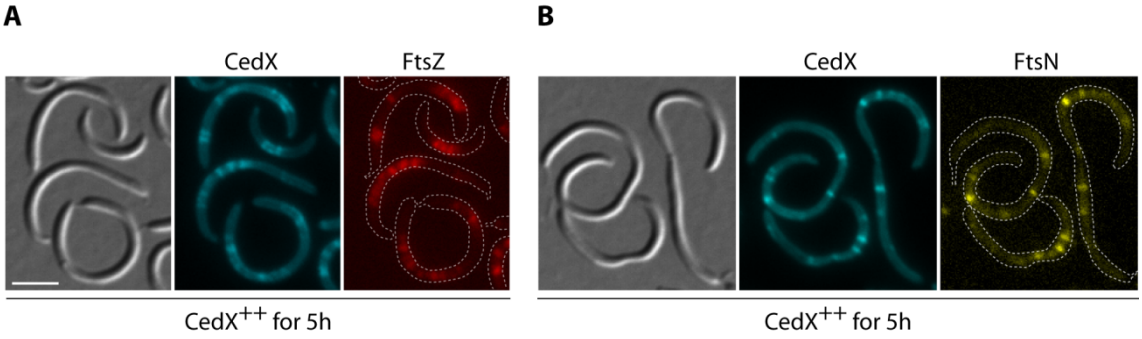

Fig. 10. Effect of CedX overproduction on the localization of FtsZ and FstN. (A) Localization of FtsZ after 5 h of CedX-CFP overproduction ($CedX^{++}$) in strain SS112 (P_{van}::P_{van}-*ftsZ-mcherry* pP_{xyl}-*cedX-cfp*). Two hours before analysis, expression of *ftZ-mcherry* was induced with 0.5 mM vanillate. CedX-CFP synthesis was induced by addition of 0.3 % xylose. Cells were analyzed by DIC and fluorescence microscopy. (B) Localization of FtsN after 5 h of CedX-Venus overproduction ($CedX^{++}$) in strain SS17 (*ftsN::cfp-ftsN* pP_{xyl}-*cedX-venus*). Cells were analyzed by DIC and fluorescence microscopy. Note that fluorescence images are false-colored (bar: 3µm).

2.1.3 Searching for a CedX interaction partner

To identify a possible interaction partner of CedX, coimmunoprecipitation (Co-IP) followed by mass spectrometric (MS) analysis of co-purified proteins was carried out. Mass spectrometry was performed in collaboration with J. Kahnt and L. Søgaard-Andersen (Dept. of Ecophysiology, MPI Marburg). For this purpose, a *C. crescentus* strain that produced a CedX-HA (hemagglutinin) derivative was generated. Owing to the low expression of *cedX* from its native promoter [96], *cedX-HA* was placed under the control of the xylose-inducible promoter and expressed from a self-replicating plasmid in a *ΔcedX* background. Transient protein-protein interactions were stabilized by crosslinking with paraformaldehyde prior to immunoprecipitation, which was carried out with cell extract of wild-type *C. crescentus* in parallel to control for unspecific binding to the HA-affinity beads.

In total, three independent Co-IP experiments were performed in which FtsZ, FtsK, FtsL, FtsQ, FtsN, FzlC, TolR and TipN were copurified at least once. Interaction of CedX with FtsZ and FtsN was confirmed by immunoblot analysis after coimmunopreciptation (Fig. 11A). In addition, several hypothetical proteins were detected by MS. Assuming that interaction with CedX requires subcellular colocalization, direct interaction partners of CedX should also show polar and/or midcell localization in *C. crescentus*. Therefore, 24 of the identified hypothetical proteins were fused to the red fluorescent protein mCherry and examined for their localization *in vivo*. None of these protein fusions displayed a similar localization pattern as CedX. In addition, deletion of five of these proteins in combination with *cedX* did not yield a visible phenotype in *C. crescentus* (data not shown) suggesting that these copurified proteins do not specifically interact with CedX.

In *C. crescentus*, several cell division proteins have been described to cause only minor cell division defects upon deletion. To exclude that CedX shares an overlapping function with either of these proteins, I generated *C. crescentus* strains that carried a double deletion mutation in CedX in combination with a) the FtsZ-stabilizing protein ZapA [58], b) the FtsZ-interacting, bifunctional

oxidoreductase homolog KidO [123], c) the polarity factor and late cell division protein TipN [69], [83] and d) the FtsZ-interacting protein FzlC [54]. In addition, localization of fluorescent protein fusions to ZapA, KidO, TipN, FzlC and TolA, a protein involved in septal membrane invagination [50], were examined in Δ*cedX* cells. Neither of the combinations examined gave rise to an enhanced phenotype or disturbed localization of the fluorescent fusion proteins compared to wild-type background (data not shown), indicating that CedX is not functionally redundant with the tested cell division proteins.

To further validate identified protein interactions, I examined whether CedX can interact with known divisome components in a bacterial adenylate cyclase two-hybrid (BACTH, Fig. 11B) assay [78]. This assay is based on the reconstitution of the catalytic domain of *Bordetella pertussis* adenylate cyclase, which has been split into a T18 and T25-fragment. Functional complementation is achieved when two putative interacting proteins, genetically fused to either the T18 or the T25 fragment, physically interact. Interaction leads to cAMP synthesis, which in turn triggers the expression of catabolic genes, e.g. for the degradation of maltose. Activation of the *mal* regulon yields red colonies, whereas no interaction between the target proteins produces white colonies on indicator plates. As suggested by coimmunoprecipitation, CedX strongly interacts with itself, FtsN, FtsL and TolR. Additionally, CedX physically contacts TolA and ZapA (Fig. 11A), albeit interaction with ZapA was only detected in one configuration. No interaction was observed with FtsK and FtsI (data not shown). The detected interaction between CedX and TipN was only weak and presumably does not reflect a functional relationship, which is in agreement with previous experiments (see above). During BACTH experiments it was found that FtsZ did not show any interaction with either itself or with other cell division proteins. The reason for this may be due to the conserved function of FtsZ among bacteria. *C. crescentus* FtsZ hybrid moieties could interact with *E. coli* FtsZ molecules and thereby become unavailable for the interaction with their cognate BACTH partner. A similar observation was reported for FtsA hybrid analysis by Karimova and co-workers [77]. Also, the T18 or T25 fragment itself may interfere with FtsZ interaction.

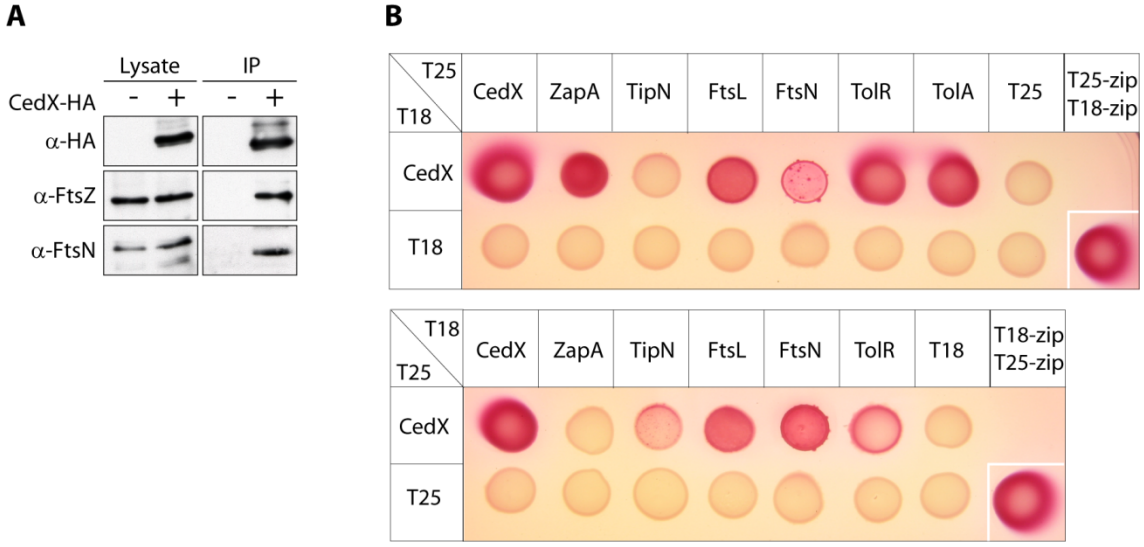

Fig. 11. CedX interaction studies. (A) Coimmunoprecipitation analysis with lysates of wild-type *C. crescentus* and strain SS48 (cedX::*ced-HA* pP$_{xyl}$-*cedX-HA*). CedX-HA was precipitated using anti-HA-affinity beads. Coprecipitated proteins were probed with anti-HA, anti-FtsZ and anti-FtsN serum. (B) Bacterial two-hybrid analysis. *E. coli* BTH101 reporter strain was transformed with plasmids encoding fusions of the T25 and T18 fragments of *Bordetella pertussis* adenylate cyclase to CedX and the listed proteins or the yeast GCN4 leucin-zipper region (zip) as a positive control. Transformants were grown in LB media and spotted onto MacConkey agar supplemented with 1 % maltose. Interaction between the two adenylate cyclase fragments is indicated by the formation of red colonies.

Although interaction of CedX with TipN was previously indicated by Co-IP/MS studies, the results of the deletion and localization studies as well as the reported functions of TipN as a cell polarity factor [69, 83], do not support functionally overlapping roles for TipN and CedX. Nevertheless, Co-IP/MS results and BACTH analyses demonstrate direct interaction of CedX with several components of the cell division apparatus, in particular late cell division proteins. However, the exact role that CedX plays during these interaction remains to be elucidated.

Functional characterization of a non-essential protein is complicated by the lack of a phenotype under normal growth conditions. Although several lines of evidence suggest that CedX is part of the divisome, the exact function of CedX cannot be deduced from these results. Since overproduction of CedX inhibits cell division, we decided to perform a screen for suppressor mutants that could tolerate high levels of CedX-CFP and thereby provide information about the specific target of CedX interaction. For this purpose, *C. crescentus ΔcedX* cells were first mutagenized by UV light and then transformed with the xylose-inducible CedX-CFP overproduction plasmid as described by Radhakrishnan et al. [123]. Suppressor mutants arose readily on PYE agar supplemented with xylose, even without UV treatment. 96 potential mutant strains were isolated and assessed by fluorescence microscopy to check for CedX-CFP production and localization, respectively. About 1/3 of the mutants had lost the CedX-CFP signal and were dismissed from further analyses, whereas the remaining 2/3 of the isolated mutants showed normal, diffuse or wild-type-like CedX localization (data not shown). To rule out suppressor mutations that had been acquired in the introduced plasmid, the CedX-CFP protein level was determined in 40 mutants by immunoblot analysis. In addition, the absence of mutantions in the plasmid-borne *cedX* gene was confirmed by sequence analysis for 10 of these strains (data not shown). Based on the CedX interaction studies, we speculated that a suppressor mutation in one of the cell division proteins may circumvent CedX overproduction. Therefore, genomic DNA of ten authentic mutant strains was purified, and for each strain *ftsZ*, *ftsA*, *ftsK*, *ftsL*, *ftsQ*, *ftsW*, *ftsE*, *ftsN*, *zapA* and *tipN* were sequenced. However, no suppressor mutation could be identified in any of these genes suggesting that a modification of a yet unknown factor may allow *C. crescentus* to escape division inhibition by excess cellular CedX.

2.1.4 Functional analysis of CedX

To identify structural domains of CedX that are required for midcell localization and blocking cell division, I performed a functional analysis of mutant CedX proteins (Fig. 12). For this purpose, CedX derivatives were fused to the fluorescent proteins CFP or Venus and produced from a plasmid-borne gene under the control of a xylose-inducible promoter in a Δ*cedX* background. The size and integrity of the fusions were verified by immunoblot analysis (Fig. 12C). *C. crescentus* cells overproducing full-length CedX, consisting of the transmembrane (TM) domain and the proline-rich C-terminal tail, displayed the characteristic cell division phenotype and CedX localization pattern. Removal of the C-terminal part, which is not part of the proline-rich region, did not suppress the CedX overproduction phenotype. By contrast, deletion of the TM domain or the proline-rich segment rendered the protein non-functional. Cells that synthesized the soluble $CedX_{\Delta 1\text{-}32}$ derivative showed diffuse cytoplasmic fluorescence. However, in some predivisional cells, $CedX_{\Delta 1\text{-}32}$-Venus accumulated at midcell indicating that this mutant protein can still interact with the divisome, albeit inefficiently.

By contrast, CedX derivatives lacking the proline-rich region failed to produce polar or midcell foci and instead showed diffuse membrane localization. These findings suggest that the transmembrane anchor and the proline-rich regions are essential for localization and protein-protein interaction.

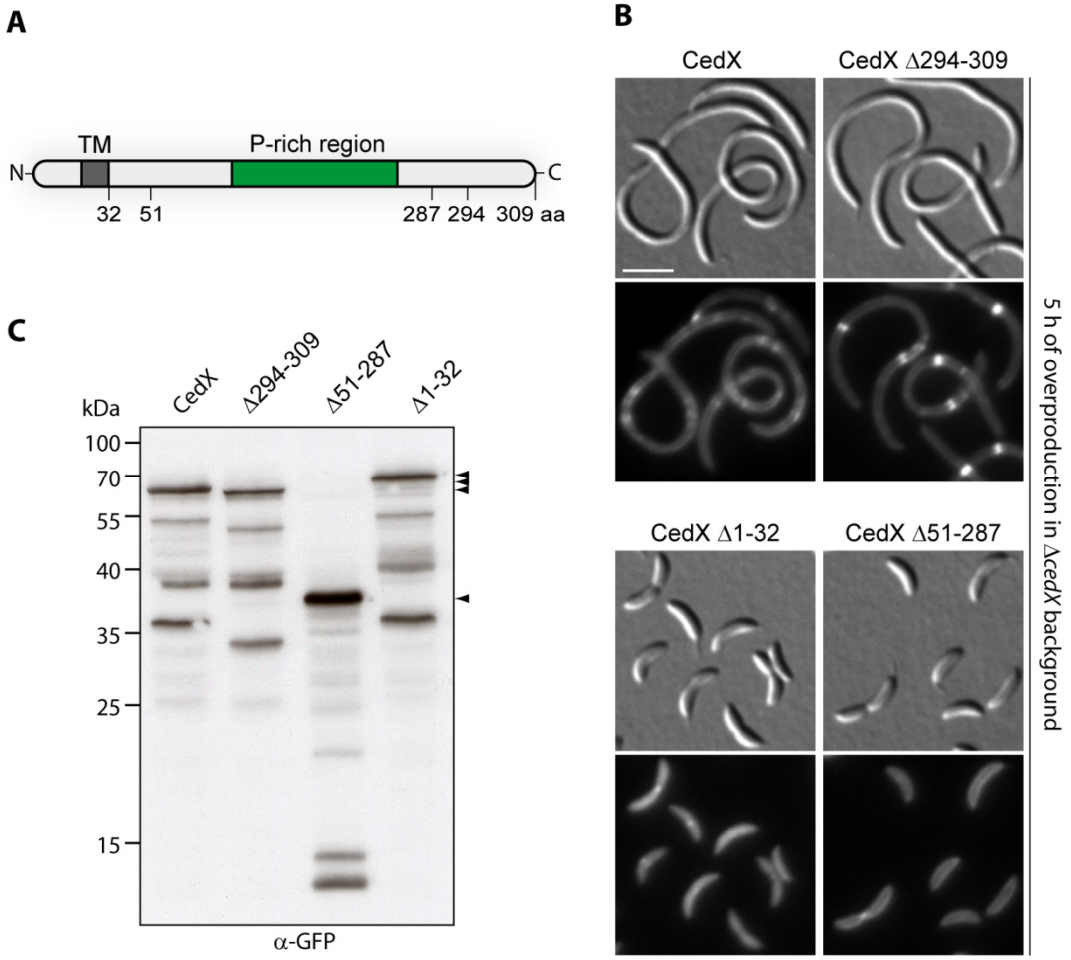

Fig. 12. Functional analysis of CedX mutant derivatives. (A) Schematic representation of CedX. The transmembrane domain (TM) and the proline-rich region (P-rich) are shown in grey and green, respectively. Numbers refer to the position of amino acid (aa) residues to indicate the site of deletions in CedX. (B) Subcellular localization and functionality of CedX mutant derivatives fused to Venus in the *ΔcedX* mutant background. Strains SS113 (pP_{xyl}-*cedX-cfp*), SS63 (pP_{xyl}-*cedX*$_{\Delta 294-309}$-*venus)*, SS49 (pP_{xyl}-*cedX*$_{\Delta 1-32}$-*venus*) and SS65 (pP_{xyl}-*cedX*$_{\Delta 51-287}$-*venus)* were grown in PYE containing 0.3 % xylose for 5 h and visualized by DIC and fluorescence microscopy (bar: 3 µm). (C) Stability of CedX-Venus mutant derivatives in the *ΔcedX* mutant background. Strains SS113 (pP_{xyl}-*cedX-cfp*), SS63 (pP_{xyl}-*cedX*$_{\Delta 294-309}$-*venus)*, SS49 (pP_{xyl}-*cedX*$_{\Delta 1-32}$-*venus*) and SS65 (pP_{xyl}-*cedX*$_{\Delta 51-287}$-*venus)* were grown in PYE containing 0.3 % xylose. After 5 h of induction, samples were withdrawn from the culture and subjected to immunoblotting using anti-GFP serum. Arrow heads indicate the expected molecular masses oft he different proteins.

2.1.5 CedX is a late cell division protein

The Z-ring provides the scaffold for the localization of downstream divisome components. Without FtsZ the divisome fails to assemble, which blocks cell division and causes filamentous growth. To test whether CedX is part of the divisome and thus requires FtsZ for midcell localization, I investigated the effect of FtsZ depletion on CedX localization (Fig. 13A). For this purpose, a copy of *cedX-venus* was ectopically introduced into a conditional *ftsZ* mutant strain. When depleted of FtsZ, CedX was dispersed within the filaments. After 40 min of restoration of FtsZ

synthesis, constriction sites appeared, identifying future sites of cell division. Concurrently, CedX accumulated at the sites of constriction and formed clearly visible foci.

Next, I examined whether the CedX localization behavior is also dependent on the late cell division protein FtsN (Fig. 13B). Therefore, *cedX-venus* was expressed ectopically in a conditional *ftsN* mutant strain. Again, after depletion of FtsN, CedX-Venus was completely dispersed in the cell. It should be noted that under conditions of FtsN depletion, midcell localization of other divisome components, such as FtsZ, FtsA, FtsK and FtsI is still ensured [100]. Taken together, CedX localization requires FtsZ and FtsN, suggesting that CedX is indeed a cell division protein.

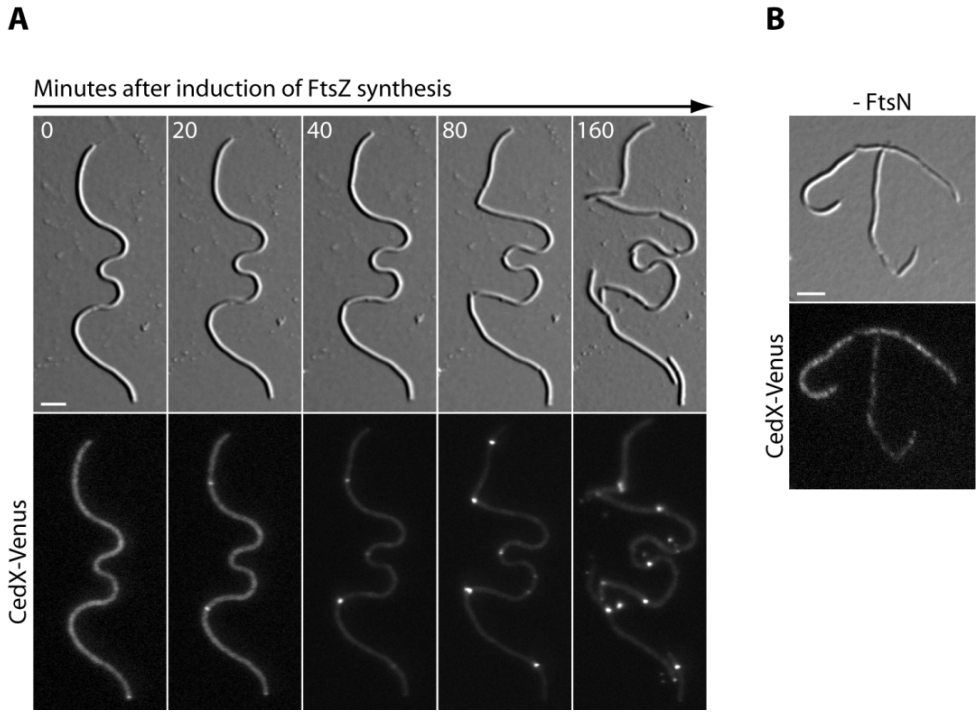

Fig. 13. Localization of CedX is dependent on FtsZ and FtsN. (A) Dependence of CedX localization on FtsZ. Strain SS37 (*ftsZ*::P_{xyl}-*ftsZ*, P_{van}::P_{van}-*cedX-venus*) was grown in PYE supplemented with 0.3 % xylose to mid-exponential phase. Cells were washed and depleted of FtsZ by incubation in PYE without xylose for another 8 h. CedX-Venus production was induced with 0.5 mM vanillate 2 h prior to analysis. Cells were mounted on a 1 % M2G agarose pad supplemented with 0.3 % xylose to initiated FtsZ synthesis and visualized by DIC and fluorescence microscopy at the indicated timepoints. (B) Dependence of CedX localization on FtsN. Strain SS20 (*ΔvanA ΔftsN* P_{van}::P_{van}-*ftsN* P_{xyl}::P_{xyl}-*cedX-venus*) was grown in PYE supplemented with 0.5 mM vanillate to mid-exponential phase. Cells were washed and depleted of FtsN by incubation in PYE without vanillate for another 15 h. CedX-Venus production was induced with 0.3 % xylose 1 h prior to analysis. Cells were visualized by DIC and fluorescence microscopy (bar: 3 µm).

Based on the findings from the FtsZ/FtsN depletion studies, CedX may be part of the late cell division complex, which requires FtsN for localization. To gain information on the timing of CedX recruitment to the divisome, I analyzed the localization dynamics of CedX and compared it to those of FtsZ, FtsA and FtsN in synchronized cells using time-course microscopy (Fig. 14). FtsZ midcell localization was observed after 45 min in more than 80 % of the cells, followed by FtsA after 90 min. Both CedX and FtsN accumulation peaked at 120 min. The localization dynamics of FtsZ, FtsA and FtsN are in agreement with previously published data [100]. Furthermore, this analysis provides evidence that CedX is a late recruit to the divisome.

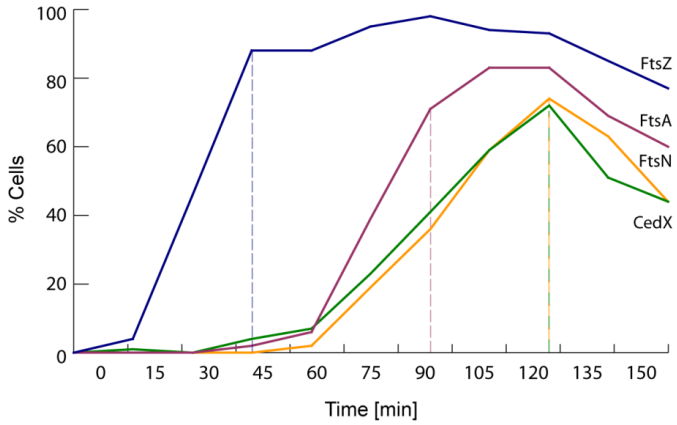

Fig. 14. Timing of CedX midcell localiziation. Strains SS10 (*cedX*::*cedX-mCherry* P_{van}-*ftsZ-venus*), SS38 (*ftsN*::*cfp-ftsN* P_{xyl}::P_{xyl}-*cedX-venus*), SS56 (*cedX*::*cedX-mcherry* P_{xyl}-*venus-ftsA*) were grown in M2G to mid-exponential phase. One hour before synchronization, fluorescent fusions were induced by addition of either 0.3 % xylose or 0.5 mM vanillate. Isolated swarmer cells of these strains were resuspended in M2G supplemented with 0.3 % xylose or 0.5 mM vanillate. The localization of the respective protein fusions was visualized in 15 min intervals using DIC and fluorescence microscopy. The graph shows the number of cells that displayed midcell localization of the respective fusion protein as a function of the cell cycle. The dashed lines denote the timepoint at which at least 70 % of the cells showed midcell localization of the respective protein fusion. At least 100 cells were analyzed per timepoint.

Recently, Goley at al. [54] reported that the localization of FtsZ-binding proteins to the divisome can be enhanced by exploiting the overexpression phenotype of the *ftsZ-G109S* mutation. This mutation causes a reduced FtsZ GTPase activity that leads to the accumulation of stable FtsZ filaments and the formation of extended constriction within the cell body. The authors demonstrated that only proteins that directly interact with FtsZ localized to the constrictions.

To test whether CedX directly interacts with FtsZ, CedX localization was visualized in a strain that overproduced FtsZ-G109S (Fig. 15). Fluorescence microscopy of the mutant strain clearly showed colocalization of CedX with the extended constriction sites. This observation implies that CedX directly interacts with FtsZ and supports our hypothesis that CedX is part of the divisome.

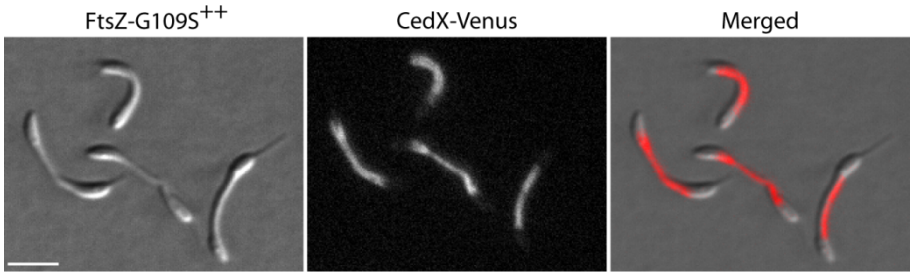

Fig. 15. CedX localizes to constrictions caused by overproduction of the FtsZ-G109S mutant derivative. Cells of strain SS148 (P_{xyl}::P_{xyl}-*cedX-venus* pP_{xyl}-*ftsZ-G109S*) were cultured in PYE to mid-exponential phase. Synthesis of FtsZ-G109S and CedX-Venus was induced with 0.3 % xylose for 3 ½ h and analyzed by DIC and fluorescence microscopy. Note that xylose-induced synthesis of CedX-Venus from the chromosomal P_{xyl}-promoter for 3 ½ h does not cause the previously described CedX overproduction phenotype (data not shown) (bar: 3 µm).

2.2 Crossband formation and stalk compartmentalization

In the second part of this chapter, I will describe the identification and characterization of the so-called stalk proteins StpABCD. I will provide evidence that these four proteins form multiprotein complexes that constitute crossbands, which act as periplasmic diffusion barriers and physically separate the stalk and the cell body.

2.2.1 Identification of StpAB

The *C. crescentus* cell cycle produces two morphological distinct daughter cells with different cell fates. Whereas the stalked cell can immediately enter a new round of replication, the newborn swarmer sibling has first to differentiate into a stalked-cell in order to become replication competent. This swarmer-to-stalked-cell transition is an obligatory and irreversible checkpoint in the developmental program during which stalk outgrowth is initiated. The stalk is an extension of the cell envelope that is segmented at irregular intervals by so-called crossbands. These disk-like structures are believed to consist of peptidoglycan and to fulfill a stabilizing function [74, 139].

To identify proteins that are involved in stalk biogenesis and morphogenesis, we focused on open reading frames that were transcriptionally upregulated during the swarmer-to-stalked-cell transition [96]. Candidate genes were fused to *mcherry* and ectopically expressed from the xylose-inducible promoter in *C. crescentus*. The resulting strains were examined for localization of the fluorescent protein fusion to the stalked pole. This screen led to the identification of the two thus far uncharacterized proteins CCNA_02562 and CCNA_02561 [94], now designated stalk protein A (StpA) and stalk protein B (StpB), respectively. StpA has a molecular mass of 59.1 kDa and is encoded immediately upstream of StpB, which has a predicted mass of 50.5 kDa.

In general, *C. crescentus* is cultured in a phosphate-rich, complex medium (PYE). Using this medium, ectopically produced StpA-mCherry and StpB-mCherry were found to specifically localize to the stalk (Fig. 16A). To better visualize the subcellular localization of StpA and StpB, cells were cultured in low-phosphate medium (M2G^{-P}), which triggers elongation of the stalk [55]. Interestingly, in elongated stalks, StpA and StpB localized in distinct foci along the length of the stalk, which resembled the distribution of crossbands. In addition, it was found that the characteristic crossband-like localization pattern of StpA-mCherry was maintained in a *ΔstpB* background, whereas normal StpB-mCherry localization was dependent on StpA (Fig. 16B). In the majority of the Δ*stpA* cells I observed bright StpB foci in the cell body and only a few cells showed single StpB foci in the stalk suggesting that StpB stability could be controlled by StpA or StpB molecules are randomly targeted to the stalk and aggregate upon accumulation in the cell body.

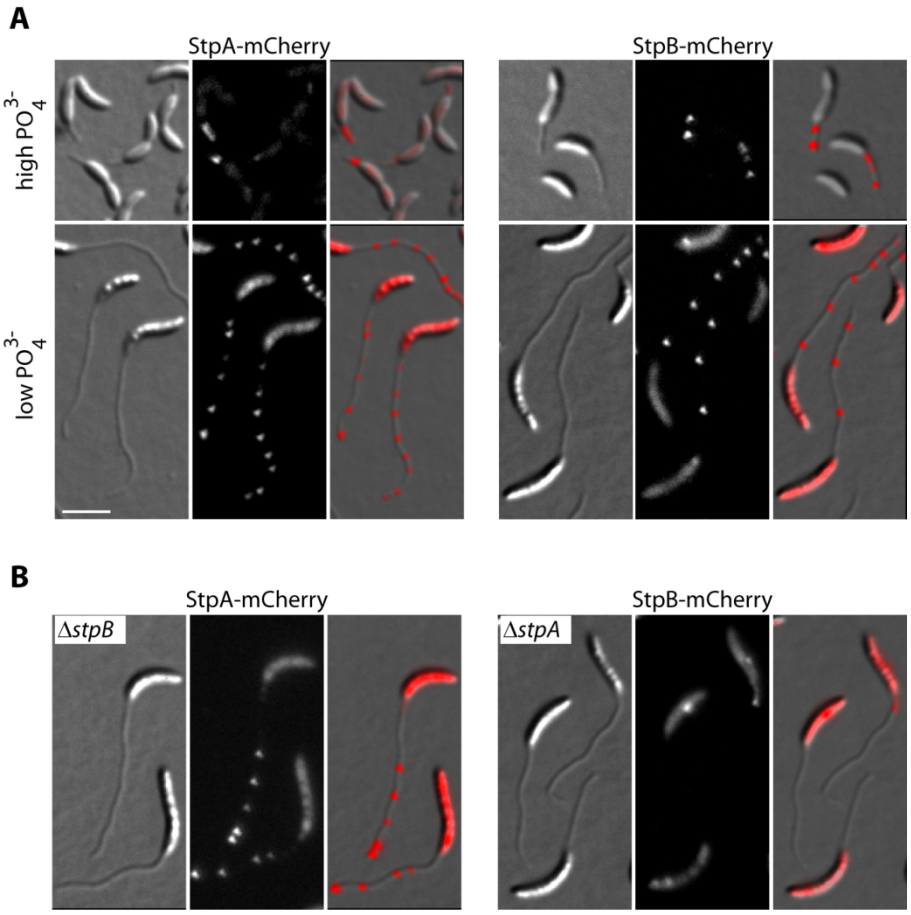

Fig. 16. Identification of StpAB. (A) Localization of StpA and StpB in live cells. Cells of strain SW30 (P_{xyl}::P_{xyl}-*stpB-mcherry*) and SW33 (P_{xyl}::P_{xyl}-*stpA-mcherry*) were grown overnight in PYE or $M2G^{-P}$ medium that contained 0.3 % xylose. Cells were visualized by DIC and fluorescence microscopy. (B) Loss of the stalk-specific localization of StpB without StpA. Strain SS141 (*ΔstpA* P_{xyl}::P_{xyl}-*stpB-mcherry*) and SS142 (*ΔstpB* P_{xyl}::P_{xyl}-*stpA-mcherry*) were cultured overnight in $M2G^{-P}$ medium supplemented with 0.3 % xylose and imaged by DIC and fluorescence microscopy (bar: 3 µm).

2.2.2 StpAB are specifically sequestered to the stalk periplasm

Bioinformatic analysis indicated that StpA is an inner membrane protein with three Sel1-like tetratricopeptide repeat sequences, which fold into a structural motif reported to mediate protein-protein interactions [15]. StpB is supposed to be a soluble periplasmic protein.

To confirm the predicted localization of StpA and StpB, protein fractionation of wild-type *C. crescentus,* in which the native copy of *stpB* was replaced by a *stpB-His* fusion, was performed (Fig. **17**A). Whereas StpA exclusively co-sedimented with the cell membranes, StpB was detected in both the membrane and soluble fraction. However, StpB was rendered soluble in StpA-deficient cells. This finding supports the earlier observation that StpA acts as a recruitment factor for StpB (Fig. 16B) and suggests a physical interaction that tethers a certain number of StpB molecules to the membrane.

Direct interaction of StpA and StpB would require that the C-terminus of StpA is oriented to the periplasm. To clarify the membrane topology, I constructed a C-terminal gene fusion of *stpA* and *stpB,* respectively, to the TEM-1 β-lactamase gene (*bla*). In order to confer resistance to β-lactam

antibiotics, such as ampicillin, β-lactamases need to be translocated into the periplasm. The respective gene fusion was placed under the xylose-inducible promoter in the β-lactam-sensitive strain CS606 [173]. Expression of both *stpA-bla* and *stpB-bla* restored resistance to ampicillin to CS606, demonstrating that StpA and StpB are targeted to the periplasm (Fig. 17B).

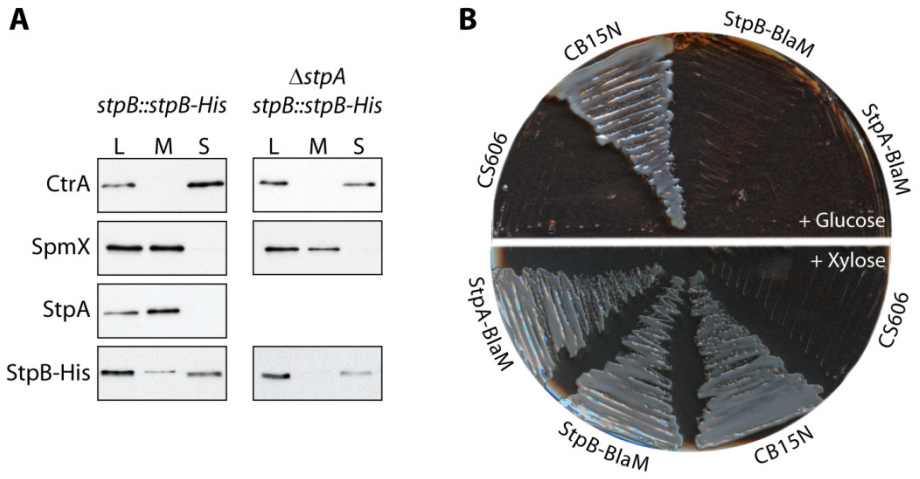

Fig. 17. Subcellular localization and membrane topology of StpA and StpB. (A) Subcellular localization of StpA and StpB. Whole cell lysates (L) of SS233 (*stpB*::*stpB-His*) and SS220 (*ΔstpA stpB*::*stpB-His*) were fractionated into membrane (M) and soluble (S) proteins followed by immunoblot analysis with anti-StpA and anti-His antiserum. To control fractionation efficiency, samples of each fraction were probed for the soluble response-regulator CtrA [122] and the integral membrane protein SpmX [124]. (B) Membrane topology of StpA and StpB. Cells of CB15N (wild-type), CS606 (Δ*bla*), SS165 (Δ*bla* P_{xyl}::P_{xyl}-*stpB-bla*) and SS172 (Δ*bla* P_{xyl}::P_{xyl}-*stpA-bla*) were patched onto PYE agar supplemented with 50 µg/ml ampicillin containing either 0.2 % glucose or 0.3 % xylose.

Next, I explored whether StpA and StpB synthesis correlated with the onset of stalk outgrowth. Therefore, the molecular abundance of StpA and StpB was monitored over the cell cycle in wild-type *C. crescentus,* in which the endogenous *stpB* gene was replaced by a *stpB-His* fusion (Fig. 18A). In agreement with microarray data [96], both proteins accumulated during the swarmer-to-stalked cell transition. Notably, StpA was completely absent in swarmer cells, which begs the question whether StpA is actively degraded at the beginning of the developmental cycle. To address this question, I examined the protein stability in cells that carried a xylose-inducible copy of *stpA* in a *ΔstpA* background. Immunoblot analysis demonstrated that StpA was stable in isolated swarmer cells (Fig. 18B), supporting the notion that StpA synthesis is regulated at the transcriptional level [85]. Additionally, I determined the cell cycle-dependent localization of StpB-mCherry produced from its native promoter in wild-type *C. crescentus* by time-course microscopy (Fig. 18C). Whereas no StpB-mCherry fluorescence signal was observed in swarmer cells, a polar StpB-mCherry focus formed between the 60 and 90 min timepoint, a period after which stalk outgrowth has already been initiated. Notably, when stalked cells were separated from newborn swarmer cells after completion of the cell cycle by density centrifugation and allowed to progress through another division cycle, a second StpB-mCherry focus appeared at the stalked pole after 60 min (Fig. 11C). By contrast, isolated newborn swarmer cells did not display polar StpB foci initially. Taken together these findings suggest that StpA and StpB synthesis require the developmental transition into a stalked cell.

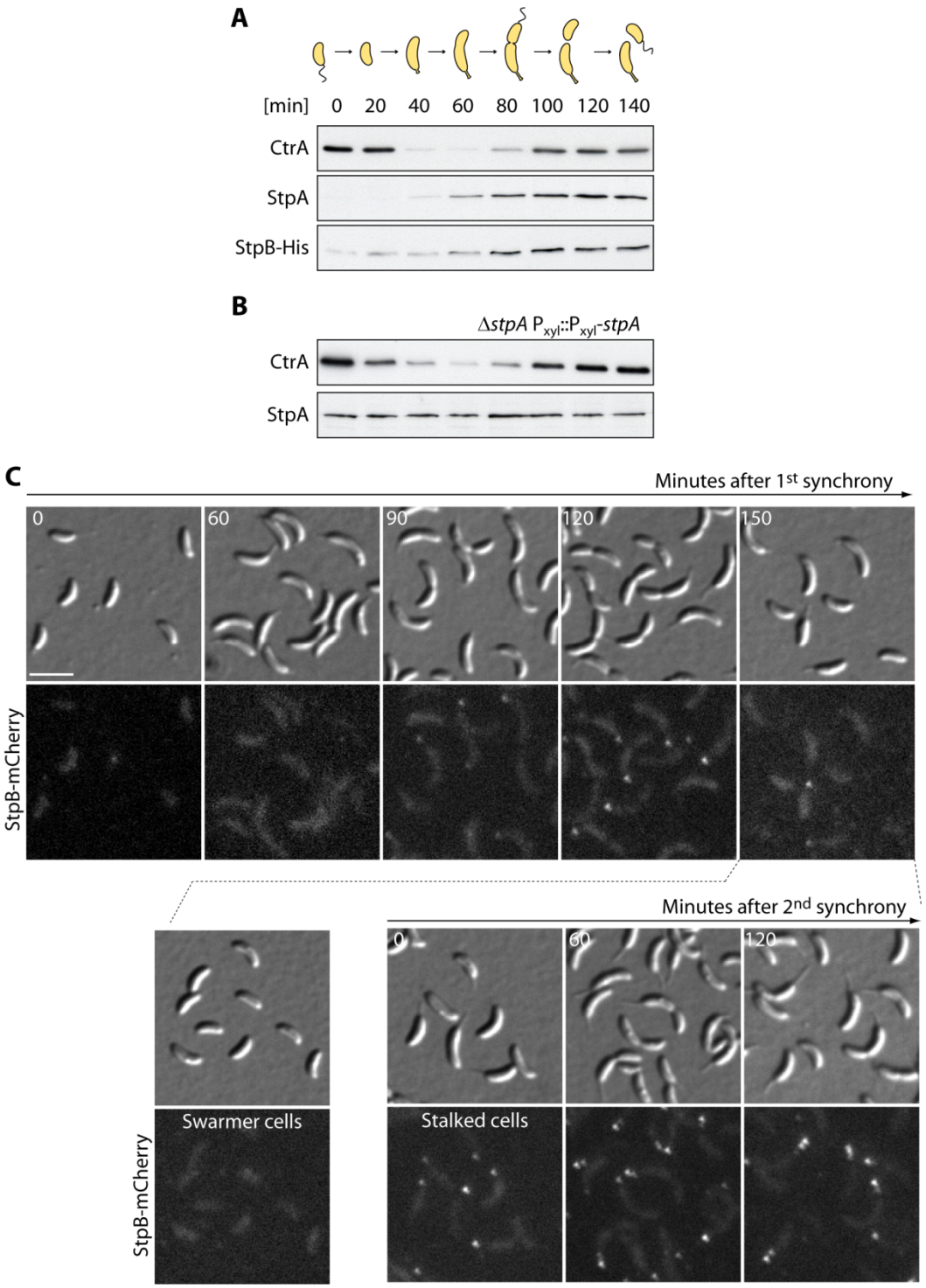

Fig. 18. StpA and StpB are cell cycle-regulated. (A) Cell cycle-dependent abundance of StpA and StpB. Swarmer cells of strain SS233 (*stpB*::*stpB-His*) were grown in M2G for one cell cycle. Samples were taken from the culture in 20 min intervals and probed with anti-CtrA, anti-StpA and anti-His antiserum. The schematic illustrates the different morphological stages of the cell cycle. (B) StpA is not actively degraded in swarmer cells. Exponentially growing cells of strain SS189 (Δ*stpA Pxyl*::*Pxyl-stpA*) were induced with 0.3% xylose 1 h prior to synchronization. Isolated swarmer cells were transferred to M2G without inducer. StpA protein levels were monitored in 20 min intervals and analyzed by immunoblotting using anti-CtrA and anti-StpA antiserum. (C) Cell cycle-dependent localization of StpB. Isolated swarmer cells of strain SS160 (*stpB*::*stpB-mcherry*) were grown in M2G for one cell cycle. At the indicated timepoints, cells were visualized by DIC and fluorescence microscopy. After completion of the first cell cycle, stalked cells were isolated from the culture and allowed to progress through a second cell cycle. Swarmer siblings from the first cell cycle lacked a StpB-mCherry signal at the beginning of the new cycle. Cells were imaged at the indicated timepoints (bar: 3 µm).

2.2.3 Crossband formation requires StpAB

The crossband-like localization pattern of StpAB in live cells suggested a role of the proteins in stalk morphogenesis and encouraged us to analyze the stalk ultrastructure by electron microscopy and electron cryo-tomography (Fig. 19). Intriguingly, both methods revealed that StpAB-deficient cells consistently lack crossbands. In addition, a deletion of either *stpA* or *stpB* was sufficient to abolish crossband synthesis (data not shown).

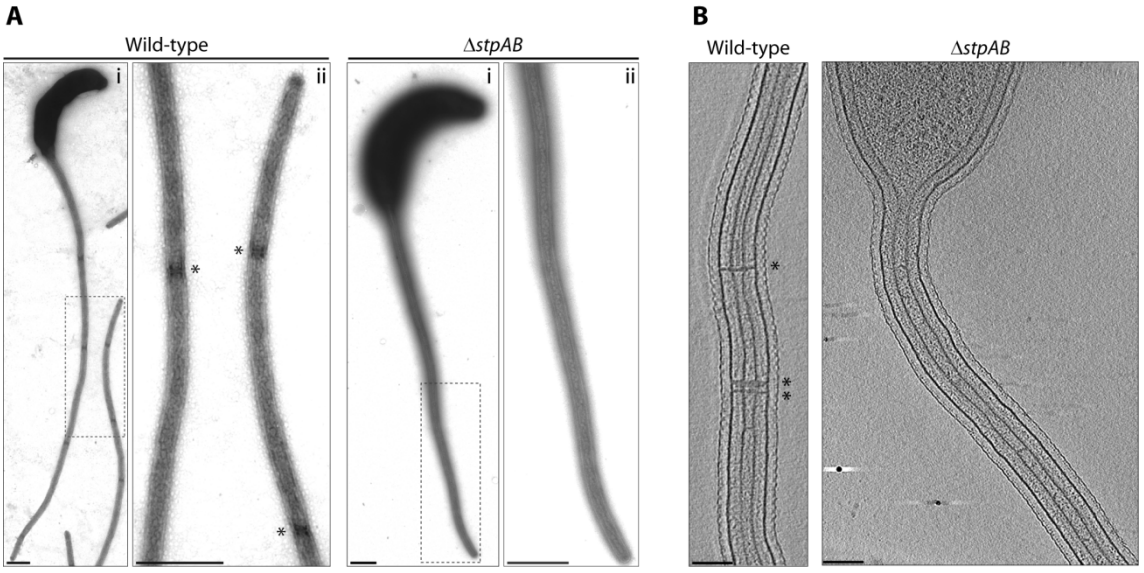

Fig. 19. StpAB-deficient cells lack crossbands. (A) Electron microscopy of wild-type *C. crescentus* and strain SW51 (Δ*stpAB*). Cells were grown in M2G^{-P}, contrasted with uranylacetate and analyzed. The dashed rectangle in (i) indicates the magnified region in (ii). Asterisks denote crossbands (bars: 500 nm). Images were taken in collaboration with K. Bolte (Dept. of Biology, Philipps University, Marburg). (B) Electron cryo-tomography of wild-type *C. crescentus* and SW51 (Δ*stpAB*) after growth in PYE. The images show a longitudinal section of the stalk. Images were taken by A. Briegel (CalTech, USA). Asterisks denote crossbands (bars: 100 nm).

The investigation of crossbands is complicated by the fact that crossbands are only discernible by electron microscopy. Thus, I was wondering whether one could take advantage of the distinct StpB-mCherry localization to study the role of StpAB in crossband formation.

To address this question, I determined the number of StpB-mCherry foci and crossbands per μm stalk in *C. crescentus* cells visualized by fluorescence and electron microscopy, respectively (Fig. 20). From the analyzed electron micrographs of wild-type cells (n=68 cells), I deduced that one crossband is inserted every 2.5 μm of the stalk. This distribution correlates with the spacing of StpB-mCherry (*stpB*::*stpB-mcherry*) foci (n=316 cells) per μm stalk. Interestingly, when I examined cells that produced StpA-mCherry (n=194 cells) from the xylose-inducible promoter, I found that the number of crossband signals per μm stalk was significantly increased compared to cells producing StpB-mCherry from the native promoter (student *t*-Test, $P<0.0001$) meaning that on average one crossband was formed every 1.67 μm stalk length. Notably, I did not observe such an increase in crossband frequency in cells that produced StpB-mCherry (n=120 cells) from the xylose-inducible promoter. Together, these findings support the notion that StpAB are involved in the formation of crossbands, which can be visualized by light microscopy using a fluorescent protein fusion to StpB. Furthermore, quantification of signals from inducible fluorescent protein fusions to either StpA or StpB indicates that constitutive production of StpA but not StpB leads to

an increase in the number of StpA foci per µm stalk. This observation implies that the total number of crossbands is linked to the number of StpA molecules in the cells.

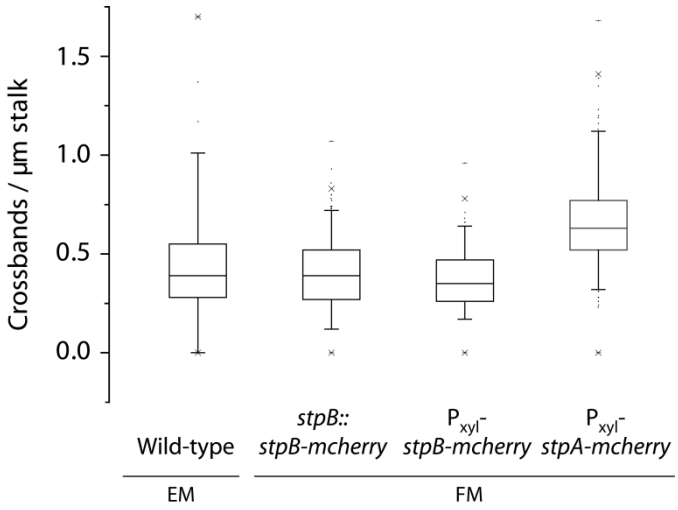

Fig. 20. Distribution of crossbands in the stalk. Cells of wild-type *C. crescentus*, SS160 (*stpB*::*stpB-mcherry*), SW30 (P_{xyl}::P_{xyl}-*stpB-mcherry*) and SW33 (P_{xyl}-P_{xyl}::*stpA-mcherry*) were grown in M2G^{-P} medium containing 0.3 % xylose. Cells were visualized by electron (EM) or fluorescence (FM) microscopy. From the respective images, the number of crossbands and StpA/B-mCherry foci per µm stalk were determined and the comparision of the data sets is graphically displayed in a box-whisker-plot. The box and the band represent the middle 50 % and the median of the data. The whiskers denote the range of the data set between the 5th and 95th percentile. The symbols "-" and "x" represent the minimum/maximum and the 1th/99th percentile of the data set. Single values outside the whisker range indicate outliers. In total 68, 316, 120 and 194 stalks of wild-type, SS160 (*stpB*::*stpB-mcherry*), SW30 (P_{xyl}::P_{xyl}-*stpB-mcherry*) and SW33 (P_{xyl}::P_{xyl}-*stpA-mcherry*) cells, respectively, were analyzed. Electron micrographs used for the analysis of wild-type *C. crescentus* were taken in collaboration with K. Bolte (Dept. of Biology, Philipps University, Marburg).

To determine the region(s) of StpA and StpB required for their localization and function in crossband formation, a series of protein truncations were generated and tagged with the red fluorescent protein mCherry. These protein fusions were produced from the xylose-inducible promoter (Fig. 21B). The size and integrity of the fusions were verified by immunoblot analaysis (data not shown).

The characteristic localization pattern of StpA was completely lost in mutant derivatives that lacked either the Sel1 domains or had the cytoplasmic and transmembrane domain replaced with the β-lactamase export sequence to facilitate translocation into the periplasm. By contrast, stalk-specific localization of StpB was not impaired by a replacement of the signal peptide with the β-lactamase export sequence or by a 159 amino acid C-terminal truncation. To corroborate the fluorescence data, the generated strains were analyzed by electron microscopy. As suggested by fluorescence microscopy, only cells that produced full-length StpA were able to form crossbands. Interestingly, although all three StpB derivatives displayed normal localization, the shortest StpB (aa 27-315) construct could not restore crossband formation (data not shown).

Therefore, I conclude that StpA requires the membrane anchor and the Sel1 domains for localization and interaction. One of its interaction partners could be StpB, which displays a largely unknown domain structure. However, whereas translocation of StpB into the periplasm seems to be sufficient for localization, the function of StpB in crossband formation appears to depend on the C-terminal region of the protein.

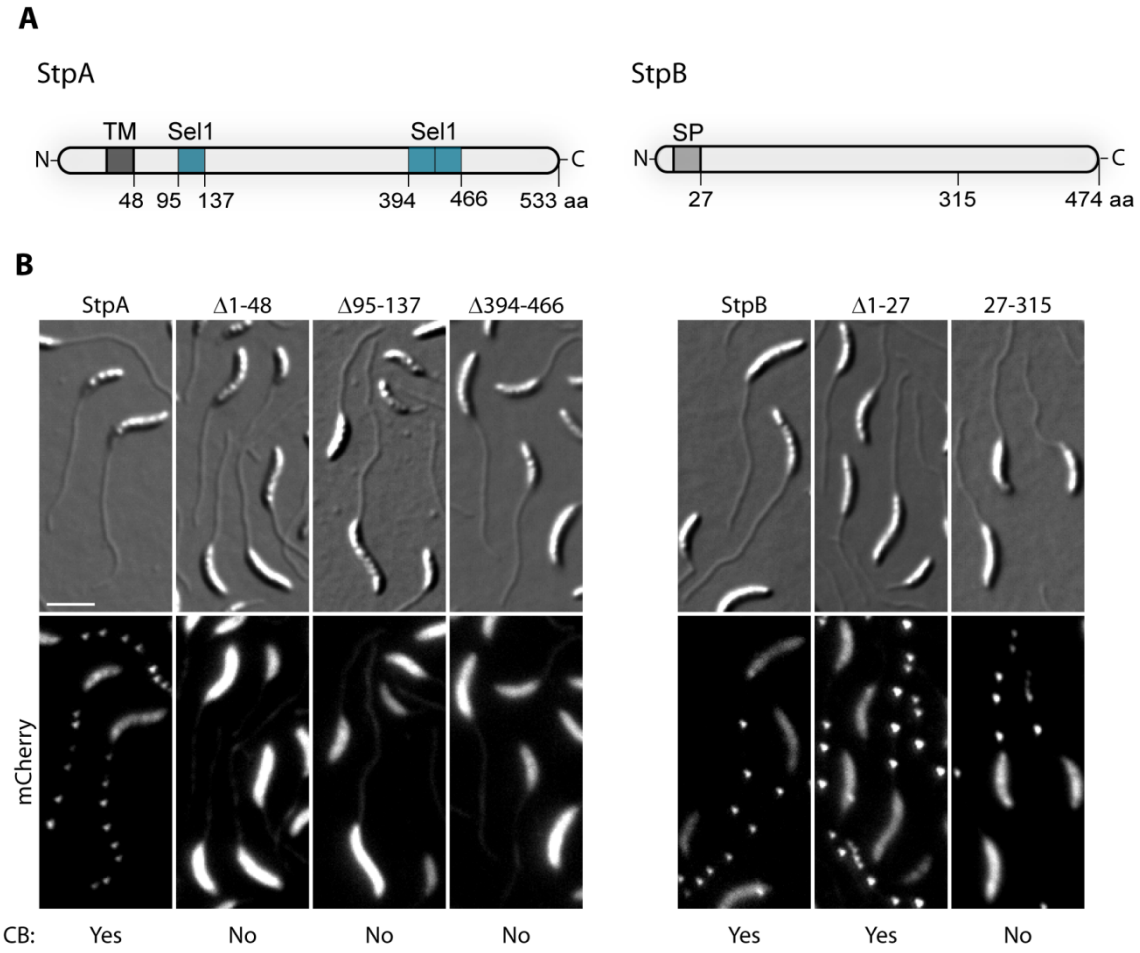

Fig. 21. Functional analysis of StpAB mutant derivatives. (A) Schematic representation of StpA and StpB. The transmembrane helix (TM), the Sel1 domains (Sel1) and the signal peptide (SP) are shown in dark grey, blue and light grey, respectively. Numbers refer to the position of amino acid (aa) residues to indicate the sites of deletions in StpA or StpB. (B) Localization and functionality of StpA and StpB mutant derivatives tagged with mCherry. StpA mutant strains SW33 (P_{xyl}::P_{xyl}-*stpA-mcherry*), SS163 (P_{xyl}::P_{xyl}-*bla*^{ss}-*stpA*$_{\Delta 1\text{-}48}$-*mcherry*), SS193 (Δ*stpA* P_{xyl}::P_{xyl}-*stpA* $_{\Delta 95\text{-}137}$-*mcherry*), SS158 (P_{xyl}::P_{xyl}-*stpA* $_{\Delta 394\text{-}466}$-*mcherry*), and StpB mutant strains SS146 (Δ*stpB* P_{xyl}::P_{xyl}-*stpB-mcherry*), SS169 (Δ*stpB* P_{xyl}::P_{xyl}-*bla*^{ss}-*stpB* $_{\Delta 1\text{-}27}$-*mcherry*), SS179 (Δ*stpB* P_{xyl}::P_{xyl}-*bla*^{ss}-*stpB* $_{27\text{-}315}$-*mcherry*) were grown in M2G^{-P} supplemented with 0.3 % xylose for 24 h and visualized by DIC and fluorescence microscopy (bar: 3 µm). Mutant strains were analyzed for the presence (yes) or absence (no) of crossbands (CB) by electron microscopy as indicated below the images.

2.2.4 Identification of StpAB interaction partners

The similar localization pattern and the results of the phenotypic analysis indicated that StpA and StpB interact *in vivo* and are either structural components of crossbands or part of their synthesis machinery. To identify possible interaction partners, I generated a strain that produced a His-tagged derivative of StpB from its native locus in an otherwise wild-type strain and performed coimmunopreciptiation studies.

Cells were grown under phosphate-limiting conditions and fixed with formaldehyde. Whole cell lysates were incubated with anti-His magnetic beads, and coimmunoprecipitated proteins were probed with anti-StpA antiserium or analyzed by mass spectrometry (J. Kahnt, Dept. of Ecophysiology, MPI Marburg). As suggested by previous experiments, StpA was copurified with

StpB and could be detected by immunoblot analysis (Fig. 22A). This interaction was also confirmed by mass spectrometry. Moreover, StpB appeared to specifically interact with two hitherto uncharacterized proteins, CCNA_02560 and CCNA_02271 [94], to which I will henceforth refer to as StpC and StpD, respectively. Interestingly, StpC is encoded immediately downstream of StpB with a one base pair overlap. The reason why this protein had escaped our attention so far is due to its incorrect annotation in the *C. crescentus* CB15 genome [106], which had been used up to this time as the reference sequence. StpC is a glycine-rich protein with a single transmembrane helix and a molecular mass of 21 kDa. The second protein, StpD, which was also incorrectly annotated, is located elsewhere on the chromosome and folds into a 29.3 kDa protein with one predicted transmembrane domain close to the N-terminal end.

If StpC or StpD interact with StpB, we expect a similar crossband-like localization pattern. Therfore, I generated xylose-inducbile copies of *stpC* and *stpD* fused to a fluorescent protein in *C. crescentus*. Strikingly, both fusion proteins mirrored the characteristic StpA and StpB localization pattern (Fig. 22B). Previous experiments had demonstrated that StpA acts as a recruitment factor for StpB (Fig. 16B). To determine whether this is also true for StpC and StpD, I investigated the rank of StpCD in the localization hierarchy (Fig. 22B). Whereas StpC localization depended on both StpA and StpB, StpD only requires StpA for recruitment to the stalk.

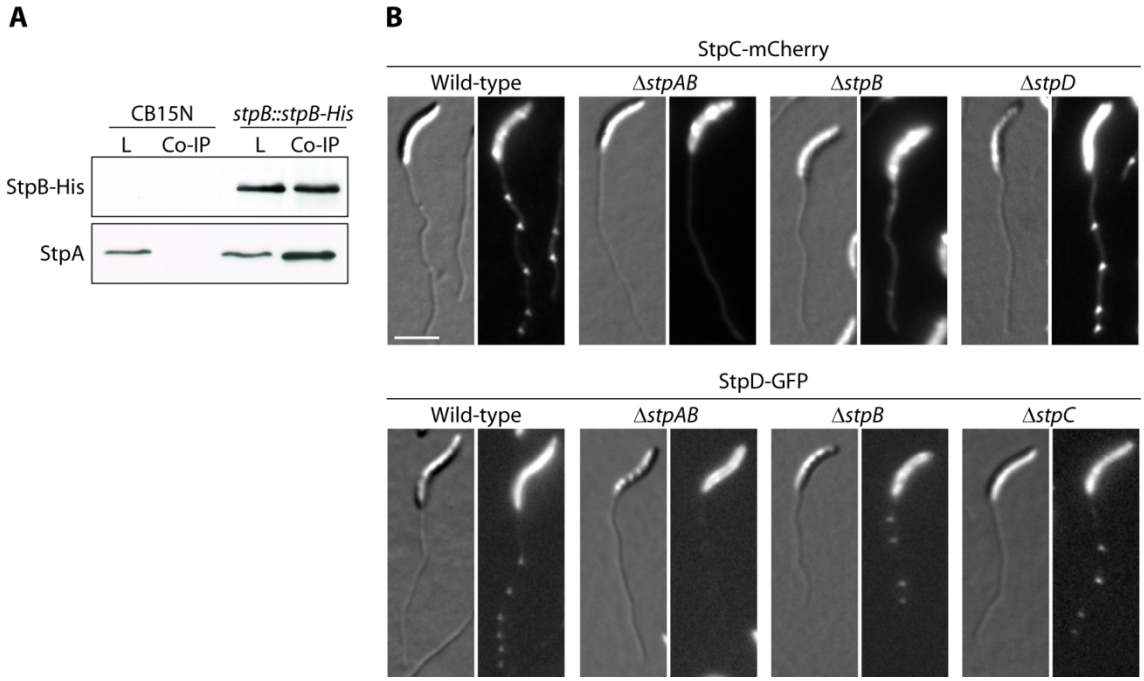

Fig. 22. Identification of StpB interaction partners. (A) Coimmunoprecipation analysis. His-tagged StpB was precipitated (Co-IP) from cell lysate (L) of strain SS233 (*stpB*::*stpB-His*) using anti-His coupled magnetic beads. Precipitated samples were analyzed by immunobloting with anti-His and anti-StpA antiserum. As a control, lysate of wild-type *C. crescentus* (CB15N) was analyzed in parallel. (B) Localization of StpCD. The localization of a xylose-inducible copy of StpC fused to mCherry was evaluated in strain SS228 (P_{xyl}::P_{xyl}-*stpC-mcherry*), SS236 (Δ*stpAB* P_{xyl}::P_{xyl}-*stpC-mcherry*), SS265 (Δ*stpB* P_{xyl}::P_{xyl}-*stpC-mcherry*), SS263 (Δ*stpD* P_{xyl}::P_{xyl}-*stpC-mcherry*). StpD-GFP localization was analyzed in strain SS226 (P_{xyl}::P_{xyl}-*stpD-gfp*), SS234 (Δ*stpAB* P_{xyl}::P_{xyl}-*stpD-gfp*), SS264 (Δ*stpB* P_{xyl}::P_{xyl}-*stpD-gfp*) and SS240 (Δ*stpC* P_{xyl}::P_{xyl}-*stpD-gfp*). Cells were grown in M2G^{-P} with 0.3 % xylose for 24 h and visualized by DIC and fluorescence microscopy (bar: 3 µm).

Due to the fact that the available microarray data on the cell cycle-regulated expression of genes in *C. crescentus* [85] is based on the old (partially incorrect) genome annotation [106], we lacked information on the transcriptional regulation of *stpC* and *stpD* over the cell cycle. Therefore, I monitored the abundance of StpC and StpD by means of a C-terminal His-tag fusion (Fig. 23A). The hybrid proteins were produced in place of the respective wild-type protein and detected by immunoblot analysis. Similar to StpAB, both proteins accumulated at the onset of stalk outgrowth. Next, I verified the predicted membrane topology of StpC and StpD by performing protein fractionation studies and the TEM-1 β-lactamase (*bla*) assay as described above. In agreement with the bioinformatic analysis, StpC and StpD were cosedimented with membrane proteins after fractionation of whole cell lysates (Fig. 23B). Furthermore, TEM-1 β-lactamase fusions to StpC and StpD evidenced that the C-termini of both proteins are directed towards the periplasm (Fig. 23C). Additionally, StpCD-deficient cells still harbor crossbands as evidenced by electron microscopy (data not shown), indicating that these two proteins might be accessory components in crossband formation.

Taken together, protein-interaction studies demonstrated that StpB is part of a multiprotein complex, in which StpA appears to be the crucial component for assembly. The complex is comprised of at least four proteins; StpABC and StpD. StpCD are also synthesized in a cell cycle-dependent manner and sequestered to the stalk periplasm, but they are not required for crossband formation under the conditions tested.

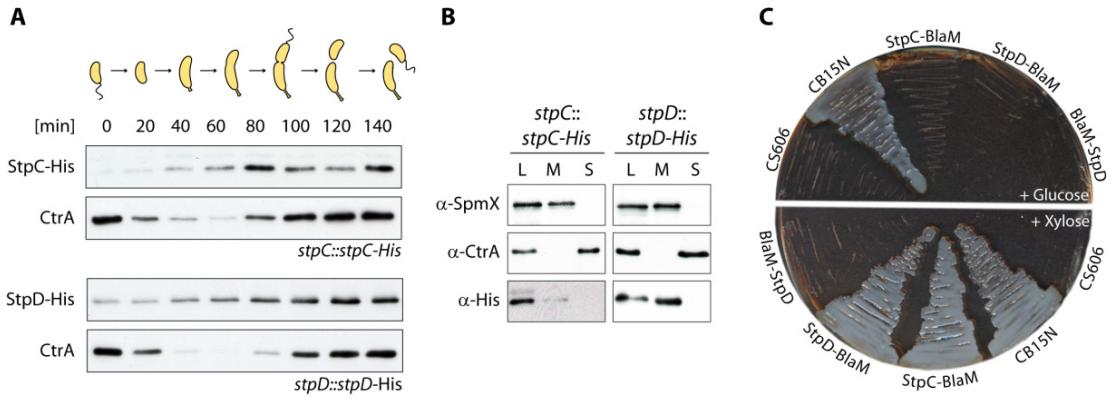

Fig. 23. Cell cycle-dependent abundance and membrane topology of StpC and StpD. (A) Cell cycle-regulated abundance of StpC and StpD. Swarmer cells of strain SS247 (*stpC*::*stpC-His*) and SS244 (*stpD*::*stpD-His*) were grown in M2G for one cell cycle. Samples were taken from the culture in 20 min intervals and analyzed by immunoblotting using anti-CtrA and anti-His antiserum. The schematic displays the morphological development of *C. crescentus* over the cell cycle. (B) Subcellular localization of StpC and StpD. Whole cell lysates (L) of strain SS247 and SS244 were fractionated by ultracentrifugation into membrane (M) and soluble (S) proteins. Samples of each fraction were probed with anti-His antiserum. The fractionation efficiency was confirmed by immunoblot analysis using anti-SpmX [124] and anti-CtrA [122] antiserum. (C) Membrane topology of StpC and StpD. Cells of wild-type *C. crescentus* (CB15N), CS606 (Δ*bla*), SS273 (Δ*bla* P_{xyl}::P_{xyl}-*stpC-bla*), SS274 (Δ*bla* P_{xyl}::P_{xyl}-*stpD-bla*) and SS275 (Δ*bla* P_{xyl}::P_{xyl}-*bla-stpD*) were grown on PYE agar with 50 µg/ml ampicillin and with either 0.2 % glucose or 0.3 % xylose.

2.2.5 StpABCD colocalize with crossbands

Several lines of evidence imply that StpABCD are involved in crossband formation. But thus far, I lacked concrete evidence that these four proteins indeed spatially overlap with crossbands. To address this issue, I first colocalized StpA, StpB and StpC with StpD in cells grown under phosphate limitation. As indicated by the similar localization pattern of cells producing only a single fluorescent protein fusion, StpD colocalized with StpA, StpB and StpC (Fig. 24A).

Secondly, in collaboration with A. Briegel (CalTech, USA), correlated fluorescence light microscopy and electron cryo-tomography was performed. This technique provides information on both the localization of a fluorescent protein fusion and structural details of the same area previously imaged. We used a *C. crescentus* strain that produced StpB-mCherry from the xylose-inducible promoter. Cells were first imaged by fluorescence microscopy, plunge frozen and then, tilt series were recorded from the same set of cells and correlated with the fluorescence micrographs (Fig. 24B). In support with previous results, StpB-mCherry explicitly colocalized with crossbands and thus, by implication, StpACD also colocalize with crossbands.

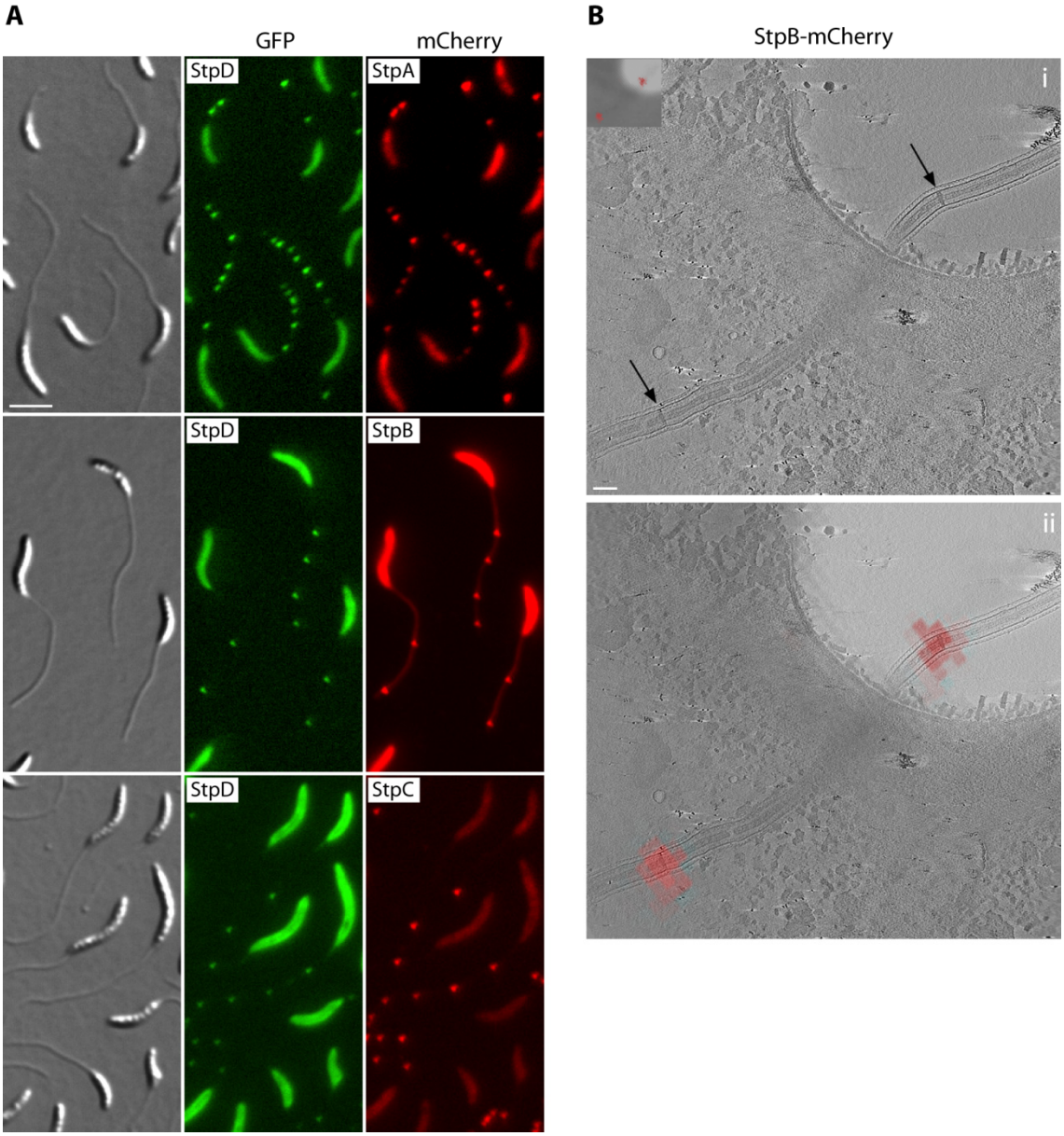

Fig. 24. StpABCD colocalize with crossbands. (A) Colocalization in live cells. Cells of strain SS243 (*stpD*::*stpD-gfp* P_{xyl}::P_{xyl}-*stpA-mcherry*), SS237 (*stpB*::*stpB-mcherry* P_{xyl}::P_{xyl}-*stpD-gfp*) and SS249 (*stpD*::*stpD-gfp* P_{xyl}::P_{xyl}-*stpC-cherry*) were grown in $M2G^{-P}$ with 0.3 % xylose for 24 h and visualized by DIC and fluorescence microscopy (bar: 3 µm). (B) Colocalization of StpB-mCherry with crossbands in *C. crescentus*. Strain SW30 (P_{xyl}::P_{xyl}-*stpB-mcherry*) was grown in $M2G^{-P}$ with 0.3 % xylose. Cells were fixed on electron microscopy grids and imaged, first by low-magnification phase contrast/fluorescence microscopy (merged image left inset) and then by electron cryo-tomography (ECT). Shown is (i) an ECT slice of the stalk with arrows pointing to crossband structures and (ii) a correlated image of a fluorescence light micrograph and an ECT image of the same cell (bar: 100 nm). Correlated fluorescence light microscopy and electron cryo-tomography was performed by A. Briegel (CalTech, USA).

Next, I asked whether StpABCD are dynamically recruited to already existing crossbands. If this were the case, photobleaching of selected StpB-mCherry foci should lead to the recovery of each bleached signal. However, fluorescence-recovery-after-photobleaching (FRAP) experiments with a strain that produced StpB-mCherry in place of the native gene demonstrated that bleached StpB-mCherry signals did not recover over time. This observation implies that StpB, and presumably also StpACD, form static protein complexes and that most likely no diffusion of components between adjacent StpABCD complexes takes place.

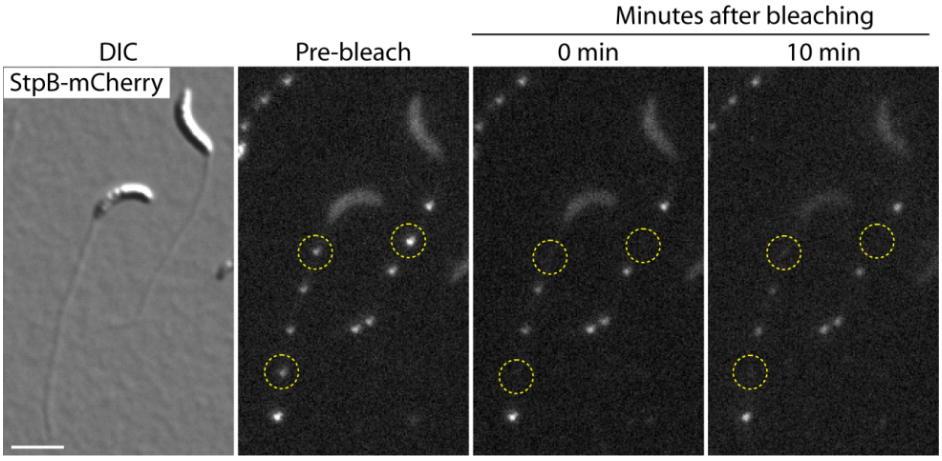

Fig. 25. StpB localization is static. Fluorescence-recovery-after-photobleaching (FRAP) experiments with strain SS160 (*stpB*::*stpB-mcherry*). Cells were grown in M2G^{-P} and imaged by DIC/fluorescence microscopy to identify StpB-mCherry localization. A laser pulse was applied to selected regions (yellow circles) and StpB-mCherry signals were completely bleached. Immediately after the laser pulse and 10 min later, fluorescence images were taken of the same region (bar: 3 µm).

Earlier studies suggested that crossbands partially consist of peptidoglycan [139], and this particular mode of murein synthesis was reported to require FtsZ [38]. To clarify whether crossband formation was indeed dependent on FtsZ, I generated a conditional *ftsZ* mutant strain (*ftsZ*::P_{xyl}-*ftsZ*) that carried a *stpB-mcherry* fusion under a vanillate-inducible promoter to visualize crossband formation. In cells that were depleted of FtsZ for 6 h, StpB-mCherry foci were still observed in the stalk, proving that crossbands are synthesized in an FtsZ-independent manner (Fig. 26). Moreover, I confirmed the distinct StpB-Cherry localization in cells that lacked PbpC, a peptidoglycan synthase recently implicated in stalk morphogenesis [81], and cells deficient of several other penicillin-binding proteins (data not shown).

Based on these findings, I hypothesize that the StpABCD complex is not only involved in crossband synthesis but also constitutes the crossband structure. Although the obtained results indicate that crossband formation does not depend on peptidoglycan synthesis, peptidoglycan may still partially contribute to overall crossband stability.

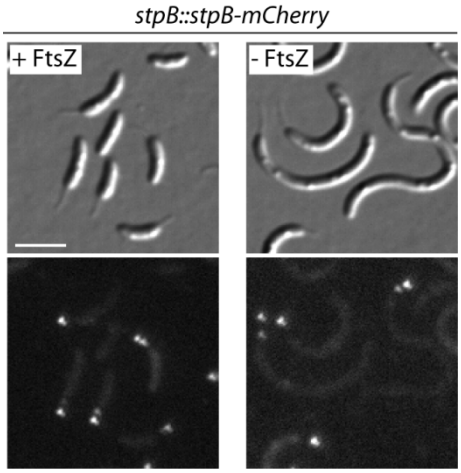

Fig. 26. Crossband synthesis is independent of FtsZ. Isolated swarmer cells of strain SS191 (*ftsZ*::P_{xyl}-*ftsZ* P_{van}::P_{van}-*stpB-mcherry*) were released into M2G medium with and without 0.3 % xylose. After 6 h of incubation, cells were imaged by DIC and fluorescence microscopy. StpB-mCherry production was induced with 0.5 mM vanillate for 2 h (bar: 3 µm)

2.2.6 Physiological role of crossbands

Blast searches revealed that StpABCD are conserved in other stalked alpha-proteobacteria such as *Brevundiomnas* or *Asticcacaulis* species. Thus, crossbands might be a general feature in stalked, non-budding bacteria. It has been suggested that crossbands fulfill a stabilizing and architectural function [74]; however, the role of these structures in stalk formation is still unclear.

First, I compared the growth of wild-type *C. crescentus* and strains devoid of crossband proteins. Cells of each mutant strain grew to equal optical densities in liquid medium. This observation was also confirmed by a dilution series of wild-type cells and cells of strains SW51 (Δ*stpAB*), SS250 (Δ*stpCD*) and SS259 (Δ*stpABC*) (Fig. 27A). Apart from the lack of crossbands, cells of strain SW51 did not display any defects in stalk biogenesis, such as stalk length (data not shown).

Second, I asked whether crossbands could protect the cells against cytoplasmic or periplasmic leakage when stalks were sheared off by mechanical force. To test this idea, wild-type *C. crescentus* and StpAB-deficient cells were grown under phosphate-limiting conditions and treated with a warring blender as described by Jordan and co-workers [75]. Neither wild-type nor crossband-mutant cells showed a loss in viability upon removal of stalks (Fig. 27B).

Third, I performed a growth competition assay to study whether wild-type *C. crescentus* could out-compete crossband-deficient cells under conditions of extended phosphate-starvation. To this end, cultures of wild-type *C. crescentus* and strain SW51 (Δ*stpAB*) were adjusted to the same optical density, mixed at equal proportions and grown in phosphate-limiting medium. As cells stop to divide after depletion of phosphate, I diluted the cells in complex medium to restart development. I repeated this cycle four times before a dilution series of the cells was plated onto PYE agar. Single colonies that formed on these plates, and on plates with cells from the initial cell suspension, were screened for the presence of *stpAB* by PCR. Again, I could not detect a shift in the composition of the population, which would indicate that either one of the genetic backgrounds provides an advantage in a low-phosphate environment.

However, the growth conditions tested might not have been stringent enough to select for a particular genotype and therefore, this competition assay should be repeated applying modified selection conditions.

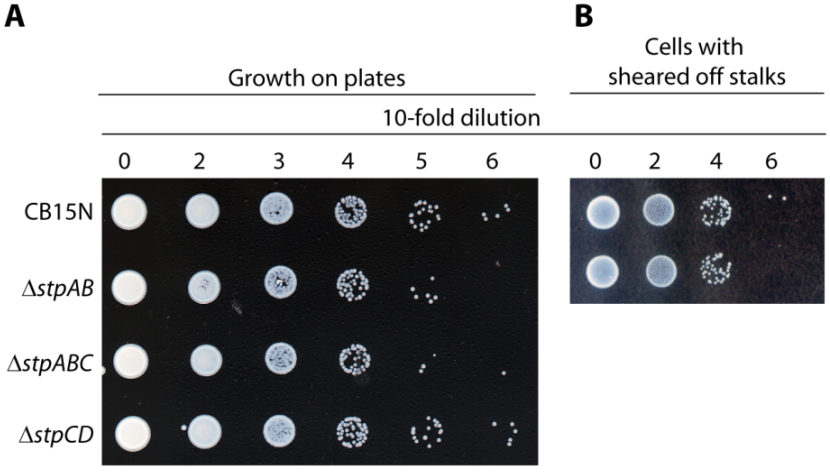

Fig. 27. Crossbands are not essential under normal growth conditions. (A) Growth on agar plates. Wild-type *C. crescentus* (CB15N), SW51 (Δ*stpAB*) SS259 (Δ*stpABC*) and SS250 (Δ*stpCD)* were grown in PYE for 24 h, diluted to an OD_{600} of 0.16, serially diluted as indicated and spotted on PYE agar. (B) Growth on agar plates after removal of stalks. Wild-type *C. crescentus* (CB15N) and strain SW51 (Δ*stpAB)* were grown in $M2G^{-P}$. Stalks were sheared off in a warring blender for 3 min at 4°C. Cells were diluted to an OD_{600} of 0.14, serially diluted and spotted as indicated on PYE agar.

In previous experiments, I observed that constitutive induction of StpA-mCherry increased the number of fluorescent "crossband-signals" in the stalk (Fig. 20). I reasoned that the cellular levels of StpA and/or StpB may determine the frequency of crossband structures. Therefore, I investigated the effect of StpAB overproduction on crossband formation. Strain SS160 (*stpB*::*stpB-cherry*) was provided with a self-replicating plasmid that carried *stpAB* under the control of the xylose-inducible promoter (Fig. 28A). It should be noted that the promoter causes leaky expression of its downstream genes. This effect is pronounced when the promoter is located on a multi-copy plasmid, causing elevated expression of the gene of interest even without inducer. When cells were cultured under phosphate-limiting conditions without xylose, stalks harbored significantly more StpB-mCherry foci. In fact, single foci could hardly be resolved. This localization pattern was lost upon induction of StpAB overproduction. Moreover, cell and stalk morphogenesis were severely affected and cell viability was dramatically reduced (Fig. 28A, B). Cell bodies were elongated with pointed cell poles. The vast majority of the cells lacked stalks and those that carried a stalk did not display the characteristic crossband-like localization of StpB. In general, StpB-mCherry localization within the cells was dispersed, which was not due to degradation as evidenced by immunoblot analysis (Fig. 28C). To better visualize cell morphology defects, we used electron microscopy. I could indeed confirm that the increased number of StpB-foci corresponded to a significantly accumulation of crossbands in the stalks. Previously described "stalkless" cells turned out to be cells with very short stalks or deformed cell poles often without any crossband structures (Fig. 28D).

Taken together, the detrimental effect of StpAB overproduction is interesting but also puzzling. It is not surprising that constitutive synthesis of two cell cycle-regulated proteins becomes detrimental to the cells as it is an energy consuming process, particularly under nutrient starvation. However, I speculate that the observed phenotype is directly linked to stalk biogenesis and morphogenesis – two processes that involve the localization of StpAB and the formation of crossbands.

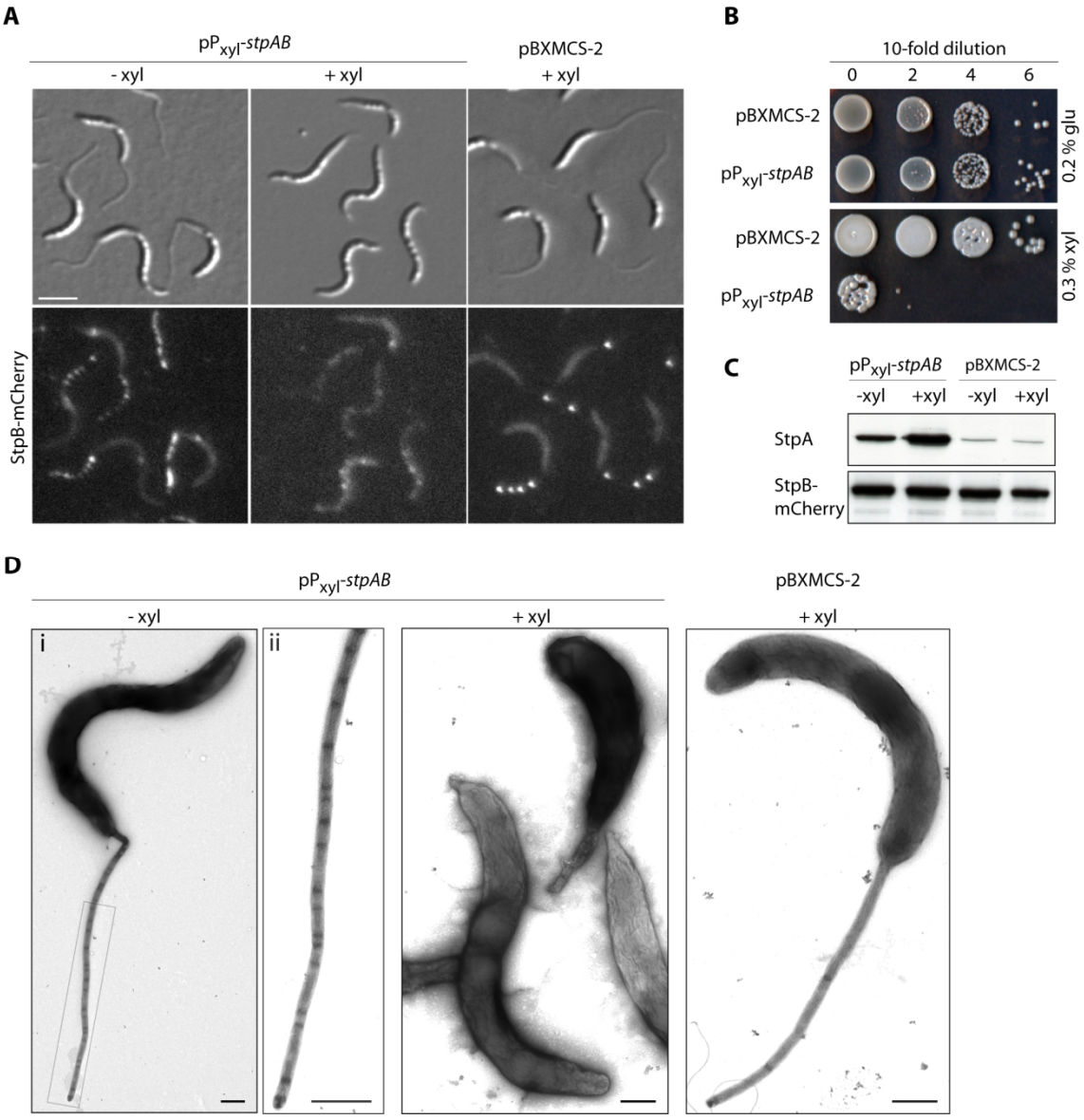

Fig. 28. Effect of StpAB overproduction. (A) Localization of StpB upon StpAB overproduction. Cells of strain SS214 (*stpB*::*stpB-mcherry* pP_{xyl}-*stpAB*) were grown for 24 h in $M2G^{-P}$ with or without 0.3 % xylose. *C. crescentus* cells carrying the empty plasmid pBXMCS-2 (SS258, *stpB*::*stpB-mcherry*) were used as a control. Cells were visualized by DIC and fluorescence microscopy (bar: 3 µm). (B) Growth on PYE agar. *C. crescentus* strains SS258 (*stpB*::*stpB-mcherry* pBXMCS-2) and SS214 (*stpB*::*stpB-mcherry* pP_{xyl}-*stpAB*) were grown in PYE for 24 h, diluted to an OD_{600} of 0.16, serially diluted as indicated and spotted on PYE agar containing either 0.2 % glucose or 0.3 % xylose. (C) Abundance of StpA and StpB-mCherry. Immunoblot analysis of cell lysates obtained from strain SS214 (*stpB*::*stpB-mcherry* pP_{xyl}-*stpAB*) and SS258 (*stpB*::*stpB-mcherry* pBXMCS-2) during growth with and without xylose. (D) Ultrastructure of cells overproducing StpAB. Cells of strains SS214 (*stpB*::*stpB-mcherry* pP_{xyl}-*stpAB*) and SS258 (*stpB*::*stpB-mcherry* pBXMCS-2) were grown in $M2G^{-P}$ in the absence or presence of inducer, contrasted with uranylacetate and imaged by electron microscopy. The dashed rectangle in (i) indicates magnified the region magnified in (ii). Electron micrographs were taken in collaboration with K. Bolte (Dept. of Biology, Philipps University, Marburg) (bars: 500 nm).

Earlier reports suggested that crossbands may form a structural barrier in the stalk [74]. To test this hypothesis, I investigated the diffusion of proteins between the stalk and the cell body in wild-type and StpAB-deficient cells by fluorescence microscopy.

First, I examined the diffusion of periplasmic proteins. For this I used the soluble red fluorescent protein tdimer2, which was fused to the signal sequence of the *E. coli* TorA protein to facilitate translocation to the periplasm [76]. tdimer2 was produced from the xylose-inducible promoter in a strain that concurrently carried a StpD-GFP fusion to visualize crossbands. To test for periplasmic compartmentalization, I carried out fluorescence-loss-in-photobleaching (FLIP) experiments (Fig. 29A). In untreated cells, diffuse red fluorescence was detected along the stalk and the cell body periplasm, while StpD-GFP localized in its typical pattern. When a laser pulse was applied to the cell pole furthest away from the stalk, tdimer2 fluorescence was completely bleached in the cell body. The bleached area extended all the way to the crossband closest to the stalk base, which was marked by the StpD-GFP fusion (*stpD*::*stpD-gfp*). No significant recovery of fluorescence in the cell body was observed after 10 min. Notably, in about 20 % of the cells, tdimer2 fluorescence was also observed up to the second latest crossband, indicating that crossband assembly may still have been in progress at the time of the bleaching experiment. By contrast, in FLIP experiments with a StpAB-deficient strain, tdimer2 was completely bleached throughout the cell including the stalk, suggesting that tdimer2 diffusion is unrestrained in the periplasm surrounding the entire cell in the absence of crossbands.

Second, I wondered whether inner membrane proteins are also compartmentalized by crossbands (Fig. 29B). For this purpose I used either wild-type *C. crescentus* that produced StpD-GFP or strain SW51 (Δ*stpAB*) in combination with a xylose-inducible copy of the *gspG* homologue (*CCNA_00175)* fused to *mcherry*. GspG (general secretion pathway protein G) is an inner membrane component of the type II secretion system (T2SS), which was recently also identified in *C. crescentus* [87]. I performed pulse-labeling experiments, in which cells were first allowed to grow in low-phosphate medium without inducer. After 36 h, when stalks are already elongated but "unlabeled" by the fluorescent fusion protein, synthesis of GspG-mCherry was induced with xylose followed by an additional growth period. In crossband-deficient cells of strain SW51, GspG-mCherry fluorescence was visible in the entire cell including the stalk. However, in wild-type *C. crescentus*, GspG-mCherry molecules were prevented from passing the newest, or in few cases the second newest, crossband visualized by StpD-GFP. These results were also confirmed by FLIP experiments (data not shown) demonstrating that inner membrane proteins cannot freely diffuse between the stalk and the cell body in wild-type *C. crescentus*.

Finally, I tested the mobility of outer membrane proteins. For this purpose, I perfomed pulse-labeling of cells that produced the outer membrane lipoprotein ElpS (CCNA_00169) fused to mCherry [87] (Fig. 29B). Again, in cells lacking StpAB, ElpS-mCherry fluorescence could be detected in the entire cell body including the stalk. In wild-type cells, on the other hand, diffusion of the outer-membrane protein was limited to the cell body and up to the second newest crossband proving that also outer membrane proteins are compartmentalized. These results were confirmed using mCherry tagged versions of the outer membrane protein CCNA_01475 or the TonB-dependent receptor CCNA_00170 (data not shown).

In summary, crossbands act as protein diffusion barriers that compartmentalize the periplasm, inner and outer membrane proteins within the stalk and physically separate the stalk from the cell body. Hence, crossband formation represents a novel mechanism to topologically restrict protein mobility within a cell.

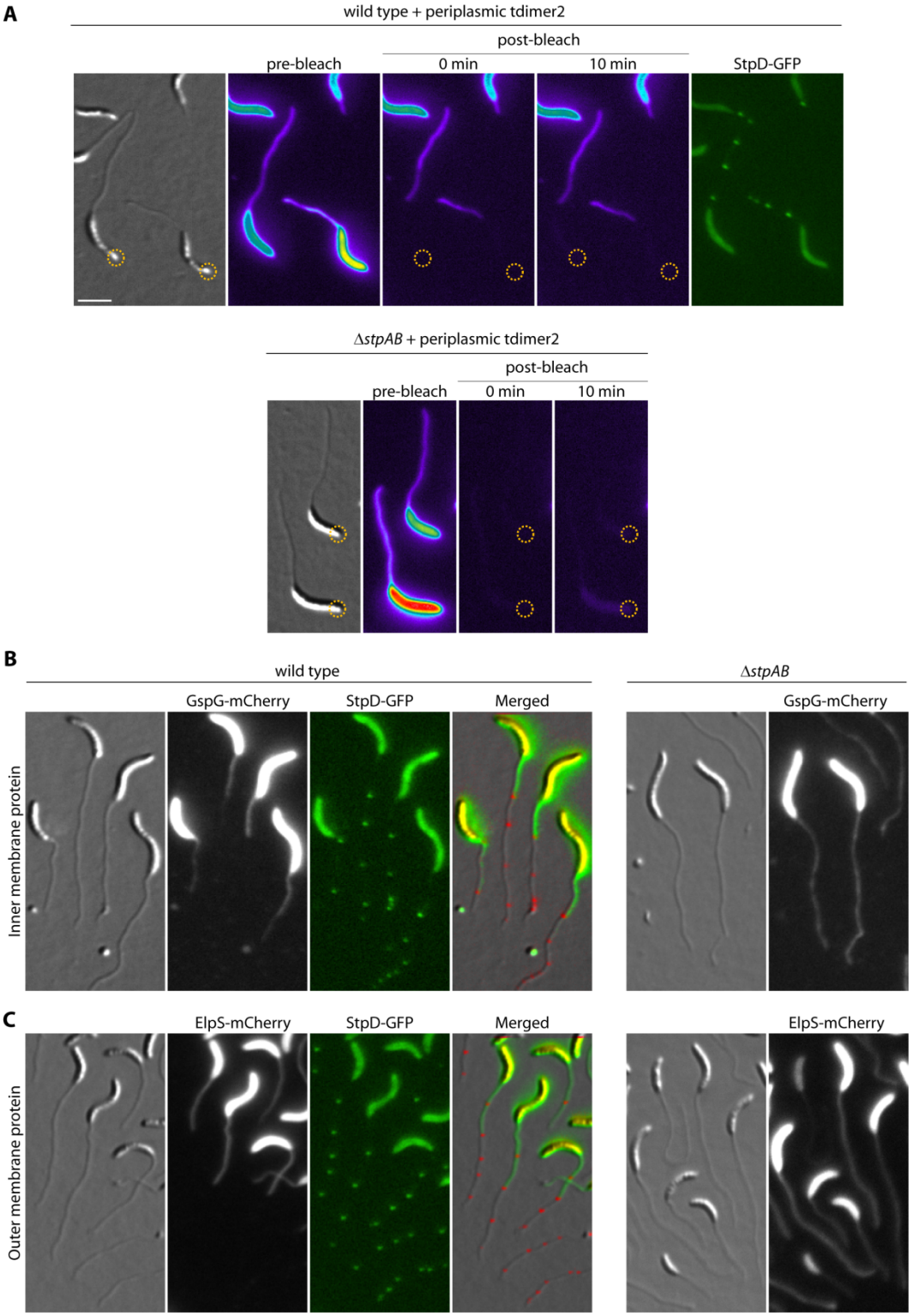

Fig. 29. Stalk compartmentalization by a protein diffusion barrier. (A) Analysis of compartmentalization of periplasmic tdimer2 using fluorescence-loss-in-photobleaching. Cells of strain SS269 (*stpD*::*stpD-gfp* pP$_{xyl}$-*tdimer2*) and SS216 (Δ*stpAB* pP$_{xyl}$-*tdimer2*) were grown in M2G^{-P} containing 0.3 % xylose for 24 h. Cells were mounted on an agarose pad and exposed to a laser pulse in the regions indicated by a yellow circle. Cells were visualized by DIC and fluorescence microscopy before and after photobleaching. (B) Compartmentalization of (i) inner membrane proteins and (ii) outer membrane proteins demonstrated by pulse-labeling experiments. Cells of strains SS277 (*stpD*::*stpD-gfp* P$_{xyl}$::P$_{xyl}$-*gspG*), SS272 (Δ*stpAB* P$_{xyl}$::P$_{xyl}$-*gspG*), SS283 (*stpD*::*stpD-gfp* P$_{xyl}$::P$_{xyl}$-*elpS*), and SS284 (Δ*stpAB* P$_{xyl}$::P$_{xyl}$-*elspS*) were grown first in M2G^{-P} for 36 h and then induced with 0.1 % xylose followed by an additional growth period. After 11 h of incubation, cells were visualized by DIC and fluorescence microscopy (bar: 3 µm).

3 DISCUSSION

3.1 CedX – An accessory divisome stabilizer

This study aimed at the identification and characterization of novel cell division proteins in *C. crescentus* that could stabilize the divisome by acting as an adapter for localized protein-protein interaction. Physical interaction of proteins can be promoted by proteins with unstructured regions that can bridge the distance between putative interaction partners or provide an anchor for localization. Based on a bioinformatic screen, the proline-rich protein CedX was identified. In general, proline-rich proteins are wide-spread in eukaryotes and prokaryotes where they fulfill diverse functions including a role in cell envelope composition [7, 113], signal transduction [80, 149] or immune response [20, 70]. From the conformational perspective, proline stretches have the propensity to organize into exposed polyproline helices that can act as flexible "sticky arms" [84, 177]. Biochemical fractionation and bioinformatical analysis of wild-type *C. crescentus* evidenced that CedX is an inner membrane protein with a proline-rich C-termainal tail that is directed towards the cytoplasm. It is therefore conceivable that this unstructured C-terminal tail of CedX reaches into the cytoplasm and provides an adaptor-like structure to stabilize or mediate protein-protein interactions. In fact, several cell division proteins, e.g. ZipA [61], FtsN [100], FtsK [10, 166] or FtsZ (alpha-proteobacteria only, unpublished) harbor short proline-rich segments suggesting that these unstructured regions provide structural flexibility that is crucial for protein function and divisome assembly.

3.1.1 CedX localization

Assembly of the divisome starts with the accumulation of FtsZ at the future division site. With the exception of the two FtsZ-positioning proteins SsgB of *Streptomyces coelicolor* [176] and PomZ of *Myxococcus xanthus* [A. Treuner-Lange & K. Aguiluz, unpublished], every protein known to be targeted to midcell requires the FtsZ-provided scaffold for localization. This prerequisite applies also to CedX, implicating CedX as a component of the cell division apparatus.

Time-course experiments evidenced that CedX is dynamically recruited to midcell in predivisional *C. crescentus* cells. This localization pattern is also dependent on the essential late cell division protein FtsN [4, 30, 100]. Consistent with previous studies [99-100, 180], I found that FtsZ arrives at midcell within the first third of the cell cycle, whereas both FtsN and CedX accumulate in the last third of the cell cycle. Based on the FtsN-dependent localization and the temporal order of recruitment to midcell, CedX qualifies for the group of late cell division proteins [51, 100]. The biological activities of late cell division proteins are diverse including chromosome segregation (FtsK/SpoIIIE, TipN [121, 143]), divisome stabilization (FtsQ/DivIB, FtsL, FtsB/DivIC), peptidoglycan remodeling (DipM, FtsN, FtsW, FtsI, AmiC) or outer membrane invagination (Tol-Pal complex) [34, 51, 65]. Thus, and for reasons that will be discussed below (see 3.1.3), CedX

could be involved in the stabilization of protein-protein interactions during late stages of cell division.

3.1.2 CedX phenotype

Overproduction of CedX completely inhibited cytokinesis. This overproduction effect has been described for a number of essential (FtsZ [170], FtsA [165], FzlA [54], FtsN [100]) and non-essential (SulA [102], EzrA [60], ZapC [62]) cell division proteins. A stoichiometric imbalance of divisome components can block divisome maturation or accelerate disassembly of the cell division machinery. In other words, excess CedX could saturate Z-ring binding sites and thereby sterically impede the recruitment of downstream divisome components or titrate out divisome components essential for the progression and completion of cytokinesis. This interpretation, however, raises the question of how CedX can interact with FtsZ. Interestingly, FtsZ sequence alignments revealed that in alpha-proteobacteria FtsZ contains an additional unstructured proline-rich insertion upstream of the highly conserved carboxy-terminal region. This region is exposed on the FtsZ surface [90] and known to directly interact with FtsA [37] and ZipA [91], two proteins that anchor FtsZ to the inner membrane. Functional analysis of CedX mutant derivatives supports the idea that the proline-rich region is required for protein-protein interaction. The exact mechanism underlying the CedX-FtsZ interaction remains unknown, but it is conceivable that CedX binds to this additional unstructured region of FtsZ, which in turn stabilizes FtsZ filaments either directly or indirectly by mediating the localization of a yet unknown factor.

An increase in the cellular level of CedX led to smooth filaments and dramatically reduced the viability of *C. crescentus* cells. The absence of membrane constrictions and the observation that FtsN colocalizes with the multiple Z-ring-like structures indicates that processes following FtsN recruitment, such as membrane invagination and peptidoglycan remodeling, are disturbed. The effect of cell lysis after extended induction of CedX synthesis is probably not directly related to the function of CedX but rather caused by the energy consuming maintenance of the multiple Z-ring structures or/and instabilities in the cell envelope due to continuous filamentous growth.

Attempts to identify suppressor mutations in the *C. crescentus fts* genes that would allow escaping lethal filamentation by CedX failed, supporting the notion that a yet unknown factor might be involved in the observed overproduction phenotype.

Further phenotypic analyses demonstrated that Δ*cedX* cells show normal growth rates and morphology, indicating that CedX is dispensable under the applied laboratory conditions including different incubation temperatures, growth media and UV stress. The latter is in line with a recent study on the SOS response in *C. crescentus* [28]. Among the genes that are regulated during UV-induced DNA damage, *cedX* was not found to be a target of LexA, which is a central player in the cellular response to DNA damage [136].

The number of proteins that associate with the divisome but are not essential for viability in *E. coli*, *B. subtilis* or *C. crescentus* has constantly increased over the last years. This list includes ZapA [58], ZapB [42], ZapC [40, 62], EzrA [60], FzlA/C [54], FtsP [134], SulA [102], SepF [63, 145] and YmgF [79]. Many of these accessory divisome components become essential for cell division only under certain stress conditions, such as oxidative stress [134], low osmotic strength [128, 142] or disturbed Z ring stability [40, 62-63, 129, 145]. Unlike for *E. coli*, many of the conditional *fts* mutants are not available for *C. crescentus,* which complicates the identification of a synthetic lethal or sick phenotype. In addition, CedX may share an overlapping function with a yet unknown cell division

protein. Functional redundancy in different aspects of cell division has been reported for ZipA/FtsA [114], SepF/FtsA [73] or ZapABC [40, 62]. Thus, I speculate that CedX stabilizes divisome assembly under specific physiological conditions. However, the nature of this condition is still unknown.

3.1.3 CedX interaction network

Bacterial two-hybrid analysis, coimmunoprecipitation studies and *in vivo* colocalization experiments strongly suggest that CedX physically interacts with the divisome. Several lines of evidence support the notion that CedX interacts with FtsZ and stabilizes the division machinery during late stages of divisome assembly (Fig. 30).

First, CedX binds to FtsZ. *In vivo* interaction of FtsZ and CedX was evidenced by coimmunoprecipitation experiments. Moreover, CedX was found to exclusively localize to extended membrane constrictions caused by the overproduction of the FtsZ-G109S (GTPase-imparied) mutant derivative in *C. crescentus*. Goley and coworkers [54] proposed that such a specific localization pattern indicates direct binding to FtsZ because it was exclusively observed for the FtsZ-stabilizing proteins FtsA, FtsE, FtsX and ZapA, but not by the late cell division proteins FtsW, FtsI, FtsQ [51] or the FtsZ-inhibitor MipZ [157]. However, experimental evidence corroborating direct binding of CedX to FtsZ is still lacking. It remains to be clarified whether CedX can also induce higher-ordered FtsZ structures *in vitro* as it has been reported for the FtsZ-binding proteins ZapA [58], SepF [59, 145], FzlA/C [54] or ZapC [40, 62].

Second, CedX is not involved in the initial set-up of the Z-ring at midcell. In *E. coli*, *B. subtilis* and *C. crescentus*, FtsZ protofilament bundling (ZapAC, SepF, FzlA), anchoring to the membrane (FtsA, ZipA) and early stabilization (ZapB, FzlC) is performed by several FtsZ-binding proteins that arrive almost simultaneously or shortly after FtsZ at the incipient division site [3, 40, 54, 62]. CedX is recruited to the Z-ring after a significant delay (~75 min). Although protein-protein interactions between CedX-ZapA and CedX-FzlC were detected by coimmunoprecipitation or bacterial two-hybrid analysis, these contacts are probably established during divisome maturation. Furthermore, *C. crescentus* cells with a Δ*cedX ΔzapA* or Δ*cedX ΔfzlC* double mutation did not display a synergistic phenotype, suggesting that CedX is not involved in the initial stabilization of the divisome.

Finally, CedX is a late recruit to the divisome. Previous work in *E. coli* [2, 52], *B. subtilis* [49] and *C. crescentus* [99-100] has demonstrated that the divisome is not assembled in a strictly linear order but rather from several functional modules. In addition to its localization dynamics, CedX was found to interact with at least two divisome modules. On the one hand CedX appears to be associated with FtsN, TolA and TolR, three bitopic membrane proteins that are involved in the organization of peptidoglycan remodeling [12, 99-100] and outer-membrane invagination during cytokinesis [50, 180], processes that are initiated significantly after establishment of the Z-ring. Thus, interaction of CedX with FtsN, TolA and TolR could possibly explain the lack of constrictions in filamentous *C. crescentus* cells after overproduction of CedX. On the other hand, CedX interacts with FtsL. In *E. coli* and *B. subtilis*, FtsL belongs to the late cell divison proteins, forming a widely conserved subcomplex with FtsQ/B that is required for multiple protein-protein interactions [22-23, 51, 56]. Consistently, FtsQ was also detected among the proteins that coprecipitated with CedX, presumably due to its interaction with FtsL. This subcomplex localizes independently of FtsN [24] and fulfills an important, yet unknown, function in Z-ring stabilization [31, 33, 52, 56-57].

Collectively, CedX is called into action during late stages of divisome assembly at which time it interacts with both FtsZ and the divisome modules FtsQLB and FtsN/TolA/TolR (Fig. 30). How are these interactions established? CedX is targeted to midcell by its transmembrane helix, which in turn is probably required for the interaction with FtsN, TolA, TolR and FtsL. In addition, I speculate that the proline-rich carboxy-terminus is involved in the interaction with FtsZ. Although the precise function of CedX during divisome assembly is still unclear, it is conceivable that CedX supports the stabilization and coordination of cytoplasmic and periplasmic processes that are crucial for successful cell division. Since CedX lacks any known catalytic domains, I propose that it fulfills a structural function. Thus, CedX could participate in linking different functional modules of the divisome to the Z-ring. At this point, however, it cannot be excluded that an additional, thus far unidentified factor is required for the proposed protein-protein interactions.

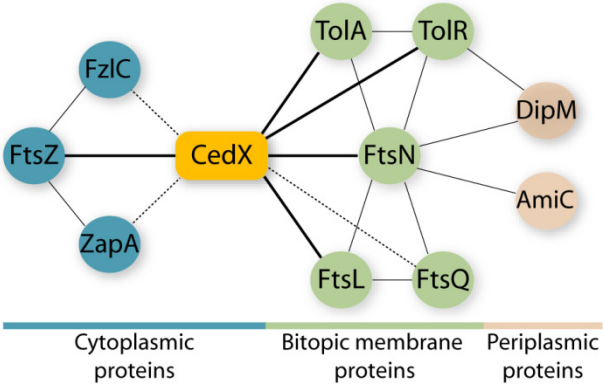

Fig. 30. CedX interaction network. CedX protein-protein interactions as determined by fluorescence microscopy, coimmunoprecipitation and bacterial two-hybrid analysis. Bold lines indicate direct interactions that have been confirmed by at least one method. Dashed lines denote putative indirect interactions. Thin black lines are interactions described by others (see text for details). Note: For simplicity, not every reported interaction is depicted in this scheme.

3.2 Crossbands – Protein diffusion barriers in stalks

The *C. crescentus* stalk is a tubular extension of the cell envelope layers and it has been described as an "organelle" streamlined for the uptake of nutrients [163]. Early reports on the stalk ultrastructure of *C. crescentus* noted the presence of annual structures, also termed crossbands, which traversed the stalk at irregular intervals [117]. Although crossbands were believed to fulfill an architectural and stabilizing role [74, 139], the exact function and biosynthesis of these structures has remained an enigma ever since they have been observed for the first time.

In order to advance the knowledge about the structural and molecular mechanisms that underlie stalk formation, I attempted to identify proteins that are involved in stalk biogenesis and/or morphogenesis. For this purpose, the *C. crescentus* transcriptome [85] was screened for genes that were specifically upregulated during stalk outgrowth and the *in vivo* localization of candidate genes was determined. In total, four proteins were identified, which not only showed a distinct stalk localization pattern but also formed a multiprotein complex. This complex turned out to be the major constituent of crossbands.

3.2.1 Crossband formation

With the exception of early reports on the crossband ultrastructure [66, 74] and the finding that crossbands are produced at the end of each division cycle [120, 152], nothing is known about the mechanisms that underlie crossband formation. Owing to the fact that crossbands are only discernible by electron microscopy, the study of their synthesis has simply not been very straightforward. Since I was able to demonstrate that the distribution of StpB-mCherry signals correlates with the number of crossbands in the stalk, crossband formation can now be traced by fluorescence microscopy. Having identified four proteins that constitute crossbands, I will try to answer several questions concerning crossband formation.

First, when are crossbands made in the *C. crescentus* life cycle? Under non phosphate-limiting conditions, the *C. crescentus* developmental program is tightly regulated in time and space [27]. Synthesis of the crossband proteins StpABCD is initiated during the obligatory swarmer-to-stalked-cell transition. Despite the cell cycle-dependent regulation of *stpABCD* expression, no motif for the transcriptional activation by the respective cell cycle regulator CtrA could be identified in the upstream regioin of these genes [85]. Upon protein synthesis, all four proteins are specifically sequestered to the stalk membrane and periplasm, where they assemble into crossband complexes. Coinciding with medial membrane constrictions in predivisional cells and after stalks had been significantly elongated, StpB-mCherry formed visible foci at the stalk base indicating that StpB, and by implication StpACD, are not involved in initial stalk biogenesis. This conclusion is also corroborated by the finding that cells deficient in crossband proteins do not show any defects in stalk biogenesis. Although the appearance of crossbands was only monitored over two division cycles, these results are in line with earlier work [120, 152]. Thus, and as proposed earlier [120, 152], crossbands may serve as an indicator of "stalk age", which under non-phosphate limiting conditions appears to correlate with cell age. Remarkably, the link between crossband formation and cell cycle is lost when cells are starved for phosphate. In response to nutrient limitation, stalk synthesis continues, while other cell cycle processes are arrested [140, J. Kühn unpublished]. Despite the lack of cell division, the growing stalk is continuously segmented by crossbands at irregular intervals. This finding indicates that crossband formation is coordinated with cell division in nutrient rich environments but appears to be completely uncoupled from cell cycle processes under phosphate-limiting growth conditions. In response to phosphate starvation, a specific subset of proteins is induced including proteins involved in scavenging phosphate sources [87, J. Kühn, unpublished]. Many of these biological activities are encoded by genes that are transcriptionally activated by PhoB [55, 169], which recognizes a conserved sequence motif in the promoter region of its target gene [9, 101]. This regulatory network is also involved in stalk elongation albeit the exact targets of PhoB in this context have not been identified yet. Although previous microarray analyses indicate that at least *stpB* and *stpD* are transcriptionally upregulated in the absence of phosphate sources, no PhoB binding sites were identified upstream of *stpABCD* [J. Kühn, unpublished]. This does not exclude a possible role of PhoB in crossband formation *per se*; however, the molecular mechanism underlying constitutive crossband formation in phosphate-starved cells remains to be elucidated.

Second, how are crossbands assembled? Crossband synthesis is initiated at the stalk pole and achieved by the sequential assembly of its individual components (Fig. 31). Several lines of evidence suggest that crossband formation can be envisioned as a spontaneous, nucleation-driven process. StpA is at the top in the localization hierarchy followed by StpB and StpC. The fourth component StpD, which is encoded further upstream on the chromosome, only requires StpA for recruitment to the complex. In addition, StpA acts as a membrane anchor for the otherwise soluble StpB

molecules. Interestingly, the cellular abundance of StpA appears to be the bottleneck for *de novo* crossband formation. This hypothesis is supported by the finding that (a) in wild-type cells, a moiety of StpB molecules remains in the soluble fraction suggesting that StpA binding sites may be limited, (b) constitutive production of StpA increases the total number of crossbands per stalk, and (c) StpA is absent in swarmer cells and starts to accumulate at the onset of stalk outgrowth whereas at least StpBC are already present at low levels in swarmer cells. Protein complexes rely on and are stabilized by the interactions of its individual components. StpA contains three Sel1 repeats, which fold into structural motifs that mediate diverse interactions between one or more proteins [15]. Thus, StpA may provide both a platform for the localization of downstream crossband components and a nucleation site. Protein interaction studies demonstrated that StpB can be coprecipitated along with StpACD, supporting the idea that StpABCD form a multiprotein complex. This process is presumably triggered as soon as a critical amount of StpB molecules is topologically stabilized by StpA, which accumulates much slower in the cell than StpB during both cell cycle-regulated and uncoupled growth. Concurrently, decreasing StpA concentrations due to StpB binding may also control the termination of the StpAB-nucleation event. Once the StpAB scaffold is assembled, StpC is recruited to the immature crossband. In the absence of StpB, no crossband structures are discernible by electron microscopy (data not shown). However, StpA and StpD still localize in the distinct crossband-like pattern along the stalk, indicating that crossband formation may involve additional StpB-independent assembly steps. Electron cryo-tomographs of wild-type *C. crescentus* cells clearly showed that crossbands traverse the entire stalk periplasm. Thus, the StpABCD complex needs to penetrate the peptidoglycan layer and subsequently establish a connection to the outer membrane. How these two tasks are accomplished is unknown, but they likely involve the biological activities of additional, yet unidentified factors.

Third, if StpA is the crucial factor required for recruiting StpBCD to the stalk base, what localizes StpA to the stalk pole in the first place? So far, I have not been successful in identifying a factor in the localization hierarchy upstream of StpA. Based on current knowledge, I can exclude the following stalk pole proteins: the histidine kinase DivJ (polar morphogenesis and sensing of cytokinesis) [95, 150, 174], the cytoskeletal proteins BacAB and the interacting cell wall synthase PbpC (stalk biogenesis) [81], and also the polymeric pole-organizing protein PopZ [17-18, 42] (data not shown). Another possible hypothesis could be that StpA localization is triggered by a topological cue such as membrane curvature. In fact, recent findings suggest that the multifunctional protein DivIVA, which contributes to Z-ring positioning in *B. subtilis*, recognizes negative (concave) membrane curvature [43, 126], e.g. at the cell pole or the newly completed septum. Conversely, positive membrane curvature (convex) generated by an engulfment process in *B. subtilis* seems to be the localization cue for SpoVM [125]. In *C. crescentus*, the junction between the cell body and the stalk provides a highly positive membrane curvature. In addition to membrane curvature, the chemical composition of stalk peptidoglycan could aid in the localization of StpA. Schmidt and Stanier [139] found that stalks are more resistant to lysozyme and Poindexter and Hagenzieker [119] proposed that the peptidoglycan between the stalk and the cell body is chemically different. Since crossband assembly is initiated after stalk outgrowth, the newly formed junction to the stalk could be specifically recognized by StpA, which then interacts with StpB by a diffusion-and-capture mechanism [131].

Finally, do crossbands contain a central pore? This question cannot be answered satisfyingly due to the lack of experimental evidence. So far, electron micrographs of stalks and isolated crossbands provided only inconclusive information with respect to the overall structure of crossbands [74, 141]. In this study, I did not identify any cytoplasmic crossband components. However, StpD is a

bitopic membrane protein with a short N-terminal region located in the stalk cytoplasm. This region could potentially interact with or recruit additional crossband components.

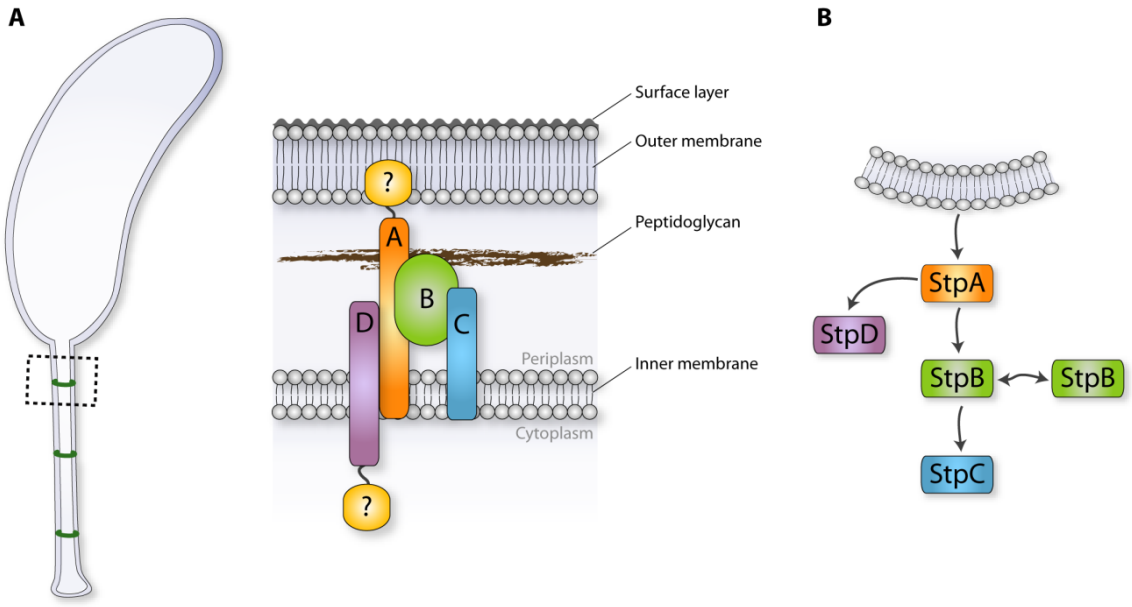

Fig. 31: Model for crossband formation. (A) Crossband assembly. Crossband assembly in the stalk periplasm of *C. crescentus* can be envisioned as a nucleation-driven process in which StpA (orange) and StpB (green) form the crossband scaffold. StpC (blue) and StpD (purple) are accessory crossband proteins. In yellow, possible yet unidentified crossband proteins are depicted. (B) Localization hierarchy. StpA provides the membrane anchor for StpB, which self-interacts and localizes StpC. StpD only requires StpA for proper localization. See text for details.

3.2.2 Physical compartmentalization by a protein diffusion barrier

The current study revealed that crossbands act as protein diffusion barriers. Using fluorescence loss in photobleaching and pulse-labeling experiments, I could demonstrate that inner membrane proteins, periplasmic proteins and outer membrane proteins cannot freely diffuse between stalk and cell body. These findings beg the question about the physiological significance of crossband formation. To address this question we first need to clarify the function of the *C. crescentus* stalk.

C. crescentus thrives in oligotrophic aquatic environments, where inorganic phosphorus is the most common limiting nutrient [111]. As mentioned earlier, low phosphate concentrations significantly enhance lengthening of the *C. crescentus* stalk [55, 137, 140]. Over the past years, the *C. crescentus* stalk has been envisioned as a nutrient scavenging antenna [163]. This hypothesis is based on proteomic analyses of purified stalks revealing that the stalk is enriched in outer membrane transport proteins, whereas it lacks most of the inner membrane components for essential cellular processes or active translocation of nutrients into the cytoplasm [72, 163]. Recently, Wagner et al. [163] used a combination of mathematical modeling of diffusive transport and cellular phosphate uptake experiments to show that the rate of nutrient uptake in diffusion-limited environments is more efficient if cells harbor a long stalk. Based on the theoretical and experimental results, Wagner and co-workers proposed a periplasmic diffusion model for the uptake and transport of nutrients by the stalk and the cell body. This model suggests that nutrient molecules, such as phosphate, are taken up by the stalk and are immediately bound by a high-affinity binding protein in the stalk periplasm.

Captured nutrients then travel along the stalk periplasmic space into the cell body periplasm, where they are actively transported into the cell body cytoplasm, which acts as a nutrient sink.

This model is clearly not in agreement with the current findings as the mobility of the nutrient-binding protein would be limited by crossbands. Thus, I favor a different hypothesis of the stalk function. In nature, *C. crescentus* permanently attaches to surfaces via the holdfast found at the tip of the stalk. To escape an existing surface biofilm or expose the immobilized cell to bulk nutrients, *C. crescentus* elongates its stalk. Concurrently, the lengthening of the stalk results in an increase of membrane surface area. In high phosphate medium, stalk length is about 1.5 μm (r=0.05 μm), which accounts for approximately 10 % additional membrane surface (cell body: r=0.25 μm, l=2.5 μm). However, upon elongation of the stalk to 8 μm this membrane surface area increases to 30 % with respect to the cell body (cell body: r=0.5 μm, l=3.5 μm, after growth in $M2G^{-P}$ for 24 h)[J. Kühn unpublished and data not shown]. In the absence of crossbands, the mobility of periplasmic, inner and outer membrane proteins would be unlimited in the entire cell. Membrane proteins make up approximately 20 % to 30 % of the total protein in a bacterial cell [164], and they are involved in diverse functions in the cells including signal transduction, ATP synthesis or metabolite exchange. The maintenance of a pool of physiologically active proteins in the cell body membranes (and periplasm) is thus an energy-consuming task. Hence, physical compartmentalization of the stalk and the cell body by crossbands could minimize these costs and prevent a constant dilution of this active protein pool due to constitutive stalk growth. Moreover, physical compartmentalization of the *C. crescentus* cell could also allow faster adaptation to a sudden environmental cue (e.g. nutrient availability) that requires the induction and accumulation of a different set of periplasmic or membrane proteins.

Apart from intracellular compartmentalization, crossbands have been suggested to provide protection against the leakage of cellular proteins upon disruption of the stalk [139] However, *C. crescentus* cells that are devoid of crossbands did not display a decrease in the survival rate after mechanical removal of the stalk from the cell body. Thus, a potential "protective" barrier function appears rather unlikely.

While a certain degree of compartmentalization by crossbands is beneficial to restrict protein mobility, overproduction of crossbands reduces the viability of *C. crescentus* dramatically. Under normal growth conditions, StpA controls the initiation of crossband formation at the stalk base. Hence, an artificial increase of cellular StpA (and StpB) could trigger ectopic crossband formation (or at least StpAB scaffold formation). Excessive compartmentalization of the periplasmic space could disrupt essential biological activities. However, the exact nature of the observed phenotype remains to be clarified. It will be interesting to investigatethe cell ultrastructure to determine whether crossbands-like structures can also be found in the cell body under overexpression condtions.

One question that has remained unsolved in this study is whether crossbands also account for a cytosolic diffusion barrier. The inner diameter of the stalk is about 40 nm [163]. Thus, there is hardly any cytoplasm present in the stalk, which could interfere with attempts to detect cytoplasmic proteins in the stalk. So far, no cytoplasmic stalk protein has been identified, neither by mass spectrometry of purified stalks [72, 163] nor by an imaging-based high-throughput screen [172]. Hence, there is no suitable marker protein to test this hypothesis. Notably, cytoplasmic GFP (<5 nm diameter) or ribosomes (<20 nm diameter) cannot enter the stalk (data not shown) [161]. Attempts to use a fluorescent dye to circumvent this problem have failed so far. One attractive hypothesis could be the existence of a cytoplasmic sorting filter at the stalk base, which prevents

random diffusion of proteins into the stalk based on specific molecular recognition. A similar sorting mechanism in combination with a membrane barrier has been recently described for axonal transport of proteins in neurons [151]. However, at this point it cannot be excluded that other molecular mechanism such as destined intracellular protein interaction networks determine the site of cytoplasmic protein localization and in *C. crescentus* [130].

3.3 Concluding remarks about rings and crossbands

Over the past years, *C. crescentus* has emerged as a versatile model system to study prokaryotic cell biology. Two key processes that can be easily traced in *C. crescentus* are cytokinesis and cell differentiation. In *C. crescentus*, and many other prokaryotes, proteins are often localized to their primary site of action [130]. Such subcellular destinations can be the Z-ring or cell poles. By screening for proteins that specifically localize to midcell or to the stalked pole, I identified proteins involved in cell division (CedX) and cell compartmentalization (StpABCD).

At the first glance, cell division appears to be a rather conserved process among most bacteria. However, accumulating reports demonstrate that there are variations on this common theme. These variations become specifically obvious at the level of Z-ring modulators. Here, I report the identification of a novel Z-ring stabilizing protein in *C. crescentus* – CedX. CedX is an accessory divisome component that presumably structurally stabilizes the assembly of late divisome modules and blocks completion of cytokinesis if its cellular abundance exceeds the native protein level. The collected data supports the idea that CedX associates with the divisome. However, to clarify whether CedX directly interacts with FtsZ, additional experimental proof is required. Until recently, CedX could not be overproduced in *E. coli* for subsequent purification. We believe that the unstructured C-terminal tail of the protein is prone to rapid degradation. I was able to overcome this problem by generating a maltose-binding protein (MBP)-CedX hybrid protein (data not shown). Thus, it will now be possible to test for interaction of CedX with FtsZ *in vitro* using co-sedimentation assays or surface plasmon resonance analyses. The exact function of CedX is still not understood and the level of sequence conservation indicates that CedX is a cell division protein that is specifically tailored to the needs of *C. crescentus* and a limited number of stalked alpha-proteobacteria. What these specific needs are remains to be determined.

Intracellular compartmentalization has long been regarded as a feature solely inherited by eukaryotes and different diffusion barrier mechanisms have already been reported for eukaryotes including ciliary membrane protein distribution [67] or axonal transport of membrane proteins and lipids [105, 107]. I found that in *C. crescentus*, diffusion of inner membrane, periplasmic and outer membrane proteins between the stalk and the cell body is restricted by crossbands. The basic structure of crossbands is provided by a putative StpA-B scaffold, which forms in a nucleation-like assembly process. At least two additional accessory proteins, StpC and StpD, are recruited to this scaffold. The precise function of the individual crossband components is still not understood. Crossbands act as protein diffusion barriers that physically separate the stalk and the cell body, thereby providing a novel mechanism for topologically restricting protein mobility in a bacterial cell. This compartmentalization minimizes the costs of maintaining a constant pool of physiologically active proteins in the *C. crescentus* cell body. Initial growth test did not reveal a growth advantage conferred by crossbands under laboratory growth condition. However, for *C. crescentus* growth conditions in natural habitats are much scarcer with respect to nutrient availability. Thus, a revised growth competition assay between wild-type and crossband-deficient

cells that combines more stringent depletion of phosphate with sudden growth boosts may provide further insight in the physiological role of crossbands. Although there is still room for speculation on the exact function of crossbands, it will be interesting to investigate whether this kind of protein compartmentalization is conserved among stalked alpha-proteobacteria.

In conclusion, the existence of crossbands could be another piece of mounting evidence demonstrating that prokaryotes have a highly organized subcellular architecture – similar to their eukaryotic counterparts.

4 MATERIAL AND METHODS

4.1 Materials

4.1.1 Sources of used reagents and enzymes

Common reagents used in this study were acquired from Becton Dickinson (USA), Bioline (Germany), Carl-Roth (Germany), GE Healthcare (Germany), Invitrogen (Germany), Merck (Germany), Millipore (Germany), Perkin Elmer (USA), Peqlab (USA), SIGMA-Aldrich (Germany) or Thermo Scientific (USA).

Enzymes required for the molecular manipulation and cloning of DNA were purchased from New England Biolabs (NEB, USA) or Fermentas (Canada). Size standards for DNA and proteins were obtained from New England Biolabs (NEB, USA) and Fermentas (Canada), respectively.

Specific chemicals are described in the text.

4.1.2 Buffers and solutions

Standard buffers and solutions were prepared according to Ausubel [8] and Sambrook [135] using aqua dest. When required, buffers and solutions were autoclaved (20 min at 121 °C) or filter sterilized (Sarstedt, Germany; pore size 0.22 µm). Specific buffers and solutions are described along with the respective method.

4.1.3 Media

Complex media were autoclaved for 20 min at 121 °C and 2 bar. Media additives, such as antibiotics or carbohydrates, were filter-sterilized (Sarstedt, Germany, pore size 0.22 µm) and added to the cooled down (~ 60 °C) medium. Minimal media were also filter sterilized. To solidify medium, 1.5 % (w/v) agar was added prior to autoclaving.

LB	(lysogeny broth, Miller)	1.0 % (w/v)	Tryptone
		0.5 % (w/v)	Yeast extract
		1.0 % (w/v)	NaCl
PYE	(peptone-yeast-extract)	0.2 % (w/v)	Bacto™Peptone
		0.1 % (w/v)	Yeast extract
		1 mM	$MgSO_4$
		0.5 mM	$CaCl_2$

M2G	(M2-minimal medium supplemented with glucose)	6.1 mM	Na_2HPO_4
		3.9 mM	KH_2PO_4
		10 mM	NH_4Cl
		0.5 mM	$MgSO_4$
		0.5 mM	$CaCl_2$
		0.2 % (w/v)	Glucose
		0.1 % (v/v)	$FeSO_4$/EDTA-Solution
M2G^{-P}	(Phosphate minimal medium)	20 mM	Tris/HCl (pH 7)
		10 mM	NH_4Cl
		3.9 mM	KCl
		0.5 mM	$MgSO_4$
		0.5 mM	$CaCl_2$
		0.2 % (w/v)	Glucose
		0.1 % (v/v)	$FeSO_4$/EDTA-Solution

Media additives

Antibiotics were prepared as stock solutions and added to a final concentration as listed in Table 1.

Table 1. Used antibiotics

Antibiotic	Stock solution [mg/ml]	Final concentration [µg/ml]			
		E. coli (liquid)	*E. coli* (plate)	*C. crescentus* (liquid)	*C. crescentus* (plate)
Ampicillin	100	200	200	-	50
Chloramphenicol in 70 % EtOH	10	20	30	1	1
Gentamycin	1	15	20	0.5	5
Kanamycin	50	50	50	5	25
Spectinomycin	20	50	100	25	50
Streptomycin	10	30	30	-	5

The following carbohydrates were used as media supplements: D(+)-glucose (short: glucose, G), 20 % (w/v) stock solution, 0.2 % final concentration; D(+)-xylose (short: xylose, X), 20 % (w/v) stock solution, 0.3 % final concentration and D(+)-sucrose, 3 % (w/v) final concentration added directly to the medium prior to autoclaving.

Furthermore, vanillic acid was prepared as a 50 mM stock solution and was added in a final concentration of 0.5 mM to the medium.

4.1.4 Oligonucleotides and plasmids

Oligonucleotides were designed using GeneTool Lite 1.0 and generated by either SIGMA-Aldrich (Germany) or Eurofins MWG Operon (Germany). *In silico* plasmid construction was done using Vector NTI Advance™ 11 (Invitrogen, Germany). A complete list of plasmids (Table 7) and oligonucleotides (Table 8) used in this study can be found in the appendix.

4.1.5 Strains

In this study *Caulobacter crescentus* CB15N (NA1000) [47] was used as wild-type strain. The host strain for molecular cloning and bacterial two-hybrid analysis were *Escherichia coli* TOP10 (Invitrogen) F– *mcr*A Δ(*mrr-hsd*RMS-*mcr*BC) Φ80*lacZ*Δ*M*15 Δ*lacX*74 *rec*A1 *araD*139 Δ(*ara leu*) 7697 *galU galK rpsL* (Str^R) *endA*1 *nupG* and *Escherichia coli* BTH101 (Euromedx, France) F- *cya-99 araD139 galE15 galK16 rpsL1 (*Str^R*) hsdR2 mcrA1 mcrB1*, respectively. A list of all strains used in this study can be found in the appendix (Table 6).

4.2 Microbiological and cell biological methods

4.2.1 Cultivation of *E. coli*

E. coli was grown aerobically in LB overnight at 37 °C. Liquid cultures were incubated in a shaker at 210 rpm. For growth on solid media, *E. coli* cells were streaked on LB-agar plates. When *E. coli* was under selection, LB-broth or LB-agar was supplemented with the respective antibiotic (Table 1).

To test for protein-protein interaction using *E. coli* BTH101 derivatives, cells were plated onto McConkey-agar supplemented with 1 % (w/v) D(+)-maltose, 200 µg/ml ampicillin and 50 µg/ml kanamycin. Cells were then cultivated for 24 to 48 h at 28 °C [78].

4.2.2 Cultivation of *C. crescentus*

C. crescentus strains used in this study are derivatives from the synchronizable *C. crescentus* CB15N (NA1000) [47]. *C. crescentus* was cultivated aerobically at 28°C in PYE, M2G or M2G^{-P} [44]. Liquid cultures were incubated in a shaker at 210 rpm. When *C. crescentus* was under selection, liquid or solid medium was supplemented with the respective antibiotic (Table 1).

To grow *C. crescentus* under low-phosphate conditions, a stationary PYE overnight culture was diluted 1:20 into M2G^{-P} and incubated for additional 24 h at 28 °C.

4.2.3 Storage of bacteria

For long-term storage of bacteria stains, overnight cultures were supplemented with 1/10 volume of DMSO (dimethyl sulfoxid) and stored at -80 °C.

4.2.4 Motility assay

To test for motility defects in *C. crescentus*, 2 µl of a cell suspension of an OD_{600} of 0.5 to 0.8 was spotted onto PYE solid media containing only 0.3 % (w/v) agar (soft-agar). Cells were monitored for their swimming ability for 2 days at 28 °C

4.2.5 Test for pili biogenesis

The *C. crescentus* pili-specific bacteriophage ΦCbK can infect cells, which subsequently leads to cell lysis [147]. To test for the presence or absence of pili, late-exponential phase cells were diluted 1:10 in PYE supplemented with 0.5 % (w/v) agar, poured onto a plain PYE agar plate and incubated on the bench top for 30 min. After the soft-agar had polymerized, 10 µl of ΦCbK lysate was spotted onto the plate and incubated at 28 °C for 24 h.

4.2.6 Synchronization

The *C. crescentus* cell cycle yields to two distinct cell types that can be easily separated by an adapted density gradient centrifugation [47]. During the synchronization procedure, cells were constantly kept on ice and centrifuges and required solutions were pre-cooled to 4 °C.

For small-scale isolation of swarmer cells, e.g. for time-lapse microscopy, cells were cultured in 25 ml M2G and harvested at an OD_{600} between 0.3 and 0.6. The cell pellet was resuspended in 750 µl M2 salts and carefully mixed with an equal volume of Percoll (SIGMA-Aldrich, Germany). After centrifugation at 11.000 g for 20 min, cells had been separated into stalked cells (upper band) and swarmer cells (lower band). Swarmer cells were isolated, washed once in 1.5 ml M2 salts at 8.000 g for 1 min and then released into 100 to 200 µl pre-warmed M2G.

For large-scale synchronization, e.g. for time-course experiments, cells were cultured in 1000 ml M2G to an OD_{600} of 0.6. Cells were sedimented at 8.600 g for 15 min and pellets were resuspended in 150 ml M2-salts. This cell suspension was then carefully mixed with 50 ml Ludox AS-40 pH 7-8 (SIGMA-Aldrich, Germany) and separated by centrifugation at 6.300 g for 30 min. Swarmer cells were isolated and washed twice with 50 ml M2 salts at 8.000 g for 10 and 5 min, respectively. Swarmer cells were then resuspended in pre-warmed M2G to a final OD_{600} of 0.3 to 0.4 and incubated at 28 °C. Samples for protein analysis or microscopy were taken at the given intervals.

4.3 Microscopic methods

C. crescentus cells were imaged during the mid-exponential phase of growth after immobilization on 1 % agarose pads using an Axio Imager.M1 microscope (Zeiss, Germany). Differential interference contrast (DIC) images were acquired using a Zeiss Plan Apochromat 100x/1.40 Oil DIC objective and a Cascade:1K CCD camera (Photometrics, USA). Fluorescence imaging was performed using an X-Cite®120PC metal halide light source (EXFO, Canada) in combination with ET-DAPI, ET-CFP (CFP), ET-YFP (eYFP), ET-GFP (eGFP) or ET-TexasRed (mCherry) filter cubes (Chroma, USA). Images were processed with MetaMorph® 7.1.2 (Universal Imaging Group). For cell length measurements, the MetaMorph® region measurement function was used.

Unless indicated differently, the synthesis of inducible fluorescent protein fusions in *C. crescentus* was activated during early-exponential growth with 0.5 mM vanillate or 0.3 % xylose for 2 h and 1 h, respectively. Inducible fluorescent protein fusions of cells grown under phosphate-limiting conditions were induced for 24 h with 0.3 % xylose prior to fluorescence imaging.

Flagellar staining

C. crescentus cells were grown to mid-exponential phase in PYE and fixed by addition of a solution containing paraformaldehyde and $NaPO_4$ (pH 7.5) to final concentrations of 2.5% and 30 mM, respectively. After 30 min incubation at room temperature (RT), the samples were incubated with the fluorescent stain DAPI (1.5 µg/ml, 4',6-diamidino-2-phenylindole) for another 15 min at RT in the dark [83]. The cells were mounted and imaged as described above. For presentation, the images were processed using the Metamorph "Sharpening" function to enhance the visualization of the flagella.

Time-lapse microscopy

To monitor subcellular localization of fluorescent protein fusion over the cell cycle, synchronized *C. crescentus* cells were immobilized on 1 % M2G agarose pads supplemented with the respective inducer. To protect cells from dehydration, the cover-slide was sealed with VLAP (vaseline, lanolin and paraffin at a 1:1:1 ratio). Images were taken at the given time points.

Fluorescence-recovery-after-photobleaching (FRAP) analysis

Photobleaching experiments were performed with a 561 nm solid state laser and a 2D-VisiFRAP Galvo System multi-point FRAP module (Visitron Systems, Germany). Cells were immobilized and protected from dehydration as described before. Experiments were performed at 28 °C using a PECON microscope incubator (Visitron Systems, Germany). Cells were first imaged to establish regions of interest for bleaching (2.500 ms eGFP, 2.500 ms mCherry). After a short laser pulse, cells were imaged immediately and again after 10 min (2.500 ms mCherry). FRAP settings for the different strains are summarized in Table 2.

Table 2. FRAP settings

Strain	Laser pulse [%]	FRAP time per pixel [ms]
SS216	5	3.500
SS269	5	3.500
SS272	14	10.000
JK364	14	10.000
SS160	5	750

Electron microscopy

Electron micrographs of *C. crescentus* cells were taken in collaboration with Dr. K. Bolte (Dept. Biology, FB17, Philipps University, Germany) using a Zeiss CEM902 electron microscope, operated at 80 kV and equipped with a 2048x2048 pixel CCD camera. Cells were spotted onto carbon-coated grids (100 mesh) and allowed to settle for 2 min. The grids were blotted dry, stained with 1:2 diluted supernatant of saturated 1% uranyl acetate (in H_20) for 1min, dried and imaged. Image processing and determination of stalk length was carried out using Adobe Photoshop CS2 (Adobe Systems) and the MetaMorph® 7.1.2 (Universal Imaging Group) region measurement tool.

4.4 Molecular biological methods

4.4.1 Isolation of microbial DNA

Plasmid DNA from *E. coli* and chromosomal DNA from *C. crescentus* was isolated using GenElute™ Plasmid Kit (SIGMA-Aldrich, Germany) and illustra™ bacteria genomicPrep Mini Spin Kit (GE Healthcare, Germany), respectively, following manufacturer's instructions.

Concentration and purity of purified nucleic acids was determined spectroscopically using a Nanodrop ND-1000 (Nanodrop, USA).

4.4.2 Polymerase chain reaction (PCR)

PCR amplification of specific DNA fragments was carried out using KOD Hot Start DNA Polymerase (Merck, Germany) along with the supplied reagents including 1 mM $MgSO_4$, 5 % DMSO, 0.5 µM of the respective oligonucleotide and diluted plasmid DNA (1:100) or chromosomal DNA as template DNA. Successful amplification of PCR fragments was verified by agarose gel electrophoresis (4.4.4) followed by purification of the PCR fragments using either the GeneElute™ PCR Clean-Up Kit (SIGMA-Aldrich, Germany) or GeneElute™ Gel Extraction Kit (SIGMA-Aldrich, Germany).

Plasmid uptake or correct integration of a DNA fragment into the genome of *C. crescentus* or *E. coli* cells was confirmed by colony PCR. A standard colony PCR mixture contained 1x BioMix™ Red (Bioline, Germany), 5 % DMSO, 0.5 µM of the respective oligonucleotide and whole cells (*E. coli* or *C. crescentus*) as template DNA. PCR products were verified by agarose gel electrophoresis (4.4.4).

Standard PCR cycling parameters applied for KOD and colony PCRs are given in Table 3.

Table 3. Standard PCR cycling parameters

Step	Temperature	Time	
Initiale denaturation	95 °C	3 min	
Denaturation	95 °C	45 s	25-30 Cycles
Annealing temperature	65 °C	45 s	
Elongation	72 °C	30 s per kb	
Finale Elongation	72 °C	4 min	

4.4.3 Restriction digestion and ligation of DNA fragments

Molecular manipulation of DNA fragments by restriction digestion was carried out by incubating 2-4 µg DNA with the respective restriction endonuclease (NEB, Germany; Fermentas, Canada) and the recommended buffer for 2 to 12 h at 37 °C. If required, 0.1 mg/ml bovine serum albumin (BSA; NEB, Germany) was added to the reaction mixture. To dephosphorylate 5'-ends, linearized plasmid DNA was treated with shrimp alkaline phosphatase (SAP; Fermentas, Canada). Digested nucleic acids were either purified by agarose gel electrophoresis and the GenElute™ Gel Extraction Kit (SIGMA-Aldrich, Germany) or directly by using the GenElute™ PCR Clean-Up Kit (SIGMA-Aldrich, Germany).

Short sequences encoding e.g. the HA- or His-affinity tags were assembled from oligonucleotides, which were phosporylated with T4 polynucleotide kinase (PNK; Fermentas, Canada), mixed, heated to 95 °C and then annealed. Linker-DNA was ligated into previously linearized vectors.

DNA ligation was performed using T4 DNA ligase and "Rapid Ligation Buffer" (Fermentas, Canada) following the manufacturer's instructions. In general, a 3-fold molar excess of DNA insert was incubated with the recipient vector for 5-60 min at room temperature.

4.4.4 Agarose gel electrophoresis

Nucleic acids were mixed 1:10 with 10 x DNA loading buffer (50 % glycerin, 0.2 % bromphenol blue, 0.2 % xylene cyanol, 0.2 M EDTA) and separated by size in 1 % agarose gels prepared in 0.5 x TAE buffer (20 mM Tris Base, 0.175 % acetic acid, 0.5 mM EDTA). To visualize DNA fragments with UV-light using a UV-Transilluminator (UVP-BioDoc-IT™ Imaging System, UniEquip, Germany), ethidium bromide was added to the agarose gels to a final concentration of 0.005 %. DNA fragments required for downstream applications were excised from the gels and purified using the GenElute™ Gel Extraction Kit (SIGMA-Aldrich, Germany).

4.4.5 Plasmid construction

In silico construction of plasmids was performed using Vector NTI Advance™ 11 (Invitrogen, Germany). A list of constructed plasmids can be found in Table 7 of the appendix section.

Plamids for the expression of N- and C-terminal gene fusions in *C. crescentus*

To construct N- or C-terminal protein fusions that would be integrated into the *C. crescentus* genome at the *vanA* or *xylX* locus by single homologous recombination, genes of interest were PCR amplified with specific oligonucleotides that carried restriction enzymes recognition sites at the 5'-end. PCR products and recipient vectors were treated with the respective restriction endonuclease and ligated in frame as described in section 4.4.3. The following vector backbones [156], [S.Schlimpert, unpublished] were used: pXVENC-2, pVVENC-1, pXCHYC-1, pXCHYC-2, pXGFPC-2, pXBlaMC-2 and pXBlaMN-2.

To generate C-terminal protein fusions encoded at a site of interest, target genes were PCR amplified with specific oligonucleotides that carried restriction enzymes recognition sites at the 5'-end. PCR products and recipient vectors were treated with the respective restriction endonuclease and ligated as described in section 4.4.3. The following vector backbones [156] were used: pGFPC-1, pCHYC-1 and pTCYC-2.

To obtain C-terminal protein fusions to the hemagglutinin- (HA) and polyhistidine- (10xHis) affinity tags, a synthetic double strand encoding either the HA- or 10xHis-tag (Eurofins MWG Operon, Germany) was used to replace the fluorescent gene of the recipient plasmid by restriction digestion and ligation (4.4.3).

High-copy vectors for xylose-inducible gene expression in *C. crescentus*

To achieve high levels of proteins or fusion proteins in cells, genes of interest or fluorescent gene fusions were inserted into the self-replicating plasmids pBXMCS-2 or pBXMCS-6 [156]. For this purpose, the target genes were released from previously constructed plasmids for the inducible expression of N- or C-terminal protein fusion by restriction digestion followed by ligation into pBXMCS-2 or pBXMCS-6.

Plasmids for the overproduction of non-fusion proteins were generated by inserting the PCR-amplified gene of interest directly into pBXMCS-2 or pBXMCS-6.

Plasmids for the construction of markerless deletions or insertions in *C. crescentus*

In-frame deletions in specific genomic regions were generated by double homologous recombination, which left 10 to 12 of the terminal codons of the target gene in the genome. For this purpose, two fragments, 500-600 bps directly up- and downstream of the target gene, were PCR amplified, purified and fused in a second PCR by overlap extension (9 bps overlap). The final PCR product was purified, treated with the respective endonucleases and cloned into the suicide vector pNPTS138 (M.R. Alley, unpublished). This vector carries a kanamycin resistance cassette and the *sacB* gene for counter-selection. Derivatives of pNPTS138 were isolated from *E. coli* TOP10 and then used to transform wild-type *C. crescentus* by electroporation. Recombinant *C. crescentus* cells were first selected for growth in the presence of kanamycin (first recombination event). Resistant colonies were re-streaked and then cultured in plain PYE medium to late exponential phase, diluted 1:100 and spread onto PYE agar that contained 3 % sucrose to select for the second recombination event yielding either wild-type *C. crescentus* or a markerless in-frame deletion strain. Single colonies that arose on PYE-sucrose plates were tested in parallel for kanamycin sensitivity and sucrose resistance. Deletion of the target gene was verified by colony PCR.

Replacement of a native gene with a hybrid-gene fusion was achieved by a similar protocol. The target gene was first cloned in the appropriate plasmid for the construction of C-terminal gene fusions. A 500-600 bp fragment immediately downstream of the target gene was amplified from the genome by PCR, purified, treated with the respective restriction enzymes and then inserted downstream of the fusion tag in the previously constructed plasmid. The "gene-fusion-downstream" fragment was liberated from this plasmid, gel-purified and ligated into pNTPS138. Construction of the recombinant *C. crescentus* strain was carried out as described above.

Plasmids for bacterial two-hybrid analysis in *E. coli*

To generate derivatives of the bacterial two-hybrid vectors pUT18, pUT18C, pKNT25, pKT25 [78], genes of interest were PCR amplified using oligonucleotides that carried a *BglII* and a *EcoRI* cleavage site at their 5' and 3' end, respectively. PCR products were purified by agarose gel electrophoresis and ligated in both orientations into the appropriate bacterial two-hybrid vector that had previously been treated with *BamHI* and *EcoRI*.

4.4.6 DNA sequencing

DNA sequencing was performed by Eurofins MWG Operon (Germany). Sequencing reactions contained 50-100 ng purified plasmid or PCR product; sequencing oligonucleotides were provided separately. Obtained sequences were analyzed with Vector NTI Advance™ 11 (Invitrogen, Germany).

4.4.7 Preparation and transformation of chemically competent *E. coli*

Preparation of chemically competent *E. coli* was performed using a modified protocol of Sambrook [135]. *E. coli* was cultured overnight and diluted 1:100 in 250 ml LB medium. Cells were grown to an OD_{600} of 0.6, placed onto ice for 10 min and sedimented. After the cell pellet was resuspended in 15 ml ice-cold 0.1 M $CaCl_2$, the cell suspension was incubated on ice for additional 30 min.

Cells were again collected by centrifugation followed by resuspension in 4 ml of ice-cold 0.1 M $CaCl_2$ with 15 % (v/v) glycerol. Aliquots of 150 µl were snap-frozen in liquid nitrogen and stored at -80 °C.

To transform chemically competent *E. coli*, cells were thawed on ice, mixed with 15 µl of the ligation reaction or 10 ng of bacterial two-hybrid plasmids and incubated for 30 min on ice. After performing a heat-shock for 90 s at 42 °C, cells were again placed on ice for 5 min and then supplemented with 800 µl LB medium. This cell suspension was incubated for 60 min at 37 °C and then spread onto LB- or McConkey agar supplemented with the respective antibiotics. Single colonies appeared after 12-16 h (TOP10) or 24-48 h (BTH101) of incubation. Recombinant *E. coli* were re-streaked onto fresh agar plates and verified by colony PCR.

4.4.8 Preparation and transformation of electrocompetent *C. crescentus*

To prepare electrocompetent *C. crescentus,* cells were grown in 2x PYE to an OD_{600} of 1.0 and processed according to [44]. Briefly, cells were washed in ice-cold 10 % (v/v) glycerol, twice in 1 volume and once in 1/10 volume at 6.800 g, 4 °C and for 10 min. The final cell pellet was resuspended in 1/50 volume of ice-cold 10 % glycerol. Aliquots of 80 µl were snap-frozen in liquid nitrogen and stored at -80 °C.

To introduce plasmid constructs, electrocompetent *C. crescentus* cells were thawed on ice and mixed with 8 µl purified plasmid. In case of replicating plasmids, only 1 µl of purified plasmid was used. This reaction mixture was then transferred to a sterile electroporation cuvette, electroporated at 1.5 kV, 400 Ω and 25 µF and immediately mixed with 900 µl ice-cold 2x PYE. The cell suspension was allowed to recover for 2 to 3 h at 28 °C followed by selection for recombinant *C. crescentus* on PYE agar supplemented with the appropriate antibiotic for 2 to 3 days at 28 °C. Single colonies were re-streaked onto new PYE agar plates and successful plasmid integration or uptake was confirmed by colony PCR.

4.4.9 Transduction of *C. crescentus*

Transduction of *C. crescentus* was performed according to Ely [45]. First, phage lysate of the *C. crescentus* donor strain was prepared. For this purpose, 500 µl late-exponential phase cells were incubated with 2 µl phage ΦCr30 (>1000PFU/ml) for 15 min at room temperature, mixed with 5 ml PYE soft-agar (PYE + 0.3 % agar + 0.2 % (v/v) glucose) and subsequently poured onto a plain PYE plate. This plate was incubated for 24 h, after which plaque formation was visible. PYE soft-agar was resuspended by addition of 6 ml PYE followed by incubation overnight on a shaker at room temperature. The soft-agar/cell suspension was transferred to a falcon tube (Sarstedt, Germany) and 100 µl of chloroform were added to the suspension followed by vortexing for 10 s. Cell debris and residual soft-agar were sedimented by centrifugation at 4.600 g at room temperature. The supernatant consisting of active phage lysate was transferred to a new falcon tube, mixed with 100 µl chloroform, vortexed for 10 s and stored at 4 °C for up to 2 years. For transduction, the obtained phage lysate was inactivated in an ultraviolet crosslinker at 120 mJoules/cm². Late-exponential phase cells (225 µl) of the *C. crescentus* recipient strain were mixed with 25 µl of inactivated phage lysate, incubated for 60 min at room temperature and spread onto PYE agar supplemented with the appropriate antibiotic to select for chromosomal integration of the desired donor DNA. Single colonies arose after 2 to 3 days of incubation at 28 °C. *C. crescentus* colonies were re-streaked onto a new PYE plate and successful integration was verified by colony PCR.

4.4.10 UV mutagenesis of *C. crescentus*

UV mutagenesis with *C. crescentus* [123] was performed using an ultraviolet crosslinker with mid-exponential phase cells irradiated with different settings (5, 10, 20, 40 mJoules). Radiated cells were diluted 1:4 in 3 ml PYE, cultured to mid-exponential phase and made electrocompetent (4.4.8). Cells were then transformed with pSS8 (Table 7) and incubated for 3 h at 28 °C. Suppressor mutants were selected on PYE agar supplemented with 0.3 % xylose and kanamycin.

4.5 Biochemical methods

4.5.1 SDS-Polyacrylamide gel electrophoresis (SDS-PAGE)

Proteins were separated by SDS-PAGE according to Lämmli [82]. To prepare protein samples of cell lysates, mid-exponential phase cells were pelleted and resuspended in 1x sodium dodecyl sulfate (SDS) sample buffer (300 mM Tris Base, 50 % (v/v) glycerol, 5 % (w/v) SDS, 500 mM dithiothreitol, 0.05 % bromphenol blue, pH 6.8). The total volume of sample buffer added to the pellet was calculated according to the initial OD_{600} of the sample: the pellet of a culture with an OD_{600} of 1 was resuspended in 100 µl 1x sample buffer. Lysates were boiled for 10 min at 95 °C and loaded along with a molecular weight marker (PageRuler™ Prestained Protein Ladder, Fermentas, Canada) on a SDS-PAGE consisting of a 5 % stacking gel and an 11 % stacking gel (Table 4). Electrophoresis was performed in a Tris/Glycine buffer (25 mM Tris Base, 192 mM glycine, 0.1 % (w/v) SDS) at 15-30 mA per gel using a PerfectBlue™ Twin S system (Peqlab, USA).

Following electrophoresis, SDS-PAGEs were either stained for 45 min in Coomassie (40 % methanol, 10 % acidic acid, 0.1 % (w/v) Brilliant Blue R 250) and destained (20 % ethanol, 10 % acidic acid) to visualize resolved proteins directly or SDS-PAGEs were processed further for specific protein detection by immunoblot analysis (4.5.2).

Table 4. Composition of a 5 % stacking gel and an 11 % resolving gel

Component	5 % stacking gel (2.5 ml)	11 % resolving gel (5 ml)
Aqua dest.	1.43 ml	1.9 ml
500 mM Tris Base pH 6.8 0.4 % (w/v) SDS	625 µl	-
1.5 M Tris Base pH 8.8 0.4 % (w/v) SDS	-	1.25 ml
30 % Rotiphorese® NR-Acrylamide/Bis- (29:1)	417 µl	1.9 ml
TEMED (N,N,N,N-Tetramethylethylenediamine)	1.9 ml	3 µl
10 % (w/v) APS (Ammonium persulfat)	25 µl	40 µl

4.5.2 Immunoblot analysis

For specific detection of proteins, proteins were first resolved on a 11 % SDS-PAGE as described above and then transferred onto a polyvenylidene fluoride (PVDF)-membrane (Millipore, USA) by semi-dry western blot transfer. PVDF membranes were first incubated in methanol for 15 s,

washed in aqua dest. for 2 min and equilibrated in western blot transfer buffer (25 mM Tris Base, 192 mM glycine, 10 % methanol) for 5 min. Proteins were blotted onto the membrane using 2 mA/cm² for 1.5-2 h and a PerfectBlue™ Semi-Dry-Elektro Blotter (Peqlab, USA). Obtained membranes were blocked overnight in 1x TBST (10 mM Tris Base, 150 mM NaCl, 0.1 % (w/v) Tween20, pH 7.5) containing 5 % (w/v) non-fat dry milk on a shaker at 4 °C.

Detection of proteins was achieved with protein-specific antibodies or anti-sera (Table 5). For this purpose, blocked membranes were briefly washed in 1x TBST and then incubated with the primary antibody. Except for α-His, which was dissolved in 1x TBST containing 3 % BSA (bovine serum albumin), primary antibodies were provided in 1x TBST containing 5 % non-fat dry milk. Membranes were incubated for 1-2 h on a shaker at room temperature and washed trice with 1x TBST prior to incubation with the secondary antibody for 1-2 h. Secondary anti-rabbit IgG horseradish perioxidase- (HRP) or anti-mouse IgG HRP-coupled antibodies were dissolved in 1x TBST with 5 % non-fat dry milk. Next, membranes were washed three times with 1x TBST and incubated with a chemiluminescence substrate (Western Lightning™ Chemiluminescence Reagent Plus; Perkin Elmer, USA) according to manufacturer's instructions. Subsequently, signals were visualized by exposure to Amersham Hyperfilm™ ECL-Chemiluminenscence films (GE Healthcare, Germany).

Table 5: Antibodies used for immunoblot analysis

Antibody	Concentration	Comment/Reference
Primary antibodies		
α-CtrA	1:10.000	[39]
α-CedX	1:5.000	Generated by immunization of rabbits with peptide CEAIVRRPLPPRPVRE and THSDQDELPFDLDED
α-HA	1:8.000	Millipore, Germany
α-His	1:5.000	SIGMA-Aldrich, Germany
α-FtsZ (b)	1:6.000	[98]
α-SpmX	1:50.000	[124]
α-StpA	1:2.500	Generated by immunization of rabbits with peptide YPPESPDSGVPHSDEA and VSRPPRAAGERPQPRP
α-TipN	1:10.000	[69]
α-GFP	1:10.000	SIGMA-Aldrich, Germany
α-mRFP1	1:10.000	[25]
Secondary antibodies		
α-rabbit-HRP	1:20.000	Perkin Elmer, USA
α-mouse-HRP	1:5.000	SIGMA-Aldrich, Germany

4.5.3 Protein fractionation

Biochemical fractionation was performed using a modified protocol of Chen et al. [25]. *C. crescentus* was cultured in 80 ml PYE to an OD_{600} of 0.6 and harvested by centrifugation at 6215 g for 10 min at 4 °C. Cell pellets were washed once with 1 volume buffer A (0.2 M Tris-HCl pH 8) and were finally resuspended in 1/10 volume buffer B (60 mM Tris-HCl pH 8, 0.2 M sucrose, 0.2 mM EDTA). This cell suspension was incubated with 100 µg/ml phenylmethylsulfonyl fluorid (PMSF), 5 µg/ml DNaseI and 10 mg/ml lysozyme for 10 min on a shaker at room temperature. To promote cell lysis, a freeze (-80 °C)-and-thaw cycle was included prior to cell rupture by sonication (5 x 5 s, 30 % output; Branson Sonifier, Germany). Remaining intact cells and cell debris were removed by centrifugation at 4.000 g for 10 min at 4 °C. Proteins were fractionated by three subsequent ultracentrifugation steps at 100.000 g for 1 h at 4°C using a Beckman-Coulter Optima™ Max-XP ultracentrifuge. After the first centrifugation, the supernatant containing soluble proteins was removed and mixed with an appropriate amount of 2x SDS sample buffer. The pellet was washed once with 1 volume buffer A. After the third centrifugation step, the pellet was resuspended in 1 volume buffer B and mixed with 2x SDS sample buffer. Protein samples were boiled for 10 min at 95 °C and analyzed by immunoblotting using antibodies against CtrA and SpmX as controls to confirm successful separation of soluble and membrane proteins.

4.5.4 Coimmunoprecipitation and mass-spectroscopy

Proteins that were coprecipitated along with CedX and StpB were analyzed by matrix-assisted laser desorption/ionization time-of-flight (MALDI-TOF) mass spectroscropy (MS). MS analyses were performed in collaboration with Jörg Kahnt (Dept. Ecophysiology, MPI Marburg).

CedX-HA

For coimmunoprecipitation of CedX-HA, *C. crescentus* SS48 and CB15N (negative control) were cultured in 750 ml M2G. Proteins were crosslinked with 0.6 % *para*-formaledhyde (in 1x PBS pH 7.4) for 20 min at 28 °C. The reaction was quenched with 125 mM glycine (in 1x PBS pH 7.4) for 5 min at room temperature. Cells were harvested by centrifugation at 8.622 g, 4 °C for 10 min and washed once with ½ volume buffer I. Cell pellets (~1 g) were frozen in liquid nitrogen and stored at -80 °C. Cell pellets were thawed on ice, washed in 100 ml Co-IP buffer and resuspended in 1/10 volume Co-IP buffer supplemented with 10 mM $MgCl_2$, 10 mg/ml lysozyme, 5 µg/ml DNaseI and 100 µg/ml phenylmethylsulfonylfluorid (PMSF). After 30 min on ice, cells were disrupted by two french press passages at 16.000 psi. Cell debris was removed by centrifugation at 13.000 g for 5 min at 4 °C. 2 ml of cell lysate was then incubated with 80 µl EZview™ Red Anti-HA Affinity Gel (SIGMA-Aldrich, Germany) for 2 h on a rotary shaker at 4 °C. Preparation of the anti-HA affinity gel was carried out according to the manufacturer's instructions. Affinity gel-sample complexes were washed twice with wash buffer II and thrice with wash buffer III. Precipitated proteins were eluted from the affinity gel with 200 µl 0.1 M glycine-HCl pH 2.5 (in H_2O) and submitted to mass-spectroscopic analysis.

Co-IP buffer	20 mM	HEPES pH 7.4
	100 mM	NaCl
	20 %	Glycerol
	0.5 %	Triton X-100

Wash buffer I	50 mM	$NaPO_4$ pH 7.4
	5 mM	$MgCl_2$
Wash buffer II	50 mM	TrisHCl pH 7.5
	150 mM	NaCl
	1 mM	EDTA
	0.5 %	Triton X-100
Wash buffer III	100 mM	TrisHCl pH 8
	750 mM	NaCl
	1 mM	EDTA
	0.05 %	Triton X-100

StpB-His

For coimmunoprecipitation of StpB-His, *C. crescentus* strain SS233 (*stpB*::*stpB-His*) and CB15N (wild-type) were cultured in 1.000 ml $M2G^{-P}$ for 12 h. Proteins were crosslinked with 0.6 % paraformaledhyde (in 1x PBS pH 7.4) for 20 min at 28 °C. The reaction was quenched with 125 mM glycine (in 1x PBS pH 7.4) for 5 min at room temperature. Cells were harvested by centrifugation at 8.622 g, 4 °C for 10 min and washed once with ½ volume buffer I. Subsequently, cell pellets (~1 g) were frozen in liquid nitrogen and stored at -80 °C. Cell pellets were thawed on ice and resuspended in 5 ml Co-IP/lysis buffer supplemented with the Lysonase™ Bioprocessing Reagent (Merck, Germany). Since cell lysis was not complete after 40 min of incubation, cells were lysed by two french press passages at 16.000 psi and cell debris was removed by centrifugation at 16.000 g for 20 min at 4 °C. To reduce unspecific binding to the dynabeads, lysates were pre-incubated with 10 µl dynabeads protein G for 10 min at room temperature on a rotary shaker. 1 ml of pre-cleared lysate was then incubated with 50 µl dynabeads crosslinked to monoclonal α-His (SIGMA-Aldrich, Germany) for 60 min at room temperature on a rotary shaker. Preparation and crosslinking of the antibody to the beads using 5 mM *bis*-sulfosuccinimidyl (BS^3) was carried out according to the manufacturer's instructions. Bead-antibody-sample complexes were washed thrice with wash buffer II and III, respectively. Precipitated proteins were eluted from the beads with 400 µl 0.2 % formic acid pH 2.5 (in H_2O) and submitted to mass-spectroscopic analysis.

PBS (phosphate buffered saline, pH 7.4)	137 mM	NaCl
	2.7 mM	KCl
	10 mM	Na_2HPO_4
	2 mM	KH_2PO_4
Co-IP/lysis buffer	5 ml	BugBuster® (Merck, Germany)
	0.5 % (w/v)	n-Dodecyl-β-D-maltoside
	100 µg/ml	Phenylmethylsulfonylfluorid
	10 µl	Lysonase™ Bioprocessing Reagent (Merck, Germany)
Wash buffer I	20 mM	NaPO4 pH 7.4
	50 mM	NaCl
	1 mM	EDTA

Wash buffer II	50 mM	TrisHCl pH 7.5
	150 mM	NaCl
	1 mM	EDTA
	100 µg/ml	Phenylmethylsulfonylfluorid
	0.5 % (w/v)	n-Dodecyl-β-D-maltoside
Wash buffer III	100 mM	TrisHCl pH 7.5
	750 mM	NaCl
	1 mM	EDTA
	0.05 % (w/v)	n-Dodecyl-β-D-maltoside

4.6 Bioinformatic methods

C. crescentus CB15N nucleotide- and protein sequences were obtained from NCBI (http://www.ncbi.nlm.nih.gov/guide/) and were analyzed using the NCBI Blastn- or Blastp-algorithm and the EMBL SMART algorithm (http://smart.embl-heidelberg.de/).

Predictions for transmembrane domains, signal peptides or subcellular protein localization were obtained by using TOPCONS (http://topcons.cbr.su.se/), TMHMM and SignalP (both at http://www.cbs.dtu.dk/services/), PSORTb (http://www.psort.org/psortb/) and CELLO (http://cello.life.nctu.edu.tw/).

Statistical analysis of the distribution of crossbands in stalks from various strains backgrounds was performed using the *t*-Test analysis tool (2 populations, test type "independent", significance level α=0.0001) of Origin 6.1.

APPENDIX

Table 6. *C. crescentus* strains

Strain	Genotype	Construction / [Ref]
CB15N	Synchronizable derivative of wild-type strain CB15	[47]
AM52	CB15N ⊿*vanA* ⊿*ftsN* P_{van}::P_{van}-*ftsN*	[100]
AM138	CB15N P_{xyl}::P_{xyl}-*venus-ftsA*	A. Möll
CS606	CB15N Δ*bla* (Δ*CC2137*)	[173]
LS3118	CB15N Δ*pilA*	[147]
MT45	CB15N *ftsN*::*cfp-ftsN*	[100]
MT199	CB15N P_{van}::*ftsZ-eyfp*	M. Thanbichler
MT246	CB15N Δ*cedX*	M. Thanbichler
MT240	CB15N P_{van}::P_{van}-*ftsZ-mcherry*	M. Thanbichler
MT253	CB15N cedX::cedX-mcherry	M. Thanbichler
SW33	CB15N P_{xyl}::P_{xyl}-*stpA-mcherry*	Integration of pSW35 in CB15N, S. Wick
SW30	CB15N P_{xyl}::P_{xyl}-*stpB-mcherry*	Integration of pSW35 in CB15N, S. Wick
SW49	CB15N Δ*stpA*	Integration of pSW51 in CB15N S. Wick
SW50	CB15N Δ*stpB*	Integration of pSW52 in CB15N S. Wick
SW51	CB15N Δ*stpAB*	Integration of pSW53 in CB15N S. Wick
UJ506	CB15N Δ*pleC*	[5]
YB1585	CB15N *ftsZ*::P_{xyl}-*ftsZ*	[168]
CedX project		
SS1	CB15N P_{xyl}::P_{xyl}-*cedX-venus*	Integration of pSS1 in CB15N
SS2	CB15N pP_{xyl}-*cedX*	Transformation of CB15N with pMT780
SS6	CB15N pBXMCS-2	Transformation of CB15N with pBXMCS-2
SS10	CB15N cedX::cedX-mcherry P_{van}-ftsZ-venus	Transduction of Kan^R from MT199 into MT253
SS17	CB15N ftsN::cfp-ftsN pP_{xyl}-cedX-venus	Integration of pSS8 in MT45
SS20	CB15N Δ*vanA* Δ*ftsN* P_{van}::P_{van}-*ftsN*, P_{xyl}::P_{xyl}-*cedX-venus*	Transduction of Kan^R from SS1 into AM52
SS28	CB15N *cedX*::*cedX*-HA	Integration of pSS15 in CB15N
SS37	CB15N *ftsZ*::P_{xyl}-*ftsZ*, P_{van}::P_{van}-*cedX-venus*	Integration of pSS17 in YB1585
SS38	CB15N *ftsN*::*cfp-ftsN* P_{xyl}::P_{xyl}-*cedX-venus*	Transduction of Kan^R from SS1 into MT45

Strain	Genotype	Construction / [Ref]
SS48	CB15N Δ*cedX* pPxyl::*cedX*-HA	Tranformation of SS28 with pSS22
SS49	CB15N Δ*cedX* pP_{xyl}-$cedX_{\Delta 1-32}$-*venus*	Transformation of MT246 with pSS20
SS56	CB15N cedX::cedX-mcherry P_{xyl}-*venus-ftsA*	Transduction of KanR from AM138 into MT253
SS63	CB15N Δ*cedX* pP_{xyl}-$cedX_{\Delta 294-309}$-*venus*	Transformation of MT246 with pSS12
SS65	CB15N Δ*cedX* pP_{xyl}-$cedX_{\Delta 51-287}$-*venus*	Transformation of MT246 with pSS30
SS112	CB15N P_{van}::P_{van}-*ftsZ-mcherry* pP_{xyl}-*cedX-cfp*	Transformation MT240 with pSS75
SS113	CB15N Δ*cedX* pP_{xyl}-*cedX-cfp*	Transformation of MT246 with pSS75
SS148	CB15N P_{xyl}::P_{xyl}-*cedX-venus* pP_{xyl}-*ftsZ*-G109S	Transformation of SS1 with pEG284
Crossband project		
SS141	CB15N Δ*stpA* P_{xyl}::P_{xyl}-*stpB-mcherry*	Integration of pSW32 in SW51
SS142	CB15N Δ*stpB* P_{xyl}::P_{xyl}-*stpA-mcherry*	Integration of pSW35 in SW50
SS146	CB15N Δ*stpB* P_{xyl}::P_{xyl}-*stpB-mcherry*	Integration of pSW32 in SW50
SS158	CB15N P_{xyl}::P_{xyl}-$stpA_{\Delta 394-466}$-*mcherry*	Integration of pSS114 in CB15N
SS160	CB15N *stpB*::*stpB-mcherry*	Integration of pSS109 in CB15N
SS163	CB15N P_{xyl}::P_{xyl}-bla^{ss}-$stpA_{\Delta 1-48}$-*mcherry*	Integration of pSS122 in CB15N
SS165	CB15N Δ*bla* P_{xyl}::P_{xyl}-*stpB-bla*	Integration of pSS120 in CS606
SS169	CB15N Δ*stpB* P_{xyl}::P_{xyl}-bla^{ss}-$stpB_{\Delta 1-27}$-*mcherry*	Integration of pSS121 in SW50
SS172	CB15N Δ*bla* P_{xyl}::P_{xyl}-*stpA-bla*	Integration of pSS119 in CS606
SS179	CB15N Δ*stpB* P_{xyl}::P_{xyl}-bla^{ss}-$stpB_{27-315}$-*mcherry*	Integration of pSS130 in SW50
SS189	CB15N Δ*stpA* Pxyl::P_{xyl}-*stpA*	Integration of pSS138 in SW49
SS191	CB15N *ftsZ*::P_{xyl}-*ftsZ* P_{van}::P_{van}-*stpB-mcherry*	Integration of pSS142 in YB1585
SS193	CB15N Δ*stpA* P_{xyl}::P_{xyl}-$stpA_{\Delta 95-137}$-*mcherry*	Integration of pSS134 in SW49
SS214	CB15N *stpB*::*stpB-mcherry* pP_{xyl}-*stpAB*	Transformation of SS160 with pSW64
SS216	CB15N Δ*stpAB* pP_{xyl}-*tdimer2*	Transformation of SW51 with pEJ216
SS220	CB15N Δ*stpA stpB*::*stpB*-His	Integration of pSS187 in SW49
SS226	CB15N P_{xyl}::P_{xyl}-*stpD-gfp*	Integration of pSS202 in CB15N
SS228	CB15N P_{xyl}::P_{xyl}-*stpC-mcherry*	Integration of pSS204 in CB15N
SS232	CB15N stpB::*stpB-mcherry*	Integration of pSS200 in CB15N
SS233	CB15N *stpB*::*stpB*-His	Integration of pSS187 in CB15N
SS234	CB15N Δ*stpAB* P_{xyl}::P_{xyl}-*stpD-gfp*	Integration of pSS202 in SW51
SS236	CB15N Δ*stpAB* P_{xyl}::P_{xyl}-*stpC-mcherry*	Integration of pSS204 in SW51
SS237	CB15N *stpB*::*stpB-mcherry* P_{xyl}::P_{xyl}-*stpD-gfp*	Integration of pSS202 in SS232
SS239	CB15N Δ*stpC*	Integration of pSS209 in CB15N
SS240	CB15N Δ*stpC* P_{xyl}::P_{xyl}-*stpD-gfp*	Integration of pSS202 in SS239

Strain	Genotype	Construction / [Ref]
SS243	CB15N stpD::*stpD-gfp* P_{xyl}::P_{xyl}-*stpA-mcherry*	Integration of pSS205 in SW33
SS244	CB15N *stpD*::*stpD*-His	Integration of pSS206 in CB15N
SS247	CB15N *stpC*::*stpC*-His	Integration of pSS210 in CB15N
SS248	CB15N stpD::stpD-gfp	Integration of pSS205 in CB15N
SS249	CB15N *stpD*::*stpD-gfp* P_{xyl}::P_{xyl}-*stpC-mcherry*	Integration of pSS205 in SS228
SS250	CB15N Δ*stpCD*	Integration of pSS208 in SS239
SS252	CB15N Δ*stpD*	Integration of pSS208 in CB15N
SS258	CB15N *stpB*::*stpB-mcherry* pBXMCS-2	Transformation of SS160 with pBXMCS-2
SS259	CB15N Δ*stpABC*	Integration of pSS215 in SW51
SS263	CB15N Δ*stpD* P_{xyl}::P_{xyl}-*stpC-mcherry*	Integration of pSS204 in SS252
SS264	CB15N Δ*stpB* P_{xyl}::P_{xyl}-*stpD-gfp*	Integration of pSS202 in SW50
SS265	CB15N Δ*stpB* P_{xyl}::P_{xyl}-*stpC-mcherry*	Integration of pSS204 in SW50
SS269	CB15N *stpD*::*stpD-gfp* pP_{xyl}-*tdimer2*	Transformation of SS248 with pEJ216
SS272	CB15N Δ*stpAB* P_{xyl}::P_{xyl}-*gspG*	Integration of pJK86 in SW51
SS273	CB15N Δ*bla* P_{xyl}::P_{xyl}-*stpC-blaM*	Integration of pSS220 in CS606
SS274	CB15N Δ*bla* P_{xyl}::P_{xyl}-*stpD-blaM*	Integration of pSS221 in CS606
SS275	CB15N Δ*bla* P_{xyl}::P_{xyl}-*blaM-stpD*	Integration of pSS222 in CS606
SS277	CB15N *stpD*::*stpD-gfp* P_{xyl}::P_{xyl}-*gspG*	Integration of pJK86 in SS248
SS283	CB15N *stpD*::*stpD-gfp* P_{xyl}::P_{xyl}-*elpS*	Integration of pSW67 in SS248
SS284	CB15N Δ*stpAB* P_{xyl}::P_{xyl}-*elspS*	Integration of pSW67 in SW51

Table 7. Plasmids

Plasmid	Genotype/description	Reference/Source
pBXMCS-2	Plasmid for overproduction of proteins in *C. crescentus*, Kan^R	[156]
pXVENC-2	Integration plasmid for constructing C-terminal fusions to Venus under the control of P_{xyl}, Kan^R	[156]
pXCHYC-2	Integration plasmid for constructing C-terminal fusions to mCherry under the control of P_{xyl}, Kan^R	[156]
pXGFPC-2	Integration plasmid for constructing C-terminal fusions to GFP under the control of P_{xyl}, Kan^R	[156]
pXBlaMC-2	Integration plasmid for constructing C-terminal fusions to β-lactamase under control of P_{xyl}, Kan^R	This study
pXBlaMN-2	Integration plasmid for constructing N-terminal fusions to β-lactamase under control of P_{xyl}, Kan^R	This study
pVVENC-1	Integration plasmid for constructing C-terminal fusions to Venus under the control of P_{van}, $Spec/Str^R$	[156]
pVCHYC-1	Integration plasmid for constructing C-terminal fusions to mCherry under the control of P_{van}, $Spec/Str^R$	[156]

Plasmid	Genotype/description	Reference/Source
pCHYC-1	Integration plasmid for constructing C-terminal fusions to mCherry at the site of interest, Spec/Str^R	[156]
pGFPC-1	Integration plasmid for constructing C-terminal fusions to GFP at the site of interest, Spec/Str^R	[156]
pTCYC-2	Integration plasmid for constructing C-terminal fusions to the tetracysteine tag at the site of interest, Kan^R	[156]
pNPTS138	*sacB*-containing suizide vector used for double homologous recombination, Kan^R	M.R.K. Alley, unpublished
pUT18	Plasmid for constructing C-terminal fusions to T18, Amp^R	[78]
pUT18C	Plasmid for constructing C-terminal fusions to T18, Amp^R	[78]
pKT25	Plasmid for constructing C-terminal fusions to T25, Kan^R	[78]
pKNT25	Plasmid for constructing C-terminal fusions to T25, Kan^R	[78]
pUT18C-zip	Derivative of pUT18C in which the leucine zipper of GCN4 is genetically fused in frame to the T18 fragment	[78]
pKT25-zip	Derivative of pKT25 in which the leucine zipper of GCN4 is genetically fused in frame to the T25 fragment	[78]
pMT780	pBXMCS-2 carrying *cedX*	M. Thanbichler
pEJ216	Replicating plasmid carrying *torA^{ss}-tdimer2* under control of P_{xyl}, Cam^R	[76]
pEG284	Replicating plasmid carrying *ftsZ* G109S under control of P_{xyl}, Cam^R	[54]
pXBlaCHYC-1	Integration plasmid carrying the *bla* signal peptide and *mcherry* for the contruction of C-terminal fusion under the control of P_{xyl}, Spec/Strp^R	A. Möll
pAM113	pKT25 carrying *tolR* (*CC3232*)	[99]
pAM114	pUT18 carrying *tolR* (*CC3232*)	[99]
pAM119	pKT25 carrying *tolA* (*CC3231*)	A. Möll
pJK86	pXCHYC-2 carrying *gspG* (*CCNA_00175*)	J. Kühn
pMT750	pXCHYC-2 carrying *cedX* (*CCNA_02091*)	M. Thanbichler
pMT773	pNTPS138-based plasmid for constructing an in-frame deletion in *cedX*	M. Thanbichler
pMT780	pBXMCS-2 carrying *cedX*	M. Thanbichler
pMT803	pNTPS138-based plasmid for replacing native *cedX* with *cedX-mcherry*	M. Thanbichler
pSW32	pXCHYC-2 carrying *stpB*	S. Wick
pSW35	pXCHYC-2 carrying *stpA*	S. Wick
pSW51	pNTPS138-based plasmid for constructing an in-frame deletion in *stpA*	S. Wick
pSW52	pNTPS138-based plasmid for constructing an in-frame deletion in *stpB*	S. Wick
pSW53	pNTPS138-based plasmid for constructing an in-frame deletion in *stpAB*	S. Wick
pSW64	pBXMCS-2 carrying *stpAB*	S. Wick

Plasmid	Genotype/description	Reference/Source
pSW67	pXCHYC-2 carrying *elpS* (*CCNA_00169*)	S.Wick/J.Kühn
pSS1	pXVENC-2 carrying *cedX*	This study
pSS8	pBXMCS-2 carrying *cedX-venus*	This study
pSS12	pBXMCS-2 carrying-$cedX_{\Delta 294\text{-}309}$-*venus*	This study
pSS15	pNPTS138-based plasmid for replacing native *cedX* with *cedX-HA*	This study
pSS17	pVVENC-1 carrying cedX	This study
pSS20	pBXMCX-2 carrying $cedX_{\Delta 1\text{-}32}$-*venus*	This study
pSS22	pBXMCS-2 carrying *cedX-HA*	This study
pSS30	pBXMCS-2 carrying $cedX_{\Delta 51\text{-}287}$-*venus*	This study
pSS75	pBXMCS-2 carrying *cedX-cfp*	This study
pSS92	pKT25 carrying *ftsL* (*CC2561*)	This study
pSS94	pUT18C carrying *ftsL* (*CC2561*)	This study
pSS96	pUT18C carrying *ftsN* (*CC2007*)	This study
pSS99	pUT18 carrying *cedX*	This study
pS102	pKT25 carrying *ftsN* (*CC2007*)	This study
pSS104	pKNT25 carrying *cedX*	This study
pSS114	pXCHYC-2 carrying $stpA_{\Delta 394\text{-}466}$	This study
pSS109	pNTPS138-based plasmid for replacing native *stpB* with *stpB-mcherry*	This study
pSS119	pXBlaMC-2 carrying *stpB*	This study
pSS120	pXBlaMC-2 carrying *stpA*	This study
pSS121	pXBlaCHYC-1 carrying $stpB_{\Delta 1\text{-}27}$	This study
pSS122	pXBlaCHYC-1 carrying $stpA_{\Delta 1\text{-}48}$	This study
pSS124	pKNT25 carrying *tipN* (*CC1485*)	This study
pSS125	pUT18 carrying *tipN* (*CC1485*)	This study
pSSS128	pUT18 carrying *zapA* (*CC3247*)	This study
pSS129	pKNT25 carrying *zapA* (*CC3247*)	This study
pSS130	pXBlaCHYC-1 carrying $stpB_{27\text{-}315}$	This study
pSS134	pXCHYC-2 carrying $stpA_{\Delta 95\text{-}137}$	This study
pSS138	pXVENN-2-based plasmid with *venus* replaced by *stpA*	This study
pSS142	pVCHYC-1 carrying *stpB*	This study
pSS187	pTCYC-2-based plasmid carrying *stpB-His*	This study
pSS200	pXCHYC-1 carrying *stpB*	This study
pSS202	pXGFPC-2 carrying *stpD*	This study
pSS204	pXCHYC-2 carrying *stpC*	This study
pSS205	pGFPC-1 carrying *stpD*	This study
pSS206	pTCYC-2-based plasmid carrying *stpD-His*	This study

Plasmid	Genotype/description	Reference/Source
pSS208	pNTPS138-based plasmid for constructing an in-frame deletion in *stpD*	This study
pSS209	pNTPS138-based plasmid for constructing an in-frame deletion in *stpC*	This study
pSS210	pTCYC-2-based plasmid carrying *stpD-His*	This study
pSS215	pNTPS138-based plasmid for constructing an in-frame deletion in *stpC* in an Δ*stpAB* background	This study
pSS220	pXBlaMC-2 carrying *stpC* (*CCNA_02271)*	This study
pSS221	pXBlaMC-2 carrying *stpD* (*CCNA_02271)*	This study
pSS222	pXBlaMN-2 carrying *stpD* (*CCNA_02271*)	This study
pSS225	pXCHYC-2 carrying *CC1409*	This study
pSS226	pXCHYC-2 carrying *CC2327*	This study
pSS227	pXCHYC-2 carrying *CC2287*	This study

Table 8. Oligonucleotides. Note the different gene annotation, CedX (CC2012) = CCNA_02091, StpA (CC2477) = CCNA_02562, StpB (CC2476) = CCNA_02561

Name	Designation	Sequence (5‘ →3‘)
Common oligonucleotides for colony PCR and sequencing		
M13for		GCCAGGGTTTTCCCAGTCACGA
M13rev		GAGCGGATAACAATTTCACACAGG
eGYC-up		CTTGCCGTAGGTGGCATCGCCCTCG
eGYC-down		GCTGCTGCCCGACAACCACTACCTGAG
mCherry-up		CTCGCCCTCGCCCTCGATCTCGAAC
mCherry-down		GCTGCTGCCCGACAACCACTACCTGAG
RevUni		GGGGATGTGCTGCAAGGCGATTAAGTTG
IntSpec-1		ATGCCGTTTGTGATGGCTTCCATGTCG
IntSpec-2		TCTTCCGGCAGGAATTCACTCACGCC
Pxyl-for		TGTCGGCGGCTTCTAGCATGGACCG
Pvan-for		TGGACTCTAGCCGACCGACTGAGACGC
pUT18-rev		GACGCGCCTCGGTGCCCACTGC
pUT18-fw		CCAGGCTTTACACTTTATGCTTCC
pUT18C-fw		CGGCGTGCCGAGCGGACGTTCG
pUT18C-rev		TCAGCGGGTGTTGGCGGGTGTC
pKT25-for		CCGCCGGACATCAGCGCCATTC
pKT25-rev		CCGCCGGACATCAGCGCCATTC
TEM-1_rev		GCTCATCATTGGAAAACGTTCTTCG

Name	Designation	Sequence (5‘ →3‘)
CedX project		
MT665	CC2012-uni	TTAATTCATATGTGCCCACTATGAGCGAACTCGCGC
MT666	CC2012-rev	TAGAGCTCCCGTCCTCGTCGAGATCGAACGGCAACTC
MT695	CC2012-rev2	TAGAGCTCTCAGTCCTCGTCGAGATCGAACGGCA
MT698	CC2012-1	TAGAATTCCAAGCTTTCCTGGATGCGCCGCTTG
MT699	CC2012-2	TAGAGCTCCAGCAAAAGACGCGCGAGTTCGCTC
MT700	CC2012-3	TAGAGCTCCAGGACGAGTTGCCGTTCGATCTCGAC
MT701	CC2012-4	ATAAGCTTCTTCTGGTCTACATGCTGGCCTCGGTGG
MT732	CC2012-5	TATGTACAAGTAACAGCGCCTCAGCGTCCGGTCTCGAC
MT733	CC2012-6	TATAGCTAGCATTGTCCTGATCGAGCTCACGCCGG
SS9	CC2012-HA-for	AATTCGTACCCATACGACGTCCCAGACTACGCTTAACT
SS10	CC2012-HA-rev	GTACAGTTAAGCGTAGTCTGGGACGTCGTATGGGTACG
SS18	CC2012-16	ATGAGCTCCTTCCCGCCGCGCTTTCGAGAC
SS25	CC2012-TM	TTAATTCATATGGATGAGGACCGGCGCATTCGCC
SS40	CC2012-rev1	CGCTTTCGACTCGCTCTTGAGAACGTTGCGGAGGG
SS41	CC2012-fw1	AAGAGCGAGTCGAAAGCGCGGCGGGAAACC
SS42	CC2012-rev2	CGCTTTCGAGCGTACGATCGCCTCGCAGCGG
SS43	CC2012-fw2	ATCGTACGCTCGAAAGCGCGGCGGGAAACC
SS192	CC2561-10	ATGAATTCTCATCGCAACGCCCCCTGGACTTG
SS196	CC2007-4	ATGAATTCTCACTTTACGAAGCAGGATTTGCCGGAG
SS199	CC2012-1	ATAAGCTTAATGCCCACTATGAGCGAACTCGCGC
SS200	CC2012-2	ATGAATTCCCGTCCTCGTCGAGATCGAACGGCAAC
SS206	CC2561-11	ATATAGATCTCATGACGGCGGCTGGCGTCTTCAATC
SS208	CC2007-5	ATATAGATCTCATGTCCGATCCGCACCGCGGGGC
SS239	CC1485-5fw	ATATAGATCTTATGGGACCCCGGCTGTGTATGAAGC
SS240	CC1485-6rev	ATATGAATTCGAGGCCAGATCGCCGCTCGCCGCGTC
SS258	CC3247-13	ATATAGATCTTATGGCTCAGGTGACCATCCAGGTGAAC
SS259	CC3247-14	ATATGAATTCGACTCAGTCGCGAGCTTCTCGATCCGC
Crossband project		
AM_299f	10xHis	AATTCCCATCACCACCATCATCACCATCACCACCACTAGT
AM_300r	10xHis	AATTACTAGTGGTGGTGATGGTGATGATGGTGGTGAT GGG
SW56	CC2477-uni	AAAACATATGCGCGAGGCCGGGGACGCAATTGC
SW57	CC2477-rev	TAGAGCTCCGTAATTCCCTTCGTTATACGGACGCCCGC
SW58	CC2476-inf-for	GGTATGTGGTTCTGGACGGTCTGGGCATTGAA

Name	Designation	Sequence (5‘ →3‘)
SW94	DCC2477-A-for	TTAAGGATCCGGAGCTGGCCAATACGGC
SW95	DCC2477-B-rev	TTAAGAATTCGCGAAGGCGCGCAATT
SW96	DCC2477-C-for	TTAAGAATTCGATCGGGGCGGGCGT
SW97	DCC2477-D-for	TTAAGCTAGCACGCCGGGCTGGATCTTG
SW98	DCC2476-A-for	AATTGGATCCTCGGCCGTCCGAACACC
SW99	DCC2476-B-rev	AATTGAATTCGGCCCAAAGCGCCAGC
SW100	DCC2476-C-for	AATTGAATTCCGGTCCGCCGCCC
SW101	DCC2476-D-rev	AATTGCTAGCTTGAAGCAGCGGTTGTCGCC
SW102	D2476d4277-A-for	TTAAGGATCCGGAGCTGGCCAATACGGC
SW103	D2476d4277-B-rev	TTAAGAATTCGCGAAGGCGCGCAATTG
SW104	D2476d4277-C-for	TTAAGAATTCGTTCCCGCGCCTCAACAAG
SW105	D2476d4277-D-for	TTAAGCTAGCGGGGGTGAAGATGCCGAG
SW123	CC2476-rev2St	AATTGAATTCTCATCGAGGAGCTCCCCCTTGT
SS221	CC2476-1	TATGTACAAGTAAGCAAGTCTGTTCGTAGCCGGCTGGC
SS222	CC2476-2	TATAGCTAGCCGACCAGCACCGTCCTCAGCATCC
SS224	CC2477-4	TAGAATTCCTAGTAATTCCCTTCGTTATACGGACGCCCG
SS227	CC2476-TM	ATTAATTCATATGTCGCCGGACGCCAAGATCGATCAG
SS228	CC2477-TM_1	ATTAATTCATATGGACACCGGCCCCAACTTCTGGTTCC
SS230	CC2477-Sel1_rev	GGGCTTGAACGAGCCGTTGACCGCAGCGTACTG
SS231	CC2477-Sel1_fw	AACGGCTCGTTCAAGCCCTCGGCCTGGCGTC
SS232	CC2477-Sel1_rev2	CGCGTAGCCATCGCCTCGGAAGCCACCCTGG
SS233	CC2477-Sel1_fw2	GGCTACGCGCCGATCGCCGCCTATGAGCGTC
SS274	CC2476-rev2	ATGAATTCGACTGGCGGTTCATGCCGGCGATGATG
SS282	CCNA_02560-for	TTAATTCATATGAGCAAGTCTGTTCGTAGCCGGCTGG
SS283	CCNA_02560-rev	TAGAGCTCCGCATCCGACGAGGCCCGCGCCGACG
SS284	CCNA_02271-for	TTAATTCATATGCGTCATCAAATGGCGCGTCGCG
SS285	CCNA_02271-rev	TAGAGCTCCGTGATGGGCGGCGGCGGCGTGCTTG
SS394	CCNA_02271-3	ATGAATTCGAACCAGACGACCTGAAGCGGCGCAG
SS395	CCNA_02271-4	CTTGTCCTTCACGCGACGCGCCATTTGATGAC
SS396	CCNA_02271-5	CGTCGCGTGAAGGACAAGCACGCCGCCGCCGC
SS397	CCNA_02271-6	TAAAGCTTCGGCGGTTTCCAGGTGATCGAGCA
SS398	CCNA_02271-7	ATTAATTCATATGGGCTTGGCGATCATCGGCCTCG
SS399	CCNA_02560-3	ATGAATTCGAGTCAAGGCGACCGGCACGATCATG
SS400	CCNA_02560-4	GAAATTACGGGAAACGGCCAGCCGGCTACGAAC
SS401	CCNA_02560-5	GCCGTTTCCCGTAATTTCGTCGGCGCGGGCCTC

Name	Designation	Sequence (5‘ →3‘)
SS402	CCNA_02560-6	TAAAGCTTCTACGAGCAGGCGACGAAGCACCG
SS416	CCNA_02271-8	TAGGTACCATGCGTCATCAAATGGCGCGTCG
SS417	CCNA_02271-9	TAGAATTCTCAGTGATGGGCGGCGGCGGCG
SS238	CC1409-1	ATTAATTCATATGAAGAAGCTCGCTCTTTCGCTCG
SS239	CC1409-2	ATGAATTCGAGAATTTGCGCGACAGGCCGATCG
SS240	CC2327-1	ATTAATTCATATGGCCCTGGCCCTGAATCCCAATG
SS242	CC2327-2	ATGAATTCGAGGCGCCCGCGTTGAAGCGGATG
SS243	CC2287-3	GCCAATGATCGCGTGATCGGCG
SS244	CC2287-4	CATCCCGCAGGAAGCCATCATCG

REFERENCES

1. Aaron, M., Charbon, G., Lam, H., Schwarz, H., Vollmer, W., and Jacobs-Wagner, C. (2007) The tubulin homologue FtsZ contributes to cell elongation by guiding cell wall precursor synthesis in *Caulobacter crescentus*, *Mol Microbiol 64*, 938-952.

2. Aarsman, M. E., Piette, A., Fraipont, C., Vinkenvleugel, T. M., Nguyen-Disteche, M., and den Blaauwen, T. (2005) Maturation of the *Escherichia coli* divisome occurs in two steps, *Mol Microbiol 55*, 1631-1645.

3. Adams, D. W., and Errington, J. (2009) Bacterial cell division: assembly, maintenance and disassembly of the Z ring, *Nat Rev Microbiol 7*, 642-653.

4. Addinall, S. G., Cao, C., and Lutkenhaus, J. (1997) FtsN, a late recruit to the septum in *Escherichia coli*, *Mol Microbiol 25*, 303-309.

5. Aldridge, P., Paul, R., Goymer, P., Rainey, P., and Jenal, U. (2003) Role of the GGDEF regulator PleD in polar development of *Caulobacter crescentus*, *Mol Microbiol 47*, 1695-1708.

6. Arends, S. J., Kustusch, R. J., and Weiss, D. S. (2009) ATP-binding site lesions in FtsE impair cell division, *J Bacteriol 191*, 3772-3784.

7. Areschoug, T., Linse, S., Stalhammar-Carlemalm, M., Heden, L. O., and Lindahl, G. (2002) A proline-rich region with a highly periodic sequence in *Streptococcal* β protein adopts the polyproline II structure and is exposed on the bacterial surface, *J Bacteriol 184*, 6376-6383.

8. Ausubel, F., Brent, R., Kingston, R., Moore, D., Seidman, J., Smith, J., and Struhl, K. (2002) Short protocols in molecular biology: A Compendium of methods from current protocols in molecular biology., John Wiley & Sons Inc.

9. Baek, J. H., and Lee, S. Y. (2006) Novel gene members in the Pho regulon of *Escherichia coli*, *FEMS Microbiol Lett 264*, 104-109.

10. Begg, K. J., Dewar, S. J., and Donachie, W. D. (1995) A new *Escherichia coli* cell division gene, *ftsK*, *J Bacteriol 177*, 6211-6222.

11. Bernander, R., and Ettema, T. J. (2010) FtsZ-less cell division in archaea and bacteria, *Curr Opin Microbiol 13*, 747-752.

12. Bernhardt, T. G., and de Boer, P. A. (2003) The *Escherichia coli* amidase AmiC is a periplasmic septal ring component exported via the twin-arginine transport pathway, *Mol Microbiol 48*, 1171-1182.

13. Bi, E. F., and Lutkenhaus, J. (1991) FtsZ ring structure associated with division in *Escherichia coli*, *Nature 354*, 161-164.

14. Biondi, E. G., Skerker, J. M., Arif, M., Prasol, M. S., Perchuk, B. S., and Laub, M. T. (2006) A phosphorelay system controls stalk biogenesis during cell cycle progression in *Caulobacter crescentus*, *Mol Microbiol 59*, 386-401.

15. Blatch, G. L., and Lassle, M. (1999) The tetratricopeptide repeat: a structural motif mediating protein-protein interactions, *Bioessays 21*, 932-939.

16. Bodenmiller, D., Toh, E., and Brun, Y. V. (2004) Development of surface adhesion in *Caulobacter crescentus*, *J Bacteriol 186*, 1438-1447.

17. Bowman, G. R., Comolli, L. R., Gaietta, G. M., Fero, M., Hong, S. H., Jones, Y., Lee, J. H., Downing, K. H., Ellisman, M. H., McAdams, H. H., and Shapiro, L. (2010) *Caulobacter* PopZ forms a polar subdomain dictating sequential changes in pole composition and function, *Mol Microbiol 76*, 173-189.

18. Bowman, G. R., Comolli, L. R., Zhu, J., Eckart, M., Koenig, M., Downing, K. H., Moerner, W. E., Earnest, T., and Shapiro, L. (2008) A polymeric protein anchors the chromosomal origin/ParB complex at a bacterial cell pole, *Cell 134*, 945-955.

19. Boyle, D. S., Khattar, M. M., Addinall, S. G., Lutkenhaus, J., and Donachie, W. D. (1997) *ftsW* is an essential cell-division gene in *Escherichia coli*, *Mol Microbiol 24*, 1263-1273.

20. Bradley, D. J., Kjellbom, P., and Lamb, C. J. (1992) Elicitor- and wound-induced oxidative cross-linking of a proline-rich plant cell wall protein: a novel, rapid defense response, *Cell 70*, 21-30.

21. Brun, Y. V., Marczynski, G., and Shapiro, L. (1994) The expression of asymmetry during *Caulobacter* cell differentiation, *Annu Rev Biochem 63*, 419-450.

22. Buddelmeijer, N., and Beckwith, J. (2002) Assembly of cell division proteins at the *E. coli* cell center, *Curr Opin Microbiol 5*, 553-557.

23. Buddelmeijer, N., and Beckwith, J. (2004) A complex of the *Escherichia coli* cell division proteins FtsL, FtsB and FtsQ forms independently of its localization to the septal region, *Mol Microbiol 52*, 1315-1327.

24. Chen, J. C., and Beckwith, J. (2001) FtsQ, FtsL and FtsI require FtsK, but not FtsN, for co-localization with FtsZ during *Escherichia coli* cell division, *Mol Microbiol 42*, 395-413.

25. Chen, J. C., Viollier, P. H., and Shapiro, L. (2005) A membrane metalloprotease participates in the sequential degradation of a *Caulobacter* polarity determinant, *Mol Microbiol 55*, 1085-1103.

26. Costa, T., Priyadarshini, R., and Jacobs-Wagner, C. (2008) Localization of PBP3 in *Caulobacter crescentus* is highly dynamic and largely relies on its functional transpeptidase domain, *Mol Microbiol 70*, 634-651.

27. Curtis, P. D., and Brun, Y. V. (2010) Getting in the loop: regulation of development in *Caulobacter crescentus*, *Microbiol Mol Biol Rev 74*, 13-41.

28. da Rocha, R. P., Paquola, A. C., Marques Mdo, V., Menck, C. F., and Galhardo, R. S. (2008) Characterization of the SOS regulon of *Caulobacter crescentus*, *J Bacteriol 190*, 1209-1218.

29. Dai, K., and Lutkenhaus, J. (1992) The proper ratio of FtsZ to FtsA is required for cell division to occur in *Escherichia coli*, *J Bacteriol 174*, 6145-6151.

30. Dai, K., Xu, Y., and Lutkenhaus, J. (1993) Cloning and characterization of *ftsN*, an essential cell division gene in *Escherichia coli* isolated as a multicopy suppressor of *ftsA12*(Ts), *J Bacteriol 175*, 3790-3797.

31. Daniel, R. A., and Errington, J. (2000) Intrinsic instability of the essential cell division protein FtsL of *Bacillus subtilis* and a role for DivIB protein in FtsL turnover, *Mol Microbiol 36*, 278-289.

32. Daniel, R. A., Harry, E. J., and Errington, J. (2000) Role of penicillin-binding protein PBP 2B in assembly and functioning of the division machinery of *Bacillus subtilis*, *Mol Microbiol 35*, 299-311.

33. Daniel, R. A., Noirot-Gros, M. F., Noirot, P., and Errington, J. (2006) Multiple interactions between the transmembrane division proteins of *Bacillus subtilis* and the role of FtsL instability in divisome assembly, *J Bacteriol 188*, 7396-7404.

34. de Boer, P. A. (2010) Advances in understanding *E. coli* cell fission, *Curr Opin Microbiol 13*, 730-737.

35. de Pedro, M. A., Quintela, J. C., Holtje, J. V., and Schwarz, H. (1997) Murein segregation in *Escherichia coli*, *J Bacteriol 179*, 2823-2834.

36. den Blaauwen, T., de Pedro, M. A., Nguyen-Disteche, M., and Ayala, J. A. (2008) Morphogenesis of rod-shaped sacculi, *Fems Microbiol Rev 32*, 321-344.

37. Din, N., Quardokus, E. M., Sackett, M. J., and Brun, Y. V. (1998) Dominant C-terminal deletions of FtsZ that affect its ability to localize in *Caulobacter* and its interaction with FtsA, *Mol Microbiol 27*, 1051-1063.

38. Divakaruni, A. V., Baida, C., White, C. L., and Gober, J. W. (2007) The cell shape proteins MreB and MreC control cell morphogenesis by positioning cell wall synthetic complexes, *Mol Microbiol 66*, 174-188.

39. Domian, I. J., Quon, K. C., and Shapiro, L. (1997) Cell type-specific phosphorylation and proteolysis of a transcriptional regulator controls the G1-to-S transition in a bacterial cell cycle, *Cell 90*, 415-424.

40. Durand-Heredia, J. M., Yu, H. H., De Carlo, S., Lesser, C. F., and Janakiraman, A. (2011) Identification and Characterization of ZapC, a Stabilizer of the FtsZ Ring in *Escherichia coli*, *J Bacteriol 193*, 1405-1413.

41. Dworkin, M. (2006) Prokaryotic Life Cycles, *The Prokaryotes*, 140-166.

42. Ebersbach, G., Galli, E., Moller-Jensen, J., Lowe, J., and Gerdes, K. (2008) Novel coiled-coil cell division factor ZapB stimulates Z ring assembly and cell division, *Mol Microbiol 68*, 720-735.

43. Edwards, D. H., and Errington, J. (1997) The *Bacillus subtilis* DivIVA protein targets to the division septum and controls the site specificity of cell division, *Mol Microbiol 24*, 905-915.

44. Ely, B. (1991) Genetics of *Caulobacter crescentus*, *Methods Enzymol 204*, 372-384.

45. Ely, B., and Johnson, R. C. (1977) Generalized Transduction in *Caulobacter crescentus*, *Genetics 87*, 391-399.

46. Erickson, H. P., Anderson, D. E., and Osawa, M. (2010) FtsZ in bacterial cytokinesis: cytoskeleton and force generator all in one, *Microbiol Mol Biol Rev 74*, 504-528.

47. Evinger, M., and Agabian, N. (1977) Envelope-associated nucleoid from *Caulobacter* crescentus stalked and swarmer cells, *J Bacteriol 132*, 294-301.

48. Fu, G., Huang, T., Buss, J., Coltharp, C., Hensel, Z., and Xiao, J. (2010) In vivo structure of the *E. coli* FtsZ-ring revealed by photoactivated localization microscopy (PALM), *PLoS One 5*, e12682.

49. Gamba, P., Veening, J. W., Saunders, N. J., Hamoen, L. W., and Daniel, R. A. (2009) Two-step assembly dynamics of the *Bacillus subtilis* divisome, *J Bacteriol 191*, 4186-4194.

50. Gerding, M. A., Ogata, Y., Pecora, N. D., Niki, H., and de Boer, P. A. (2007) The trans-envelope Tol-Pal complex is part of the cell division machinery and required for proper outer-membrane invagination during cell constriction in *E. coli*, *Mol Microbiol 63*, 1008-1025.

51. Goehring, N. W., and Beckwith, J. (2005) Diverse paths to midcell: assembly of the bacterial cell division machinery, *Curr Biol 15*, R514-526.

52. Goehring, N. W., Gonzalez, M. D., and Beckwith, J. (2006) Premature targeting of cell division proteins to midcell reveals hierarchies of protein interactions involved in divisome assembly, *Mol Microbiol 61*, 33-45.

53. Goley, E. D., Comolli, L. R., Fero, K. E., Downing, K. H., and Shapiro, L. (2010) DipM links peptidoglycan remodelling to outer membrane organization in *Caulobacter*, *Mol Microbiol 77*, 56-73.

54. Goley, E. D., Dye, N. A., Werner, J. N., Gitai, Z., and Shapiro, L. (2010) Imaging-based identification of a critical regulator of FtsZ protofilament curvature in *Caulobacter*, *Mol Cell 39*, 975-987.

55. Gonin, M., Quardokus, E. M., O'Donnol, D., Maddock, J., and Brun, Y. V. (2000) Regulation of stalk elongation by phosphate in *Caulobacter crescentus*, *J Bacteriol 182*, 337-347.

56. Gonzalez, M. D., Akbay, E. A., Boyd, D., and Beckwith, J. (2010) Multiple interaction domains in FtsL, a protein component of the widely conserved bacterial FtsLBQ cell division complex, *J Bacteriol 192*, 2757-2768.

57. Gonzalez, M. D., and Beckwith, J. (2009) Divisome under construction: distinct domains of the small membrane protein FtsB are necessary for interaction with multiple cell division proteins, *J Bacteriol 191*, 2815-2825.

58. Gueiros-Filho, F. J., and Losick, R. (2002) A widely conserved bacterial cell division protein that promotes assembly of the tubulin-like protein FtsZ, *Genes Dev 16*, 2544-2556.

59. Gündogdu, M. E., Kawai, Y., Pavlendova, N., Ogasawara, N., Errington, J., Scheffers, D. J., and Hamoen, L. W. (2011) Large ring polymers align FtsZ polymers for normal septum formation, *EMBO J 30*, 617-626.

60. Haeusser, D. P., Schwartz, R. L., Smith, A. M., Oates, M. E., and Levin, P. A. (2004) EzrA prevents aberrant cell division by modulating assembly of the cytoskeletal protein FtsZ, *Mol Microbiol 52*, 801-814.

61. Hale, C. A., and de Boer, P. A. J. (1997) Direct binding of FtsZ to ZipA, an essential component of the septal ring structure that mediates cell division in *E. coli*, *Cell 88*, 175-185.

62. Hale, C. A., Shiomi, D., Liu, B., Bernhardt, T. G., Margolin, W., Niki, H., and de Boer, P. A. (2011) Identification of *Escherichia coli* ZapC (YcbW) as a Component of the Division Apparatus That Binds and Bundles FtsZ Polymers, *J Bacteriol 193*, 1393-1404.

63. Hamoen, L. W., Meile, J. C., de Jong, W., Noirot, P., and Errington, J. (2006) SepF, a novel FtsZ-interacting protein required for a late step in cell division, *Mol Microbiol 59*, 989-999.

64. Handler, A. A., Lim, J. E., and Losick, R. (2008) Peptide inhibitor of cytokinesis during sporulation in Bacillus subtilis, *Mol Microbiol 68*, 588-599.

65. Harry, E., Monahan, L., Thompson, L., and Kwang, W. J. (2006) Bacterial cell division: the mechanism and its precison, in *Int Rev Cytol*, pp 27-94, Academic Press.

66. Houwink, A. L. (1955) *Caulobacter*; its morphogenesis, taxonomy and parasitism, *Antonie Van Leeuwenhoek 21*, 49-64.

67. Hu, Q., Milenkovic, L., Jin, H., Scott, M. P., Nachury, M. V., Spiliotis, E. T., and Nelson, W. J. (2010) A septin diffusion barrier at the base of the primary cilium maintains ciliary membrane protein distribution, *Science 329*, 436-439.

68. Hughes, H. V., Huitema, E., Pritchard, S., Keiler, K. C., Brun, Y. V., and Viollier, P. H. (2010) Protein localization and dynamics within a bacterial organelle, *Proc Natl Acad Sci U S A 107*, 5599-5604.

69. Huitema, E., Pritchard, S., Matteson, D., Radhakrishnan, S. K., and Viollier, P. H. (2006) Bacterial birth scar proteins mark future flagellum assembly site, *Cell 124*, 1025-1037.

70. Hung, C. Y., Yu, J. J., Seshan, K. R., Reichard, U., and Cole, G. T. (2002) A parasitic phase-specific adhesin of *Coccidioides immitis* contributes to the virulence of this respiratory Fungal pathogen, *Infect Immun 70*, 3443-3456.

71. Inagaki, F., Takai, K., Hirayama, H., Yamato, Y., Nealson, K. H., and Horikoshi, K. (2003) Distribution and phylogenetic diversity of the subsurface microbial community in a Japanese epithermal gold mine, *Extremophiles 7*, 307-317.

72. Ireland, M. M., Karty, J. A., Quardokus, E. M., Reilly, J. P., and Brun, Y. V. (2002) Proteomic analysis of the *Caulobacter crescentus* stalk indicates competence for nutrient uptake, *Mol Microbiol 45*, 1029-1041.

73. Ishikawa, S., Kawai, Y., Hiramatsu, K., Kuwano, M., and Ogasawara, N. (2006) A new FtsZ-interacting protein, YlmF, complements the activity of FtsA during progression of cell division in *Bacillus subtilis*, *Mol Microbiol 60*, 1364-1380.

74. Jones, H. C., and Schmidt, J. M. (1973) Ultrastructural study of crossbands occurring in the stalks of *Caulobacter crescentus*, *J Bacteriol 116*, 466-470.

75. Jordan, T. L., Porter, J. S., and Pate, J. L. (1974) Isolation and characterization of prosthecae of *Asticcacaulis biprosthecum*, *Arch Mikrobiol 96*, 1-16.

76. Judd, E. M., Comolli, L. R., Chen, J. C., Downing, K. H., Moerner, W. E., and McAdams, H. H. (2005) Distinct constrictive processes, separated in time and space, divide *Caulobacter* inner and outer membranes, *J Bacteriol 187*, 6874-6882.

77. Karimova, G., Dautin, N., and Ladant, D. (2005) Interaction network among *Escherichia coli* membrane proteins involved in cell division as revealed by bacterial two-hybrid analysis, *J Bacteriol 187*, 2233-2243.

78. Karimova, G., Pidoux, J., Ullmann, A., and Ladant, D. (1998) A bacterial two-hybrid system based on a reconstituted signal transduction pathway, *Proc Natl Acad Sci U S A 95*, 5752-5756.

79. Karimova, G., Robichon, C., and Ladant, D. (2009) Characterization of YmgF, a 72-residue inner membrane protein that associates with the *Escherichia coli* cell division machinery, *J Bacteriol 191*, 333-346.

80. Kenney, C. D., and Cornelissen, C. N. (2002) Demonstration and characterization of a specific interaction between gonococcal transferrin binding protein A and TonB, *J Bacteriol 184*, 6138-6145.

81. Kühn, J., Briegel, A., Mörschel, E., Kahnt, J., Leser, K., Wick, S., Jensen, G. J., and Thanbichler, M. (2010) Bactofilins, a ubiquitous class of cytoskeletal proteins mediating polar localization of a cell wall synthase in *Caulobacter crescentus*, *EMBO J 29*, 327-339.

82. Laemmli, U. K. (1970) Cleavage of structural proteins during the assembly of the head of bacteriophage T4, *Nature 227*, 680-685.

83. Lam, H., Schofield, W. B., and Jacobs-Wagner, C. (2006) A landmark protein essential for establishing and perpetuating the polarity of a bacterial cell, *Cell 124*, 1011-1023.

84. Larsen, R. A., Wood, G. E., and Postle, K. (1993) The conserved proline-rich motif is not essential for energy transduction by *Escherichia coli* TonB protein, *Mol Microbiol 10*, 943-953.

85. Laub, M. T., McAdams, H. H., Feldblyum, T., Fraser, C. M., and Shapiro, L. (2000) Global analysis of the genetic network controlling a bacterial cell cycle, *Science 290*, 2144-2148.

86. Laub, M. T., Shapiro, L., and McAdams, H. H. (2007) Systems biology of *Caulobacter*, *Annu Rev Genet 41*, 429-441.

87. Le Blastier, S., Hamels, A., Cabeen, M., Schille, L., Tilquin, F., Dieu, M., Raes, M., and Matroule, J. Y. (2010) Phosphate starvation triggers production and secretion of an extracellular lipoprotein in *Caulobacter crescentus*, *PLoS One 5*, e14198.

88. Lindås, A. C., Karlsson, E. A., Lindgren, M. T., Ettema, T. J., and Bernander, R. (2008) A unique cell division machinery in the Archaea, *Proc Natl Acad Sci U S A 105*, 18942-18946.

89. Liu, G., Draper, G. C., and Donachie, W. D. (1998) FtsK is a bifunctional protein involved in cell division and chromosome localization in *Escherichia coli*, *Mol Microbiol 29*, 893-903.

90. Löwe, J., and Amos, L. A. (1999) Tubulin-like protofilaments in Ca^{2+}-induced FtsZ sheets, *EMBO J 18*, 2364-2371.

91. Ma, X., and Margolin, W. (1999) Genetic and functional analyses of the conserved C-terminal core domain of *Escherichia coli* FtsZ, *J Bacteriol 181*, 7531-7544.

92. MacRae, J. D., and Smit, J. (1991) Characterization of *Caulobacters* isolated from wastewater treatment systems, *Appl Environ Microbiol 57*, 751-758.

93. Männistö, M. K., Tiirola, M. A., Salkinoja-Salonen, M. S., Kulomaa, M. S., and Puhakka, J. A. (1999) Diversity of chlorophenol-degrading bacteria isolated from contaminated boreal groundwater, *Arch Microbiol 171*, 189-197.

94. Marks, M. E., Castro-Rojas, C. M., Teiling, C., Du, L., Kapatral, V., Walunas, T. L., and Crosson, S. (2010) The genetic basis of laboratory adaptation in *Caulobacter crescentus*, *J Bacteriol 192*, 3678-3688.

95. Matroule, J. Y., Lam, H., Burnette, D. T., and Jacobs-Wagner, C. (2004) Cytokinesis monitoring during development; rapid pole-to-pole shuttling of a signaling protein by localized kinase and phosphatase in *Caulobacter*, *Cell 118*, 579-590.

96. McGrath, P. T., Lee, H., Zhang, L., Iniesta, A. A., Hottes, A. K., Tan, M. H., Hillson, N. J., Hu, P., Shapiro, L., and McAdams, H. H. (2007) High-throughput identification of transcription start sites, conserved promoter motifs and predicted regulons, *Nat Biotechnol 25*, 584-592.

97. Mohammadi, T., van Dam, V., Sijbrandi, R., Vernet, T., Zapun, A., Bouhss, A., Diepeveen-de Bruin, M., Nguyen-Disteche, M., de Kruijff, B., and Breukink, E. (2011) Identification of FtsW as a transporter of lipid-linked cell wall precursors across the membrane, *EMBO J*.

98. Mohl, D. A., Easter, J., Jr., and Gober, J. W. (2001) The chromosome partitioning protein, ParB, is required for cytokinesis in *Caulobacter crescentus*, *Mol Microbiol 42*, 741-755.

99. Möll, A., Schlimpert, S., Briegel, A., Jensen, G. J., and Thanbichler, M. (2010) DipM, a new factor required for peptidoglycan remodelling during cell division in *Caulobacter crescentus*, *Mol Microbiol 77*, 90-107.

100. Möll, A., and Thanbichler, M. (2009) FtsN-like proteins are conserved components of the cell division machinery in proteobacteria, *Mol Microbiol 72*, 1037-1053.

101. Monds, R. D., Newell, P. D., Schwartzman, J. A., and O'Toole, G. A. (2006) Conservation of the Pho regulon in *Pseudomonas fluorescens* Pf0-1, *Appl Environ Microbiol 72*, 1910-1924.

102. Mukherjee, A., Cao, C., and Lutkenhaus, J. (1998) Inhibition of FtsZ polymerization by SulA, an inhibitor of septation in *Escherichia coli*, *Proc Natl Acad Sci U S A 95*, 2885-2890.

103. Mukherjee, A., and Lutkenhaus, J. (1994) Guanine nucleotide-dependent assembly of FtsZ into filaments, *J Bacteriol 176*, 2754-2758.

104. Murat, D., Byrne, M., and Komeili, A. (2010) Cell biology of prokaryotic organelles, *Cold Spring Harb Perspect Biol 2*, 1-18.

105. Nakada, C., Ritchie, K., Oba, Y., Nakamura, M., Hotta, Y., Iino, R., Kasai, R. S., Yamaguchi, K., Fujiwara, T., and Kusumi, A. (2003) Accumulation of anchored proteins forms membrane diffusion barriers during neuronal polarization, *Nat Cell Biol 5*, 626-632.

106. Nierman, W. C., Feldblyum, T. V., Laub, M. T., Paulsen, I. T., Nelson, K. E., Eisen, J. A., Heidelberg, J. F., Alley, M. R., Ohta, N., Maddock, J. R., Potocka, I., Nelson, W. C., Newton, A., Stephens, C., Phadke, N. D., Ely, B., DeBoy, R. T., Dodson, R. J., Durkin, A. S., Gwinn, M. L., Haft, D. H., Kolonay, J. F., Smit, J., Craven, M. B., Khouri, H., Shetty, J., Berry, K., Utterback, T., Tran, K., Wolf, A., Vamathevan, J., Ermolaeva, M., White, O., Salzberg, S. L., Venter, J. C., Shapiro, L., and Fraser, C. M. (2001) Complete genome sequence of *Caulobacter crescentus*, *Proc Natl Acad Sci U S A 98*, 4136-4141.

107. Nishimura, K., Akiyama, H., Komada, M., and Kamiguchi, H. (2007) βIV-spectrin forms a diffusion barrier against L1CAM at the axon initial segment, *Mol Cell Neurosci 34*, 422-430.

108. North, N. N., Dollhopf, S. L., Petrie, L., Istok, J. D., Balkwill, D. L., and Kostka, J. E. (2004) Change in bacterial community structure during in situ biostimulation of subsurface sediment cocontaminated with uranium and nitrate, *Appl Environ Microbiol 70*, 4911-4920.

109. Osawa, M., Anderson, D. E., and Erickson, H. P. (2008) Reconstitution of contractile FtsZ rings in liposomes, *Science 320*, 792-794.

110. Osawa, M., Anderson, D. E., and Erickson, H. P. (2009) Curved FtsZ protofilaments generate bending forces on liposome membranes, *EMBO J 28*, 3476-3484.

111. Paerl, H. W. (1982) Factors limiting productivity of freshwater ecosystems, in *K. C. Marhal (ed.), Advances in microbial ecology.* , pp 75-110.

112. Paradis-Bleau, C., Markovski, M., Uehara, T., Lupoli, T. J., Walker, S., Kahne, D. E., and Bernhardt, T. G. (2010) Lipoprotein cofactors located in the outer membrane activate bacterial cell wall polymerases, *Cell 143*, 1110-1120.

113. Patru, M. M., and Pavelka, M. S., Jr. (2010) A role for the class A penicillin-binding protein PonA2 in the survival of *Mycobacterium smegmatis* under conditions of nonreplication, *J Bacteriol 192*, 3043-3054.

114. Pichoff, S., and Lutkenhaus, J. (2002) Unique and overlapping roles for ZipA and FtsA in septal ring assembly in *Escherichia coli*, *EMBO J 21*, 685-693.

115. Poggio, S., Takacs, C. N., Vollmer, W., and Jacobs-Wagner, C. (2010) A protein critical for cell constriction in the Gram-negative bacterium *Caulobacter crescentus* localizes at the division site through its peptidoglycan-binding LysM domains, *Mol Microbiol 77*, 74-89.

116. Pogliano, J., Pogliano, K., Weiss, D. S., Losick, R., and Beckwith, J. (1997) Inactivation of FtsI inhibits constriction of the FtsZ cytokinetic ring and delays the assembly of FtsZ rings at potential division sites, *Proc Natl Acad Sci U S A 94*, 559-564.

117. Poindexter, J. L. S., and Cohen-Bazire, G. (1964) Fine structure of stalked bacteria belonging to family *Caulobacteraceae*, *J Cell Biol 23*, 587-&.

118. Poindexter, J. S. (1964) Biological Properties and Classification of the *Caulobacter* Group, *Bacteriol Rev 28*, 231-295.

119. Poindexter, J. S., and Hagenzieker, J. G. (1982) Novel peptidoglycans in *Caulobacter* and *Asticcacaulis* spp., *J Bacteriol 150*, 332-347.

120. Poindexter, J. S., and Staley, J. T. (1996) *Caulobacter* and *Asticcacaulis* stalk bands as indicators of stalk age, *J Bacteriol 178*, 3939-3948.

121. Ptacin, J. L., Lee, S. F., Garner, E. C., Toro, E., Eckart, M., Comolli, L. R., Moerner, W. E., and Shapiro, L. (2010) A spindle-like apparatus guides bacterial chromosome segregation, *Nat Cell Biol 12*, 791-798.

122. Quon, K. C., Marczynski, G. T., and Shapiro, L. (1996) Cell cycle control by an essential bacterial two-component signal transduction protein, *Cell 84*, 83-93.

123. Radhakrishnan, S. K., Pritchard, S., and Viollier, P. H. (2010) Coupling prokaryotic cell fate and division control with a bifunctional and oscillating oxidoreductase homolog, *Dev Cell 18*, 90-101.

124. Radhakrishnan, S. K., Thanbichler, M., and Viollier, P. H. (2008) The dynamic interplay between a cell fate determinant and a lysozyme homolog drives the asymmetric division cycle of *Caulobacter crescentus*, *Genes Dev 22*, 212-225.

125. Ramamurthi, K. S., Lecuyer, S., Stone, H. A., and Losick, R. (2009) Geometric cue for protein localization in a bacterium, *Science 323*, 1354-1357.

126. Ramamurthi, K. S., and Losick, R. (2009) Negative membrane curvature as a cue for subcellular localization of a bacterial protein, *Proc Natl Acad Sci U S A 106*, 13541-13545.

127. Rath, A., Davidson, A. R., and Deber, C. M. (2005) The structure of "unstructured" regions in peptides and proteins: role of the polyproline II helix in protein folding and recognition, *Biopolymers 80*, 179-185.

128. Reddy, M. (2007) Role of FtsEX in cell division of *Escherichia coli*: viability of ftsEX mutants is dependent on functional SufI or high osmotic strength, *J Bacteriol 189*, 98-108.

129. Romberg, L., and Levin, P. A. (2003) Assembly dynamics of the bacterial cell division protein FTSZ: poised at the edge of stability, *Annu Rev Microbiol 57*, 125-154.

130. Rudner, D. Z., and Losick, R. (2010) Protein subcellular localization in bacteria, *Cold Spring Harb Perspect Biol 2*, 1-14.

131. Rudner, D. Z., Pan, Q., and Losick, R. M. (2002) Evidence that subcellular localization of a bacterial membrane protein is achieved by diffusion and capture, *Proc Natl Acad Sci U S A 99*, 8701-8706.

132. Ryan, K. R., Taylor, J. A., and Bowers, L. M. (2010) The BAM complex subunit BamE (SmpA) is required for membrane integrity, stalk growth and normal levels of outer membrane β-barrel proteins in *Caulobacter crescentus*, *Microbiology 156*, 742-756.

133. Sackett, M. J., Kelly, A. J., and Brun, Y. V. (1998) Ordered expression of ftsQA and ftsZ during the *Caulobacter crescentus* cell cycle, *Mol Microbiol 28*, 421-434.

134. Samaluru, H., SaiSree, L., and Reddy, M. (2007) Role of SufI (FtsP) in cell division of *Escherichia coli*: evidence for its involvement in stabilizing the assembly of the divisome, *J Bacteriol 189*, 8044-8052.

135. Sambrook, J., Fritsch, E., and Maniatis, T. (1989) Molecular Cloning. A Laboratory Manual., Cold Spring Harbor, NY., Cold Spring Harbor Laboratory Press.

136. Sassanfar, M., and Roberts, J. W. (1990) Nature of the SOS-inducing signal in *Escherichia coli*. The involvement of DNA replication, *J Mol Biol 212*, 79-96.

137. Schmidt, J. M. (1968) Stalk Elongation in Mutants of *Caulobacter crescentus*, *J Gen Microbiol 53*, 291-298.

138. Schmidt, J. M. (1971) Prosthecate bacteria, *Annu Rev Microbiol 25*, 93-110.

139. Schmidt, J. M. (1973) Effect of lysozyme on crossbands in stalks of *Caulobacter crescentus*, *Arch. Mikrobiol. 89*, 33-40.

140. Schmidt, J. M., and Stanier, R. Y. (1966) The development of cellular stalks in bacteria, *J Cell Biol 28*, 423-436.

141. Schmidt, J. M., and Swafford, J. R. (1975) Ultrastructure of crossbands in prosthecae of *Asticcacaulis* species, *J Bacteriol 124*, 1601-1603.

142. Schmidt, K. L., Peterson, N. D., Kustusch, R. J., Wissel, M. C., Graham, B., Phillips, G. J., and Weiss, D. S. (2004) A predicted ABC transporter, FtsEX, is needed for cell division in *Escherichia coli*, *J Bacteriol 186*, 785-793.

143. Schofield, W. B., Lim, H. C., and Jacobs-Wagner, C. (2010) Cell cycle coordination and regulation of bacterial chromosome segregation dynamics by polarly localized proteins, *EMBO J 29*, 3068-3081.

144. Seitz, L. C., and Brun, Y. V. (1998) Genetic analysis of mecillinam-resistant mutants of *Caulobacter crescentus* deficient in stalk biosynthesis, *J Bacteriol 180*, 5235-5239.

145. Singh, J. K., Makde, R. D., Kumar, V., and Panda, D. (2008) SepF increases the assembly and bundling of FtsZ polymers and stabilizes FtsZ protofilaments by binding along its length, *J Biol Chem 283*, 31116-31124.

146. Skerker, J. M., and Laub, M. T. (2004) Cell-cycle progression and the generation of asymmetry in *Caulobacter crescentus*, *Nat Rev Microbiol 2*, 325-337.

147. Skerker, J. M., and Shapiro, L. (2000) Identification and cell cycle control of a novel pilus system in Caulobacter crescentus, *EMBO J 19*, 3223-3234.

148. Smith, C. S., Hinz, A., Bodenmiller, D., Larson, D. E., and Brun, Y. V. (2003) Identification of genes required for synthesis of the adhesive holdfast in *Caulobacter crescentus*, *Journal of Bacteriology 185*, 1432-1442.

149. Solheim, S. A., Petsalaki, E., Stokka, A. J., Russell, R. B., Tasken, K., and Berge, T. (2008) Interactions between the Fyn SH3-domain and adaptor protein Cbp/PAG derived ligands, effects on kinase activity and affinity, *FEBS J 275*, 4863-4874.

150. Sommer, J. M., and Newton, A. (1991) Pseudoreversion analysis indicates a direct role of cell division genes in polar morphogenesis and differentiation in *Caulobacter crescentus*, *Genetics 129*, 623-630.

151. Song, A. H., Wang, D., Chen, G., Li, Y., Luo, J., Duan, S., and Poo, M. M. (2009) A selective filter for cytoplasmic transport at the axon initial segment, *Cell 136*, 1148-1160.

152. Staley, J. T., and Jordan, T. L. (1973) Crossbands of *Caulobacter crescentus* stalks serve as indicators of cell age, *Nature 246*, 155-156.

153. Steele, V. R., Bottomley, A. L., Garcia-Lara, J., Kasturiarachchi, J., and Foster, S. J. (2011) Multiple essential roles for EzrA in cell division of *Staphylococcus aureus*, *Mol Microbiol 80*, 542-555.

154. Thanbichler, M. (2009) Spatial regulation in *Caulobacter crescentus*, *Curr Opin Microbiol 12*, 715-721.

155. Thanbichler, M. (2010) Synchronization of chromosome dynamics and cell division in bacteria, *Cold Spring Harb Perspect Biol 2*, a000331.

156. Thanbichler, M., Iniesta, A. A., and Shapiro, L. (2007) A comprehensive set of plasmids for vanillate- and xylose-inducible gene expression in *Caulobacter crescentus*, *Nucleic Acids Res 35*, e137.

157. Thanbichler, M., and Shapiro, L. (2006) MipZ, a spatial regulator coordinating chromosome segregation with cell division in *Caulobacter*, *Cell 126*, 147-162.

158. Thanbichler, M., and Shapiro, L. (2008) Getting organized--how bacterial cells move proteins and DNA, *Nat Rev Microbiol 6*, 28-40.

159. Typas, A., Banzhaf, M., van den Berg van Saparoea, B., Verheul, J., Biboy, J., Nichols, R. J., Zietek, M., Beilharz, K., Kannenberg, K., von Rechenberg, M., Breukink, E., den Blaauwen, T., Gross, C. A., and Vollmer, W. (2010) Regulation of peptidoglycan synthesis by outer-membrane proteins, *Cell 143*, 1097-1109.

160. Uehara, T., Parzych, K. R., Dinh, T., and Bernhardt, T. G. (2010) Daughter cell separation is controlled by cytokinetic ring-activated cell wall hydrolysis, *EMBO J 29*, 1412-1422.

161. Wagner, J. K., and Brun, Y. V. (2007) Out on a limb: how the *Caulobacter* stalk can boost the study of bacterial cell shape, *Mol Microbiol 64*, 28-33.

162. Wagner, J. K., Galvani, C. D., and Brun, Y. V. (2005) *Caulobacter crescentus* requires RodA and MreB for stalk synthesis and prevention of ectopic pole formation, *J Bacteriol 187*, 544-553.

163. Wagner, J. K., Setayeshgar, S., Sharon, L. A., Reilly, J. P., and Brun, Y. V. (2006) A nutrient uptake role for bacterial cell envelope extensions, *Proc Natl Acad Sci U S A 103*, 11772-11777.

164. Wallin, E., and von Heijne, G. (1998) Genome-wide analysis of integral membrane proteins from eubacterial, archaean, and eukaryotic organisms, *Protein Sci 7*, 1029-1038.

165. Wang, H. C., and Gayda, R. C. (1990) High-level expression of the FtsA protein inhibits cell septation in *Escherichia coli* K-12, *J Bacteriol 172*, 4736-4740.

166. Wang, S. C., West, L., and Shapiro, L. (2006) The bifunctional FtsK protein mediates chromosome partitioning and cell division in *Caulobacter*, *J Bacteriol 188*, 1497-1508.

167. Wang, S. P., Sharma, P. L., Schoenlein, P. V., and Ely, B. (1993) A histidine protein kinase is involved in polar organelle development in *Caulobacter crescentus*, *Proc Natl Acad Sci U S A 90*, 630-634.

168. Wang, Y., Jones, B. D., and Brun, Y. V. (2001) A set of *ftsZ* mutants blocked at different stages of cell division in *Caulobacter*, *Mol Microbiol 40*, 347-360.

169. Wanner, B. L. (1993) Gene regulation by phosphate in enteric bacteria, *J Cell Biochem 51*, 47-54.

170. Ward, J. E., Jr., and Lutkenhaus, J. (1985) Overproduction of FtsZ induces minicell formation in *E. coli*, *Cell 42*, 941-949.

171. Weart, R. B., Lee, A. H., Chien, A. C., Haeusser, D. P., Hill, N. S., and Levin, P. A. (2007) A metabolic sensor governing cell size in bacteria, *Cell 130*, 335-347.

172. Werner, J. N., Chen, E. Y., Guberman, J. M., Zippilli, A. R., Irgon, J. J., and Gitai, Z. (2009) Quantitative genome-scale analysis of protein localization in an asymmetric bacterium, *Proc Natl Acad Sci U S A 106*, 7858-7863.

173. West, L., Yang, D., and Stephens, C. (2002) Use of the *Caulobacter crescentus* genome sequence to develop a method for systematic genetic mapping, *J Bacteriol 184*, 2155-2166.

174. Wheeler, R. T., and Shapiro, L. (1999) Differential localization of two histidine kinases controlling bacterial cell differentiation, *Mol Cell 4*, 683-694.

175. Whittenbury, R., and Dow, C. S. (1977) Morphogenesis and differentiation in *Rhodomicrobium vannielii* and other budding and prosthecate bacteria, *Bacteriol Rev 41*, 754-808.

176. Willemse, J., Borst, J. W., de Waal, E., Bisseling, T., and van Wezel, G. P. (2011) Positive control of cell division: FtsZ is recruited by SsgB during sporulation of *Streptomyces*, *Genes Dev 25*, 89-99.

177. Williamson, M. P. (1994) The structure and function of proline-rich regions in proteins, *Biochem J 297 (Pt 2)*, 249-260.

178. Wu, L. J., and Errington, J. (1994) *Bacillus subtilis* SpoIIIE protein required for DNA segregation during asymmetric cell division, *Science 264*, 572-575.

179. Wu, L. J., and Errington, J. (2004) Coordination of cell division and chromosome segregation by a nucleoid occlusion protein in *Bacillus subtilis*, *Cell 117*, 915-925.

180. Yeh, Y. C., Comolli, L. R., Downing, K. H., Shapiro, L., and McAdams, H. H. (2010) The *Caulobacter* Tol-Pal complex is essential for outer membrane integrity and the positioning of a polar localization factor, *J Bacteriol 192*, 4847-4858.

181. Young, K. D. (2006) The selective value of bacterial shape, *Microbiol Mol Biol Rev 70*, 660-703.

ACKNOWLEDGEMENT

Finding the appropriate words to describe research results is more or less a technical task; however, finding the right words to express my gratitude was much harder. Writing this doctoral thesis would not have been possible without the advise, encouragement and support from a number of people around me who have contributed in various ways to the completion of this work.

First and foremost I want to thank my advisor Martin Thanbichler. The door to your office was always open whenever I needed advice, guidance or wanted to bounce off ideas. Thank you for never running out of even better ideas and for giving me the freedom to be curious and to explore.

I am indebted to my thesis committee members Prof. Dr. Renate Renkawitz-Pohl, Prof. Dr. Uwe G. Maier, and in particular to Prof. Dr. MD Lotte Søgaard-Andersen who unhesitatingly agreed to become my second reviewer.

Some of the exciting results described in this study would not have been obtained without the help of my collaborators. I am very grateful to J. Kahnt (Dept. of Ecophysiology) for the MALDI/MS analyses, M. Johannsen and Dr. K. Bolte (Dept. of Biology, Philipps-University, Marburg) for the their support in collecting countless electron micrographs of stalks, and to Dr. A. Briegel and Prof. G. Jensen (Caltech, USA) for the electron cryo-tomographs.

Special thanks go to my enthusiastic and critical readers Dr. Juliane Kühn, Dr. Jürgen Lassak and (soon to-be Dr.) Daniela Kiekebusch for helpful discussions and valuable comments on my thesis.

My time in the lab was made very enjoyable and inspiring by past and present lab members. I would like to take this opportunity to thank Stephanie Wick and Marlina Bischoff for excellent technical support. I thank all of you for a wonderful working atmosphere throughout the last years. Those cake and coffee sessions will remain unforgotten and I wish everyone all the best.

Over the past years I made very good friends who made sure that I enjoyed the life outside the lab as much as my time at the bench. Thank you, Jürgen, Anja, Julia and Dani for sharing every success and failure.

In a special way, I would like to express my deepest gratitude to my family for their encouragement and unconditional support throughout my life. I apologize for all those cut short phone calls and the birthdays I missed. Thank you for your understanding and your love.

ERKLÄRUNG

Ich versichere, dass ich meine Dissertation:

„About rings and crossbands – Characterization of proteins involved in cell division and compartmentalization in *Caulobacter crescentus*“

selbstständig, ohne unerlaubte Hilfe angefertigt und mich dabei keiner anderen als der von mir ausdrücklich bezeichneten Quellen und Hilfen bedient habe. Die Dissertation wurde in der jetzigen oder einer ähnlichen Form noch bei keiner anderen Hochschule eingereicht und hat noch keinen sonstigen Prüfungszwecken gedient.

Marburg, den ___.___.2011 _____

Susan Schlimpert